

# LETTER OF TRANSMITTAL

**To:** Guy Warren  
Remedial Project Manager  
Alaska Department of  
Environmental Conservation  
555 Cordova Street  
Anchorage, Alaska 99501

**Date:** 12/30/13

**From:** Justin Peach  
Remedial Project Manager  
NAVFAC NW  
1101 Tautog Circle, Suite  
201  
Silverdale, WA, 98315

**Subject:** Final Hydrodynamic Mobility Analysis of UXO Transport, Andrew Bay,  
OU B-2, Former Adak Naval Complex, Adak, Alaska

**Transmitting:**

Included  Under Separate Cover

**The Following:**

<input type="checkbox"/> Correspondence	<input type="checkbox"/> Memorandum
<input type="checkbox"/> Report	<input type="checkbox"/> Graphic
<input type="checkbox"/> CD/Disk	<input type="checkbox"/> Construction Drawing
<input type="checkbox"/> Survey	<input type="checkbox"/> Specification
<input type="checkbox"/> Work Plan	<input type="checkbox"/> Shop Drawing
<input type="checkbox"/> Assessment	<input type="checkbox"/> Letter
<input type="checkbox"/> Decision Document	<input type="checkbox"/> Public Press Release
<input type="checkbox"/> Site Closure	<input type="checkbox"/> Comments/Response to Comments
<input type="checkbox"/> Public Information	<input type="checkbox"/> Document for Restoration Advisory Board

**For:**

Review and Comment  
 Approval  
 Signature  
 Use and Files  
 Quotation  
 Payment  
 As Requested  
 Action Noted Below

<b>Number of Copies:</b>	<b>Sets</b> _____	<b>Sheets</b> _____	<b>Documents</b> _____
--------------------------	-------------------	---------------------	------------------------

Guy-  
Attached for your use is the Final Hydrodynamic Mobility Analysis of UXO  
Transport, Andrew Bay, OU B-2, Former Adak Naval Complex, Adak, Alaska.

Please let me know if you have any questions or comments concerning the  
document.

\_\_\_\_\_  
Justin Peach

# LETTER OF TRANSMITTAL

**To:** Christopher Cora  
Remedial Project Manager  
U.S. Environmental Protection  
Agency  
1200 6th Ave, ECL-115  
Seattle, WA 98107

**Date:** 12/30/13

**From:** Justin Peach  
Remedial Project Manager  
NAVFAC NW  
1101 Tautog Circle, Suite  
201  
Silverdale, WA, 98315

**Subject:** Final Hydrodynamic Mobility Analysis of UXO Transport, Andrew Bay,  
OU B-2, Former Adak Naval Complex, Adak, Alaska

**Transmitting:**

Included  Under Separate Cover

**The Following:**

Correspondence  Memorandum  
 Report  Graphic  
 CD/Disk  Construction Drawing  
 Survey  Specification  
 Work Plan  Shop Drawing  
 Assessment  Letter  
 Decision Document  Public Press Release  
 Site Closure  Comments/Response to Comments  
 Public Information  Document for Restoration Advisory Board

**For:**

Review and Comment  
 Approval  
 Signature  
 Use and Files  
 Quotation  
 Payment  
 As Requested  
 Action Noted Below

<b>Number of Copies:</b>	<b>Sets</b> _____	<b>Sheets</b> _____	<b>Documents</b> _____
--------------------------	-------------------	---------------------	------------------------

Chris-  
Attached for your use is the Final Hydrodynamic Mobility Analysis of UXO  
Transport, Andrew Bay, OU B-2, Former Adak Naval Complex, Adak, Alaska.

Please let me know if you have any questions or comments concerning the  
document.

\_\_\_\_\_  
Justin Peach

# LETTER OF TRANSMITTAL

**To:** Eric Lehnertz, CIH, CSP  
Environment, Health, and  
Safety Manager  
The Aleut Corporation  
5540 Tech Center Drive, Suite  
100  
Colorado Springs, CO 80919-  
2332

**Date:** 12/30/13

**From:** Justin Peach  
Remedial Project Manager  
NAVFAC NW  
1101 Tautog Circle, Suite  
201  
Silverdale, WA, 98315

**Subject:** Final Hydrodynamic Mobility Analysis of UXO Transport, Andrew Bay,  
OU B-2, Former Adak Naval Complex, Adak, Alaska

**Transmitting:**

Included  Under Separate Cover

**The Following:**

Correspondence  Memorandum  
 Report  Graphic  
 CD/Disk  Construction Drawing  
 Survey  Specification  
 Work Plan  Shop Drawing  
 Assessment  Letter  
 Decision Document  Public Press Release  
 Site Closure  Comments/Response to Comments  
 Public Information  Document for Restoration Advisory Board

**For:**

Review and Comment  
 Approval  
 Signature  
 Use and Files  
 Quotation  
 Payment  
 As Requested  
 Action Noted Below

<b>Number of Copies:</b>	<b>Sets</b> _____	<b>Sheets</b> _____	<b>Documents</b> _____
--------------------------	-------------------	---------------------	------------------------

Eric-  
Attached for your use is the Final Hydrodynamic Mobility Analysis of UXO  
Transport, Andrew Bay, OU B-2, Former Adak Naval Complex, Adak, Alaska.  
Please let me know if you have any questions or comments concerning the  
document.

\_\_\_\_\_  
Justin Peach

# LETTER OF TRANSMITTAL

**To:** Merry Maxwell  
Regional Permits Coordinator  
Alaska Maritime NWR  
US Fish & Wildlife Service  
1101 East Tudor Road  
Anchorage, Alaska 99503

**Date:** 19 Nov 2013

**From:** Justin Peach  
Remedial Project Manager  
NAVFAC NW  
1101 Tautog Circle, Suite  
201  
Silverdale, WA, 98315

**Subject:** Final Hydrodynamic Mobility Analysis of UXO Transport, Andrew Bay, OU B-2, Former Adak Naval Complex, Adak, Alaska

**Transmitting:**

Included  Under Separate Cover

**The Following:**

<input type="checkbox"/> Correspondence	<input type="checkbox"/> Memorandum
<input type="checkbox"/> Report	<input type="checkbox"/> Graphic
<input type="checkbox"/> CD/Disk	<input type="checkbox"/> Construction Drawing
<input type="checkbox"/> Survey	<input type="checkbox"/> Specification
<input type="checkbox"/> Work Plan	<input type="checkbox"/> Shop Drawing
<input type="checkbox"/> Assessment	<input type="checkbox"/> Letter
<input type="checkbox"/> Decision Document	<input type="checkbox"/> Public Press Release
<input type="checkbox"/> Site Closure	<input type="checkbox"/> Comments/Response to Comments
<input type="checkbox"/> Public Information	<input type="checkbox"/> Document for Restoration Advisory Board

**For:**

Review and Comment  
 Approval  
 Signature  
 Use and Files  
 Quotation  
 Payment  
 As Requested  
 Action Noted Below

<b>Number of Copies:</b>	<b>Sets</b> _____	<b>Sheets</b> _____	<b>Documents</b> _____
--------------------------	-------------------	---------------------	------------------------

Merry-  
Attached for your use is the Final Hydrodynamic Mobility Analysis or UXO Transport, Andrew Bay, OU B-2, Former Adak Naval Complex, Adak, Alaska.

Please let me know if you have any questions or comments concerning the report.

Thanks much.

\_\_\_\_\_  
Justin Peach

**Final**

April 2013



# Hydrodynamic Mobility Analysis of UXO Transport Andrew Bay

## **Former Adak Naval Complex**

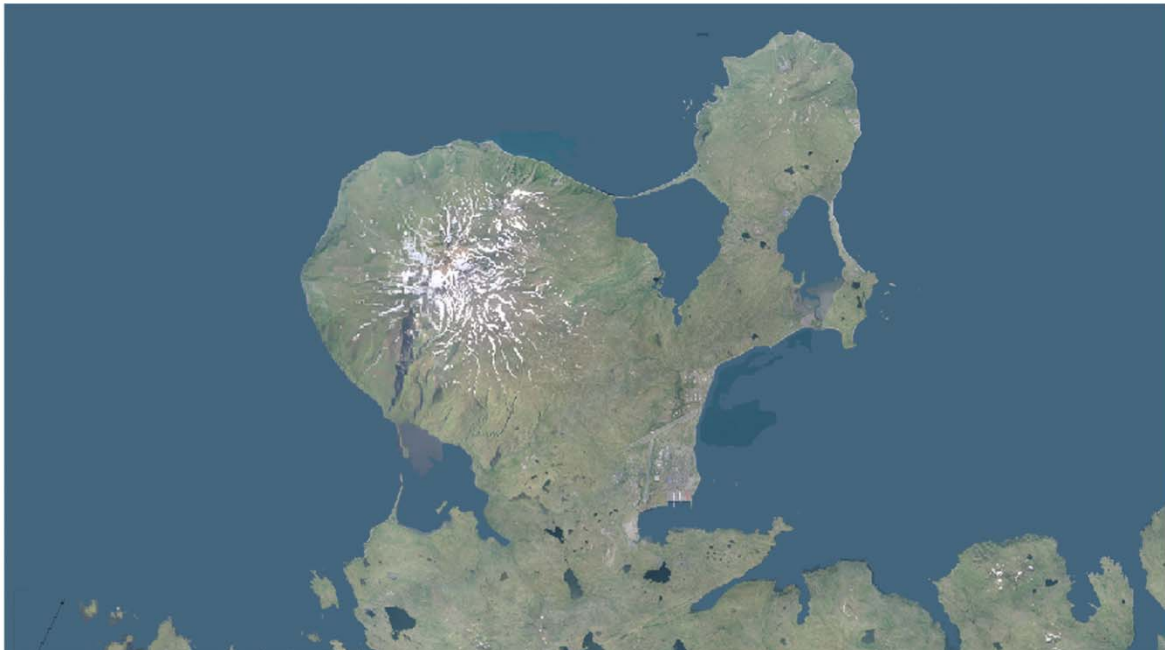
Adak, Alaska

**Department of the Navy**

**Naval Facilities Engineering Command Northwest**

1101 Tautog Circle

Silverdale, WA 98315



## EXECUTIVE SUMMARY

This study invokes the unexploded ordnance (UXO) mobility model (Wilson et al., 2008d) to quantify UXO transport in Andrew Bay by means of numerical hydrodynamic simulation based on bathymetric data, historical information on bottom composition, and historic wave climate records. The physics-based UXO Mobility Model has been demonstrated by the Environmental Security Technology Certification Program (ESTCP) using ground-truth information in a variety of environments under a variety of conditions. Two hypotheses of UXO fate and transport are evaluated with this model: 1) UXO are being transported onto the beach from offshore deposits due to long-period, high-energy waves and wave-induced currents (referred to as the *bottom wind hypothesis*); and, 2) UXO are mixed among the beach deposits of gravels, cobbles, rock and basal conglomerate, and become episodically exposed by erosion and realignment of the beach profile in response to wave climate variation (referred to as the *beach churn hypothesis*). The potential number of UXO types believed to be present in Andrew Bay are too numerous to study each particular type in hydrodynamic simulation. Therefore, a short list of canonical types was evaluated that not only represent UXO types actually recovered by Explosive Ordnance Disposal (EOD) personnel at Andrew Bay, but also spans the size and weight distribution of the potential inventory. Three general types of UXO were selected for presentation herein. The 60 mm and 81 mm mortar rounds were selected for size matching with native beach rock and for relative ease of potential mobility; the 20 mm and 40 mm rounds were selected to represent the high mobility UXO types due to their relative small size and size similarity with the gravels and smaller cobble fractions found at Andrew Bay; and the 2000 lb bomb was chosen due to its high critical shear stress value (i.e., low potential for mobility) and size similarity with the largest fractions of beach rock found at Andrew Bay. These three example categories represent the range of mobility characteristics of the typical UXO found in Andrew Bay.

The hydrodynamic simulations provide support for both the bottom wind hypothesis and the beach churn hypothesis in accounting for fate and transport of UXO at Andrew Bay. In this study, a risk assessment model was adopted that is based on the likelihood of UXO appearing on the beach of the barrier spit at Andrew Bay in response to either of these two hypotheses. The mobility analysis and the initialization of the model are based on a set of simplifying assumptions that maximize this risk and seek the most plausible outcome by the two operative hypotheses (worst-case scenario). An estimate is made of the extent of offshore waters from which UXO can conceivably reach the beach in the future, referred to as the *critical zone*. This critical zone defines the domain where future monitoring efforts should focus search and detection assets. The model simulations are conducted over a 20-year period, and the probabilities of occurrence reported below are for a 20-year simulation. To obtain a 20-year unbroken wave record, it was necessary to loop a continuous 4-year wave record from the National Oceanic and Atmospheric Administration (NOAA) Buoy #46073 five times. (No other longer continuous wave records exist in this region.)

Under the bottom wind hypothesis, the study results are summarized in Tables ES-1 through ES-3, and indicate that 1.5% of the mid-sized UXO population of 60 mm and 81 mm mortar rounds migrates onshore. Only half of that percentage moves more than a distance of 103 m upslope and toward the beach during a period of 20 years of simulation. However, a 0.01% probability of occurrence exists that a 60 mm and 81 mm mortar round might reach the

**Table ES-1. Mobility Results under the Bottom Wind Hypothesis for Mid-sized UXO Population of 60 mm and 81 mm Mortar Rounds**

<b>Transport distance (m)</b>	<b>Onshore Probability</b>	<b>Offshore Probability</b>	<b>Longshore Probability</b>
0-50	0.102827088	6.990824907	0.574729632
50-100	0.692408808	20.97247472	1.300073718
100-50	0.123404736	18.5102476	0.499527436
150-100	0.054838056	13.6535288	0.94422869
200-250	0.123404736	10.47260231	1.067430053
250-300	0.082264728	6.662703894	1.135805234
300-350	0.075415704	4.199597094	0.862094448
350-400	0.068551392	2.67423024	0.759479161
400-450	0.061702368	1.72417476	0.711585025
450-500	0.034275696	0.943897713	0.574729632
500-550	0.013713336	0.690549585	0.547421572
550-600	0.006849024	0.349233357	0.485768375
600-650	0	0.102922677	0.396912149
650-700	0.006849024	0.014074896	0.280537801
700-750	0.013713336	0.007037448	0.164268484
750-800	0.013713336	0	0.061548166
800-850	0.013713336		0.054721151
850-900	0		0.020481045
900-950	0.006849024		0.020481045
950-1000	0		0.01365403
1000-1050	0.027426672		0.020481045
1050-1100	0.006849024		0.006827015
1100-1150	0		0

**Table ES-2. Mobility Results under the Bottom Wind Hypothesis for Small-sized UXO Population of 20 mm and 40 mm Anti-aircraft Rounds**

Transport distance (m)	Onshore Probability	Offshore Probability	Longshore Probability
0-100	0.636285163	5.581539576	1.409154219
100-200	2.004653293	16.71006881	4.261493709
200-300	0.636285163	12.22980793	6.279624648
300-400	0.9988967	6.183140058	7.469815914
400-500	1.197352201	2.031535296	8.441044227
500-600	1.204212094	0.431010252	6.231712509
600-700	0.916818682	0.020729952	4.179550518
700-800	0.855199994	0	2.674572021
800-900	0.793701655		1.72394145
900-1000	0.602106047		0.943913916
1000-1100	0.567926931		0.690919911
1100-1200	0.492588457		0.348818283
1200-1300	0.396790653		0.102540933
1300-1400	0.287393412		0.013881087
1400-1500	0.177875822		0.006716655
1500-1600	0.068478581		0
1600-1700	0.068478581		
1700-1800	0.027319223		
1800-1900	0.027319223		
1900-2000	0.013719786		
2000-2100	0.034179116		
2100-2200	0.020579679		
2200-2300	0.006859893		
2300-2400	0		

**Table ES-3. Mobility Results under the Bottom Wind Hypothesis for Large-sized UXO Population of 2000 lb Bombs**

<b>Onshore Transport (m)</b>	<b>2000 lb bomb Onshore Probability</b>	<b>Offshore Transport (m)</b>	<b>2000 lb bomb Offshore Probability</b>	<b>Longshore Transport (m)</b>	<b>2000 lb bomb Longshore Probability</b>
0-5	0	0-10	22.32599505	0-10	1.314791632
5-10	0.04104	10-20	30.555339	10-20	0.445097972
10-15	0.02052	20-30	20.82816532	20-30	0.1848813
15-20	0.00684	30-40	11.26569478	30-40	0.35608439
20-25	0.00684	40-50	5.766547584	40-50	0.212297844
25-30	0.00684	50-60	2.995659464	50-60	0.1848813
30-35	0.00684	60-70	1.765230124	60-70	0.0616271
35-40	0.00684	70-80	0.889396956	70-80	0.006854136
40-45	0.00684	80-90	0.328437438	80-90	0.089013582
45-50	0	90-100	0.08235157	90-100	0.054772964
50-55	0	100-110	0.047473258	100-110	0.013708272
55-60	0.00684	110-120	0.03390947	110-120	0.013708272
60-65	0	120-130	0	120-130	0.0616271
650-700				130-140	0.006854136
700-750				140-150	0
750-800					

beach over the 20-year period from as far offshore as 1,136 m. A total of 12% of the small-sized UXO population of 20 mm and 40 mm UXO migrate onshore, and 6% move more than a distance of 606 m upslope and toward the beach over a 20-year period of time. A 0.05% probability of occurrence exists that a 20 mm or 40 mm round might reach the beach over a 20-year period from as far offshore as 2,273 m. The critical zone for the 20 mm and 40 mm rounds is the most extensive of any UXO type, so it could be used to delineate the outer boundary of the offshore UXO search area for future monitoring and remediation planning for all UXO at Andrew Bay. Only 0.11% of the large-sized UXO population of 2000 lb bombs migrates onshore, and 0.05% moves more than a distance of 19.2 m upslope and toward the beach over the 20-year period of time. The maximum distance a 2000 lb bomb can move onshore and upslope against gravity is 57.5 m, and its probability of occurrence is only 0.06%. The critical zone of the 2000 lb bomb is within the zone of active seasonal beach profile change, which would be covered by a beach profile monitoring program of the barrier spit beach for future monitoring and remediation planning, as recommended under the beach churn hypothesis. These risk assessment estimates for the bottom wind hypothesis are conditional probabilities based on the assumption that UXO populations are spread uniformly across Andrew Bay. If UXO are concentrated in patches closer to shore, the probability of beaching would be higher; conversely, if populations of UXO are concentrated further offshore, the probabilities would be lower. In addition, the 20-year wave climate data used as input to the simulations are assumed to be representative of future ocean wave activity in this area.

Under the beach churn hypothesis, the risk assessment probability is 3.0% for the likelihood of exposure of 60 mm and 81 mm mortar rounds on the beach of the barrier spit at Andrew Bay. Similar computations for the 20 mm and 40 mm UXO gives a joint probability of 1.5% for exposure on the beach

of the barrier spit, and 0.37% probability of exposure of a 2000 lb bomb. These risk assessments by the beach churn mechanism are based on the assumption that these UXO types are already blended homogeneously among the beach cobble and rock of the barrier spit. The distance offshore to closure depth, where beach profile changes no longer occur, is 1,200 m. Therefore, the critical zone of the beach churn hypothesis looks very much like that for the bottom wind critical zone of the 60 mm and 81 mm mortar rounds. Again, the 20-year wave climate data are assumed to be representative of future environmental forcing.

To improve the analysis results of the bottom wind hypothesis, it is necessary to reduce uncertainties on UXO location, bottom type, bathymetric roughness, and directional wave and current variability. Reducing these uncertainties leads to recommendations already proposed in a previous UXO study at Andrew Bay by Jones and Israel (2002), namely:

- Bathymetric measurements. The Carignan et al. (2009) bathymetry is adequate over the farfield of Andrew Bay, but additional bathymetric surveys to better resolve micro-bathymetry over the critical zone of the inner 2 km of Andrew Bay are needed. When converted to digital formats, this critical zone bathymetry should provide at least 10 m horizontal resolution of bottom roughness features.
- Directional wave measurements in Andrew Bay. Bottom-mounted, self-recording acoustic Doppler current profilers (ADCPs) could provide these measurements. A single ADCP with a co-located pressure sensor mounted at closure depth (28 m) could provide the first three moments of the shoaling wave direction spectra. A shore parallel line array of four such sensors at 50 m spacing could resolve the complete direction spectra.
- Current measurements in Andrew Bay. These measurements could be provided by the bottom-mounted ADCP measurements described above, augmented by a deep water monitoring site at the outer edge of the critical zone, 2 km offshore of the barrier spit. This deep water mooring would require an ADCP mounted to a clump weight with acoustic release, as it would be located at about 100 m depth, below operational depth of most divers.
- Sediment samples collected throughout Andrew Bay to characterize the bottom.
- UXO underwater survey using towed array magnetometers.

Improvements to the analysis results of the beach churn hypothesis require improved information on the resident UXO population numbers, types, and spatial distribution, beach aggregate size distribution, seasonal beach profile change, and directional wave and current variability. These improvements can be achieved by implementing the following recommendations, some of which are included above:

- Higher resolution bathymetric measurements, shoreward of closure depth (inside the 30 m isobath), as described above under additional bottom wind measurements.
- Shoaling wave measurements with bottom-mounted ADCPs, as described above under additional bottom wind measurements.
- Beach profile surveys in both summer and winter.
- Samples of beach aggregate and follow-on size and roundness analysis. Electro-magnetic or magnetic gradiometer surveys to detect and classify UXO blended in the beach deposits of the barrier spit. These types of land surveys have demonstrated extremely

high probabilities of detection ( $P_d$ ) and classification ( $P_c$ ) of UXO and fragments under ESTCP-sponsored programs. The equipment would require large diameter wheeled or tracked vehicles for adequate mobility and maneuverability over the beach rock and cobble fields on the beach of the barrier spit at Andrew Bay.

Offshore surveys of bottom composition based on collecting sediment samples would provide the greatest cost-benefit to evaluating the bottom wind hypothesis because it would resolve the question concerning the movable bottom versus rigid bottom formulation of the UXO mobility model in the offshore domain. Samples of beach aggregate with follow-on size and roundness analysis, combined with electro-magnetic or magnetic gradiometer surveys to detect and classify UXO blended in the beach deposits of the barrier spit, would provide the greatest cost-benefit to evaluating the beach churn hypothesis because such studies would resolve the long-term persistence of this UXO exposure mechanism.

## CONTENTS

EXECUTIVE SUMMARY .....	ii
APPENDICES .....	ii
FIGURES .....	ii
TABLES .....	v
ACRONYMS AND ABBREVIATIONS .....	vi
Section 1.0: INTRODUCTION .....	1
Section 2.0: SITE PARAMETERS AND MODEL INPUT FOR ANDREW BAY .....	4
2.1 Climate .....	4
2.2 Beach and Bottom Composition .....	6
2.2.1 Modeling Choices Related to Bottom Composition .....	7
2.3 Tides and Currents .....	10
2.4 Wave Climate.....	10
2.4.1 Modeling Choices Related to Wave Climate .....	11
2.5 UXO Types in Andrew Bay.....	15
Section 3.0: UXO MOBILITY MODELING .....	18
3.1 Technology.....	18
3.2 Technology Description .....	18
3.3 Wave Refraction/Diffraction Analysis.....	27
3.4 Bar-Berm and Shore Rise Profile Modeling .....	33
3.5 Hydrodynamic UXO Mobility Simulation.....	35
Section 4.0: RISK ASSESSMENT .....	59
4.1 Risk Assessment of Bottom Wind Hypothesis .....	59
4.2 Risk Assessment of Beach Churn Hypothesis .....	62
Section 5.0: RECOMMENDATIONS FOR FUTURE WORK .....	65
Section 6.0: REFERENCES .....	66

## APPENDICES

APPENDIX A: UXO Types in Andrew Bay	
APPENDIX B: Photographs and Engineering Drawings of Each Ordnance Type Found in the Canonical Listing in Table 2-2	
APPENDIX C: Combined Peer Review Comments and Author Responses	

## FIGURES

Figure 1-1. Adak Island Location Map .....	1
Figure 1-2. Digital Bathymetry, Farfield Adak Island, AL.....	2
Figure 1-3. Digital Bathymetry, Nearfield Adak Island, AL .....	3
Figure 2-1. Andrew Bay Area Showing Predominantly Natural, Undisturbed Land.....	5

Figure 2-2.	Area of Munitions Recovered along Andrew Lake Seawall (hatched green area), and Offshore Extent of Underwater Survey (blue dashed line) by EOD Personnel 1962-1964.....	6
Figure 2-3.	Size Distribution of Beach Rock, Cobble and Gravels Found on the Barrier Spit of Andrew Bay.....	8
Figure 2-4.	Proxy Offshore Grain Size Distribution of Shells, Sands, and Gravels from UXO Mobility Experiments Conducted at Ocean Shores, WA.....	10
Figure 2-5.	Location of NOAA Wave Buoys for Developing Wave Forcing Records for Andrew Bay UXO Mobility Modeling.....	11
Figure 2-6.	Historic Wave Record Measured by NOAA Buoy #46073 in the Southeast Bering Sea (2005-2009).....	13
Figure 2-7.	Histograms and Cumulative Probability: (a) of Wave Height; (b) Wave Period as Derived from the 1985-2011 Period of Record for NOAA Buoy #46035 (green) Compared with the 2005-2009 Period of Record for NOAA Buoy #46073 (pink).....	14
Figure 2-8.	Historic Wave Record Measured by NOAA Buoys #46073 and #46035 in the Southeast Bering Sea (2005-2009).....	15
Figure 2-9.	EOD Personnel with Recovered UXO on the Beach at Andrew Bay circa 1962.....	17
Figure 3-1.	Architecture to the Vortex Lattice UXO Mobility Model.....	20
Figure 3-2.	Computational Control Cells and Farfield Movable Boundary Conditions Used in the Vortex Lattice Computational Methodology: (a) Accretion/Erosion Wave; (b) Coupled Control Cells; and (c) Profile Changes.....	21
Figure 3-3.	Mechanics of Farfield Burial: (a) Envelope of Profile Change Gives Critical Mass; (b) Volume of Critical Mass from Elliptic Cycloids; and (c) Cross Shore Variation in Critical Mass Thickness.....	23
Figure 3-4.	Vortex Lattice Method: (a) Lattice and Horseshoe Vortex System; (b) Horseshoe Vortices Inducing Sediment Transport in Nature.....	24
Figure 3-5.	(a) Image Method for Vortex Induced Velocity at any Point near the Bed (image plane) Due to Horseshoe Vortex System of an Arbitrary Lattice Panel; (b) Schematic in the Cross-wake Plane of a Pair of Vortex Filaments Trailing out of the Page.....	25
Figure 3-6.	Moment Balance for Threshold of UXO Movement in Response to Reaction Forces Generated by Trailing Vortex Filaments.....	26
Figure 3-7.	Refraction/Diffraction Pattern of the Five Largest Storms at Andrew Bay (2005-2009).....	29
Figure 3-8.	Refraction/Diffraction Pattern of the Five Largest Storms at Andrew Bay (2005-2009).....	30
Figure 3-9.	Refraction/Diffraction Pattern of the Five Largest Storms at Andrew Bay (2005-2009).....	31
Figure 3-10.	Refraction/Diffraction Pattern of the Five Largest Storms at Andrew Bay (2005-2009).....	32
Figure 3-11.	Refraction/Diffraction Pattern of the Five Largest Storms at Andrew Bay (2005-2009).....	33
Figure 3-12.	Simulated Shore Rise/Bar-berm Cross Sectional Profile of the Barrier Spit at Andrew Bay.....	35
Figure 3-13.	Simulation of Flow Divergence Induced over 60 mm Mortar UXO by the Expansion and Contraction of Near Bed Flow Field over High and Low Spots in the Bottom Micro-bathymetry of Andrew Bay.....	37
Figure 3-14.	Vertical Velocity Profile over a 60 mm Mortar Round Resting on an Irregular Sloping Bottom at Andrew Bay.....	38

Figure 3-15.	60 mm Mortar Round Resting on an Irregular Sloping Bottom at Andrew Bay: (a) Pressure Distribution; and (b) Shear Stress Distribution.....	39
Figure 3-16.	Upgraded UXO Mobility Model Simulation of Local Flow Field around a 2000 lb Bomb UXO Resting on Hard Sloping Substrate with no Burial (rigid bottom formulation).....	41
Figure 3-17.	Mechanics of UXO Downslope Migration Progression.....	42
Figure 3-18.	Probability Density Function (red) and Cumulative Probability (blue) for Onshore Transport of 60 mm and 81 mm UXO at Andrew Bay; Based on Rigid Bottom Formulation in the Offshore Domain (seaward of the 30 m depth contour) .....	43
Figure 3-19.	Probability Density Function (red) and Cumulative Probability (blue) for Longshore Transport of 60 mm and 81 mm UXO at Andrew Bay; Based on Rigid Bottom Formulation in the Offshore Domain (seaward of the 30 m depth contour) .....	44
Figure 3-20.	Probability Density Function (red) and Cumulative Probability (blue) for Offshore Transport of 60 mm and 81 mm UXO at Andrew Bay; Based on Rigid Bottom Formulation in the Offshore Domain (seaward of the 30 m depth contour) .....	45
Figure 3-21.	A Simulation of Flow Divergence Induced over 20 mm and 40 mm UXO by the Expansion and Contraction of near Bed Flow Field over High and Low Spots in the Bottom Micro-bathymetry of Andrew Bay .....	47
Figure 3-22.	20 mm UXO Resting on an Irregular Sloping Bottom at Andrew Bay: (a) Pressure Distribution; and (b) Shear Stress Distribution .....	48
Figure 3-23.	40 mm UXO Resting on an Irregular Sloping Bottom at Andrew Bay: (a) Pressure Distribution; and (b) Shear Stress Distribution .....	49
Figure 3-24.	Probability Density Function (red) and Cumulative Probability (blue) for Onshore Transport of 20 mm and 40 mm UXO at Andrew Bay; Based on Rigid Bottom Formulation in the Offshore Domain (seaward of the 30 m depth contour) .....	50
Figure 3-25.	Probability Density Function (red) and Cumulative Probability (blue) for Longshore Transport of 20 mm and 40 mm UXO at Andrew Bay; Based on Rigid Bottom Formulation in the Offshore Domain (seaward of the 30 m depth contour) .....	51
Figure 3-26.	Probability Density Function (red) and Cumulative Probability (blue) for Offshore Transport of 20 mm and 40 mm UXO at Andrew Bay; Based on Rigid Bottom Formulation in the Offshore Domain (seaward of the 30 m depth contour) .....	52
Figure 3-27.	Simulation of Nearbed Flow over a 2000 lb UXO Bomb Resting on an Irregular Sloping Bed at Andrew Bay .....	54
Figure 3-28.	2000 lb UXO Bomb Resting on an Irregular Sloping Bottom at Andrew Bay: (a) Pressure Distribution; and (b) Shear Stress Distribution.....	55
Figure 3-29.	Probability Density Function (red) and Cumulative Probability (blue) for Onshore Transport of a 2000 lb UXO Bomb at Andrew Bay; Based on Rigid Bottom Formulation in the Offshore Domain (seaward of the 30 m depth contour) .....	56
Figure 3-30.	Probability Density Function (red) and Cumulative Probability (blue) for Longshore Transport of a 2000 lb UXO Bomb at Andrew Bay; Based on Rigid Bottom Formulation in the Offshore Domain (seaward of the 30 m depth contour) .....	57
Figure 3-31.	Probability Density Function (red) and Cumulative Probability (blue) for Offshore Transport of a 2000 lb UXO Bomb at Andrew Bay; Based on Rigid Bottom Formulation in the Offshore Domain (seaward of the 30 m depth contour) .....	58
Figure 4-1.	Critical Zone Mapping (red) for the 60 mm and 81 mm Mortar Rounds.....	61
Figure 4-2.	Critical Zone Mapping (red) for the 20 mm and 40 mm Rounds.....	62
Figure 4-3.	Critical Zone Mapping (red) for the 2000 lb Bomb .....	64

**TABLES**

Table ES-1. Mobility Results under the Bottom Wind Hypothesis for Mid-sized UXO Population  
of 60 mm and 81 mm Mortar Rounds..... iii

Table ES-2. Mobility Results under the Bottom Wind Hypothesis for Small-sized UXO Population  
of 20 mm and 40 mm Anti-aircraft Rounds..... iv

Table ES-3. Mobility Results under the Bottom Wind Hypothesis for Large-sized UXO Population  
of 2000 lb Bombs..... v

Table 2-1. Size Distribution of Beach Rock, Cobble and Gravels from a Composite Sample of the  
Beach of Barrier Spit of Andrew Bay..... 9

Table 2-2. Canonical Listing of Ordnance Recovered on the Beach at Andrew Bay ..... 16

Table 4-1. Residence Probability from Native Size Distribution and Effective Diameter of UXO..... 63

## ACRONYMS AND ABBREVIATIONS

ADCP	acoustic Doppler current profiler
EOD	Explosive Ordnance Disposal
ESTCP	Environmental Security Technology Certification Program
MSL	mean sea level
NOAA	National Oceanic and Atmospheric Administration
Pc	probability of classification
Pd	probability of detection
PEM	parabolic equation method
UXO	unexploded ordnance

## Section 1.0: INTRODUCTION

This study was prepared to assess fate and transport of unexploded ordnance (UXO) in the offshore vicinity of Andrew Bay on Adak Island in the Aleutian Island chain of Alaska (Figure 1-1). This report builds on information compiled in a previous study by Jones and Israel (2002). Andrew Bay is located on the northern side of Adak Island (Figures 1-2 and 1-3). The UXO has been routinely collected from the Andrew Bay beach since 1962, particularly after large winter storms. The continuous collection of UXO by explosive ordnance disposal (EOD) personnel from the beach over intervening years presents two hypotheses of UXO fate and transport: 1) UXO are being transported onto the beach from offshore deposits due to long-period, high-energy waves and wave-induced currents (referred to as the *bottom wind hypothesis*; or 2) UXO are mixed among the beach deposits of gravels, cobbles, rock and basal conglomerate, and become episodically exposed by erosion and realignment of the beach profile in response to wave climate variation (referred to as the *beach churn hypothesis*). The goal of the current study is to invoke the Environmental Security Technology Certification Program (ESTCP)-certified UXO mobility model (Wilson et al., 2008d) to quantify UXO transport in Andrew Bay by means of numerical hydrodynamic simulation based on bathymetric data and historic wave climate records. The probability statistics derived from the hydrodynamic transport simulations give a measure of the likelihood of either of these two possible fate and transport hypotheses.

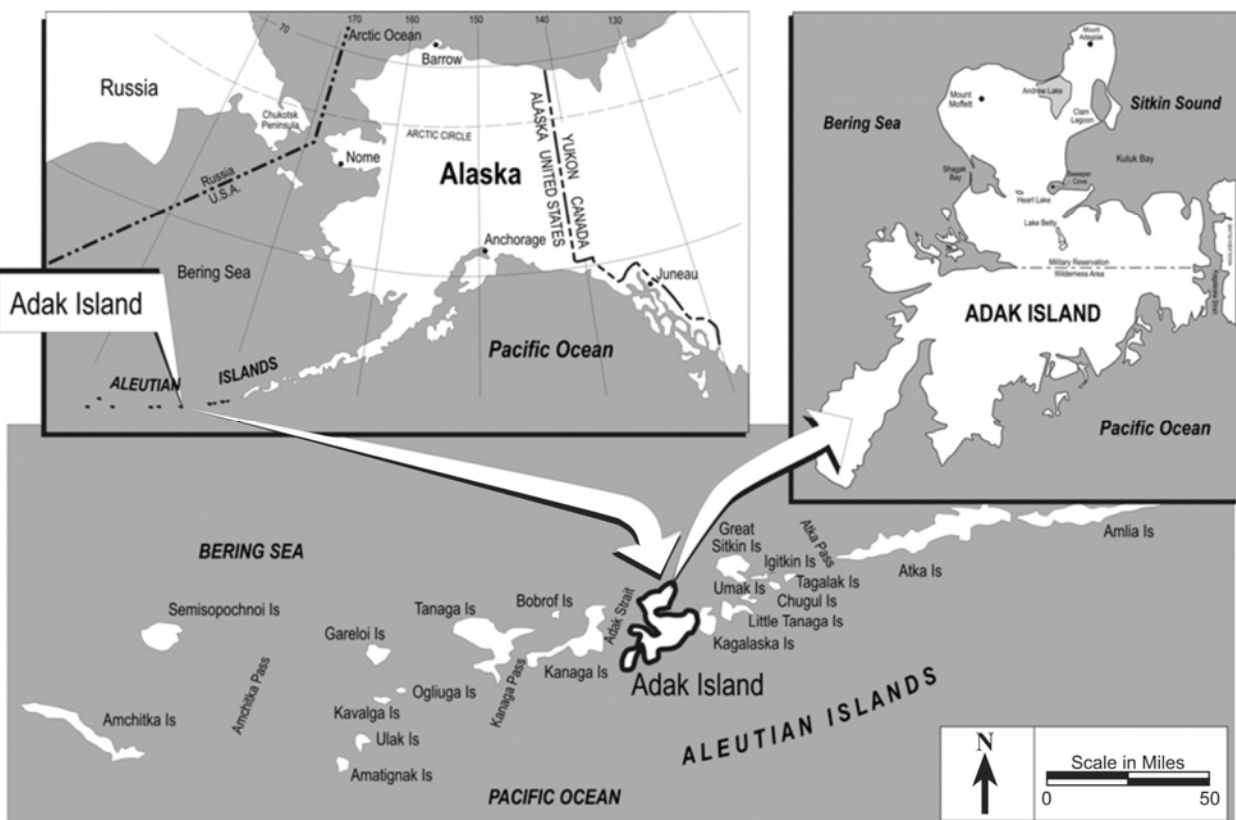
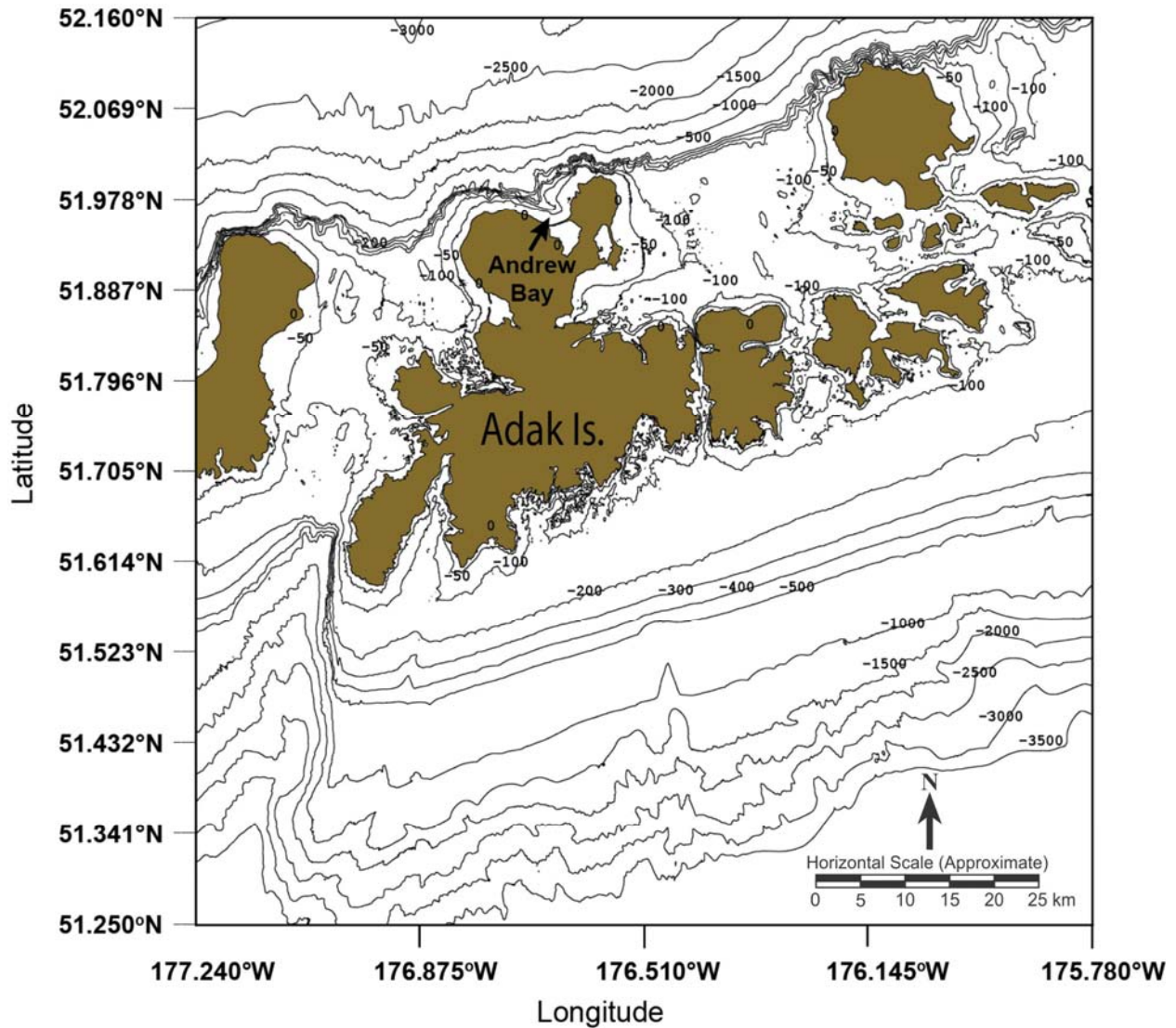


Figure 1-1. Adak Island Location Map

(from Jones and Israel, 2002)



**Figure 1-2. Digital Bathymetry, Farfield Adak Island, AL**

(Depth contours in mean sea level [MSL] datum at 500 m intervals from -3000 m through -500 m MSL; at 100 m intervals from -500 through -100 m MSL; and at 50 m intervals, from 0 m MSL to -100 m MSL. [digital data from Carignan et. al., 2009])

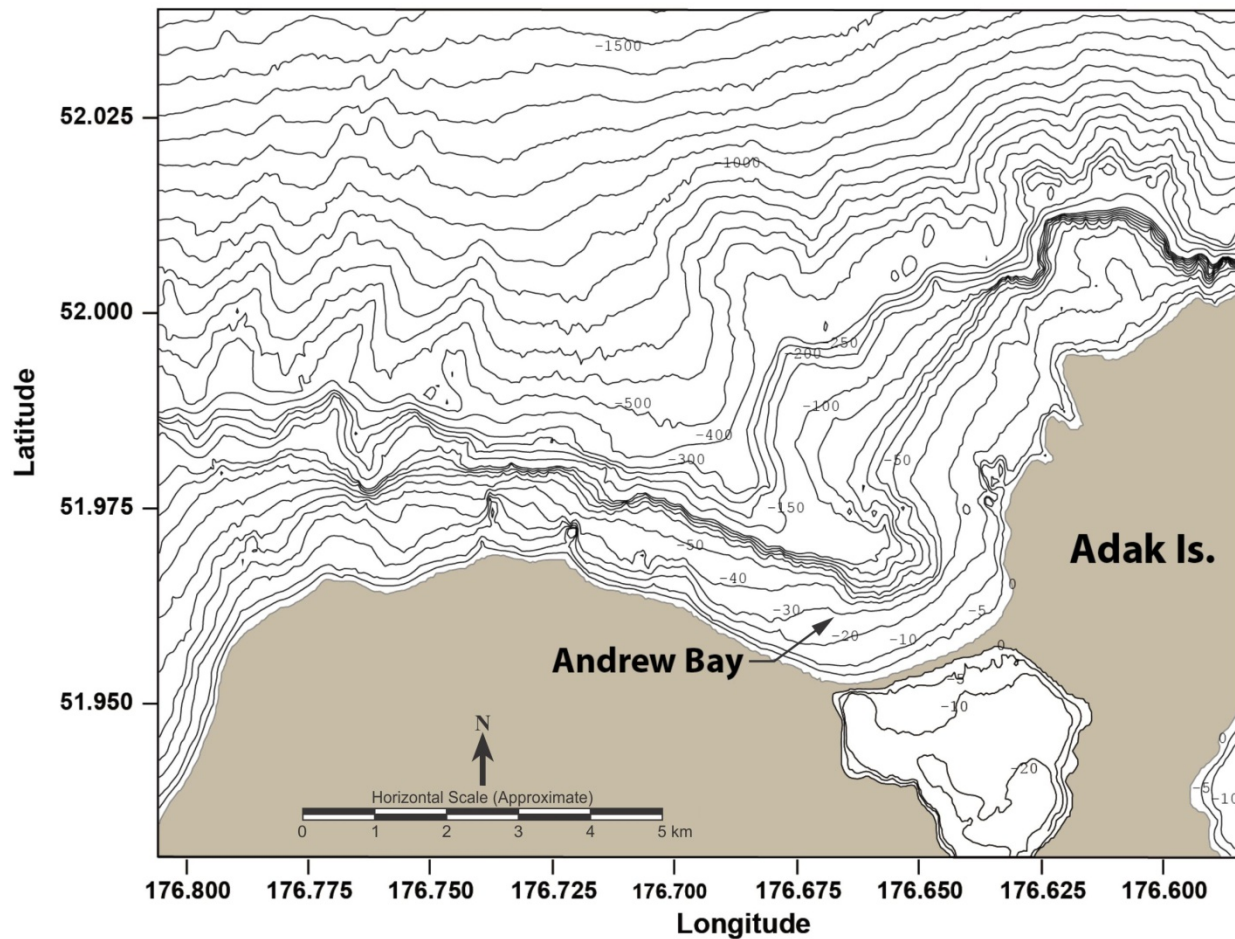


**Figure 1-3. Digital Bathymetry, Nearfield Adak Island, AL**

(Depth contours at 100 m intervals from -2000 through -300 m MSL; at 50 m intervals from -300 m through -50m MSL; at 10 m intervals from -50 m through -10 m MSL, and at -5 m intervals to 0 m MSL. [digital data from Carignan et. al., 2009])

This report is organized into five main sections. Section 2.0 reviews the UXO physical characteristics and environmental characteristics of Andrew Bay. Section 3.0 details the numerical hydrodynamic model used in the analysis of UXO mobility and presents the analysis and results of UXO mobility under various environmental conditions in the Bay. Section 4.0 presents the risk assessment of UXO mobility, identifying critical areas along Andrew Bay where transport of several canonical UXO types is likely, and Section 5.0 details the recommendations for future work in Andrew Bay.

## **Section 2.0: SITE PARAMETERS AND MODEL INPUT FOR ANDREW BAY**

Adak Island is located approximately 1,300 air miles southwest of Anchorage, Alaska, in the Aleutian Island chain. Its geographic position is  $176.045^{\circ}$  W and  $51.45^{\circ}$  N. At 725 square kilometers (280 square miles) in area, it is the largest of the group of the Aleutian Islands (Figures 1-1 and 1-2). Andrew Bay is located on the northwest shore of Adak Island. The Bay is approximately 7.6 km (4.75 miles) wide, extending from Acorn Rock on the west side to a Loran station at the base of Mount Adagdak (Figures 1-3 and 2-1). The beach is centrally located on the coast of the Bay and is bounded on either side by headlands with large rock reefs. The shoreward side of the beach is bordered by a 3.2-km (2-mile) long seawall. The seawall is a narrow area described as an elongated dike made up of boulders, cobble, and gravel with a dirt road running along the top (Foster Wheeler Environmental Corporation, 2000) and borders Andrew Lake inshore (Figure 2-2).

The beach of the barrier spit that bounds the central portion of the Bay is comprised of primarily cobble and boulder material with an estimated average size of 10 to 25 cm diameter (Section 2.4). The beach also contains many larger boulders. This material extends out to the extent of the visual surveys (30 m depth [Jones and Israel, 2002]; Figures 1-3 and 2-2). Kelp beds extend out hundreds of meters from the beach of the barrier spit and also border the east and west side of the barrier beach during the summer months (communication with EOD personnel [Jones and Israel, 2002]). Digital bathymetry of Andrew Bay at 1 arc-second resolution was obtained online and referenced as a technical memorandum from the National Geophysical Data Center, Marine Geology and Geophysics Division, Boulder, Colorado (see Carignan et al., 2009). This database was the primary source of bathymetric data used to initialize the UXO mobility model, and a bathymetric map of the nearfield Adak Island, AL, around Andrew Bay is shown in Figure 1-3.

### **2.1 Climate**

Adak Island experiences a polar maritime climate characterized by persistently overcast skies, high winds, frequent and often violent storms, and a narrow range of temperature fluctuation throughout the year. Adak is located in the region of the polar front, the zone of convergence between temperate westerly winds (which actually blow from the southwest at this latitude) and the polar easterly winds. In this area of the Aleutian Islands, this confluence of air masses creates a semi-permanent low pressure zone, particularly strong in winter, which generates the frequent low pressure (cyclonic) storms characteristic of the North Pacific region. Weather on the island can be very localized; fog, low ceilings, precipitation, and clear weather are all possible within a distance of a few miles. Storms occur during all seasons; however, the most frequent and severe storms occur in the winter. Wind conditions on Adak are controlled by the following:

- Position of the polar front
- Atmospheric pressure gradient
- Position of low (and occasionally high) pressure centers with respect to the island.

The polar front separates the southwest winds of the temperate prevailing westerlies from the northeast winds of the Arctic easterlies. The polar front is most often located north of the Aleutians, which is reflected in the dominance of southwest to west-southwest winds that comprise nearly 30 percent of both the frequency and magnitude of winds on Adak.



**Figure 2-1. Andrew Bay Area Showing Predominantly Natural, Undisturbed Land**  
(from Jones and Isreal, 2002)

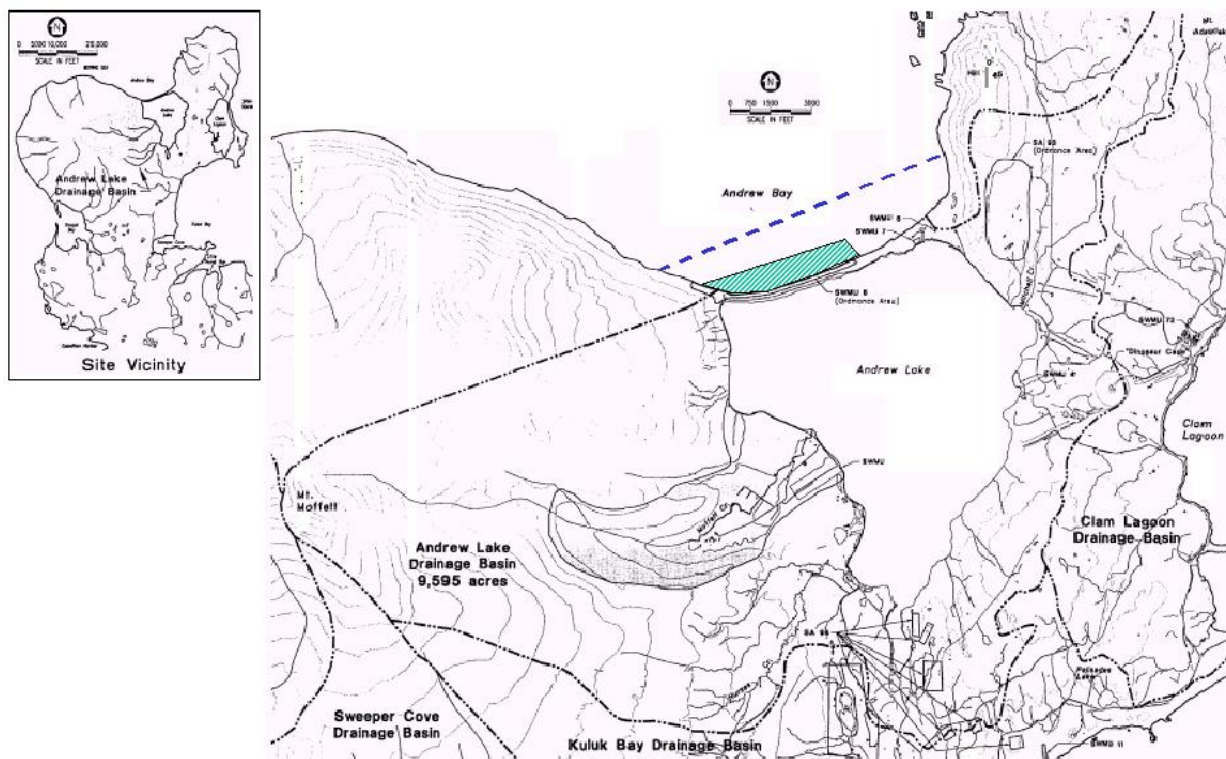


**Figure 2-2. Area of Munitions Recovered along Andrew Lake Seawall (hatched green area), and Offshore Extent of Underwater Survey (blue dashed line) by EOD Personnel 1962-1964 (from Jones and Israel, 2002)**

The polar front is also the source of a persistent zone of low atmospheric pressure, the Aleutian Low, which is situated over the North Pacific and Bering Sea. The Aleutian Low, in turn, generates frequent cyclonic disturbances that form in the area. Most frequently, storm centers pass north and then east of Adak, and the winds, drawn into the low pressure center in a counterclockwise pattern, shift from southwest through northeast as this happens. This accounts for nearly 68 percent of the wind distribution with time on Adak, though the prevailing southwesterly flow during non-storm events accounts for a significant portion of that number.

Wind conditions are typified by local shifts and rapid changes in velocity. Average wind velocity is 12 knots, with gusts in excess of 100 knots recorded during winter storms. High winds are also frequent during the summer months, with gusts over 50 knots not uncommon.

## 2.2 Beach and Bottom Composition

A cobble/rock barrier spit (Figure 2-1) spans between the headlands of Andrew Bay, partitioning Andrew Cove from Andrew Bay (Figure 2-2). This cobble/rock spit is referred to as *the beach* and is the primary search and recovery area of the numerous UXO clean-up sweeps conducted by

the EOD. Because of the extremely high energy wave climate incident on Andrew Bay, this barrier spit is not a typical sandy beach formation, but rather a steeply sloping rubble mound consisting of very coarse gravels, cobble and beach rock that have been significantly rounded by constant wave induced rolling motion. Figure 2-3 and Table 2-1 provide a size distribution of the gravels and beach rock that comprise this barrier spit. This size distribution was derived from one composited sample (blended from an unspecified number of sub-samples) of the beach deposits of the barrier spit at Andrew Bay (Carignan et al., 2009). By weight approximately 5% of the aggregate comprising the barrier spit are gravels, 7% are cobbles, and 88% are beach rock. The median size of the barrier spit material is 25-cm diameter beach rock, and some of the largest beach rock found in the rubble mound formation of the spit is 82 cm in diameter. Consequently, the preponderance of the native beach rock in the barrier spit is comparable in size to moderate to large UXO, although the beach rock is significantly more rounded in shape than the paraboloids of revolution typical of UXO ordnance (Figure 2-4). Regardless of shape differences, this size similarity would tend to promote “blending” of the UXO with the native aggregate, as opposed to more typical scour/burial behavior found at most UXO sites, where UXO are very large relative to the sediment grain sizes. The beach rock at Andrew Bay is also well sorted, with 68% of the total aggregate of the barrier spit sized between 20 cm and 50 cm in diameter. This suggests that the native beach rock, cobble and gravel have been subjected to significant hydraulic weathering typical of wave action. However, the beach rock, cobbles and gravels of the barrier spit are fluvial in origin, from five drainage basins, namely, the central Andrew Bay drainage basin, the Clam Lagoon drainage basin to the east, and the Kuluk Bay, Sweeper Cove, and Shagak Bay drainage basins to the south and west. Currently, the area surrounding Andrew Bay is predominantly natural, undisturbed land (Figures 2-1 and 2-2).

**2.2.1 Modeling Choices Related to Bottom Composition.** The presence of kelp beds extending hundreds of meters offshore from the barrier spit, and also bordering the east and west side of the barrier spit (Section 2.0), is significant in relation to bottom composition of the offshore regions of Andrew Bay. Kelp only roots on rocky, hard bottom substrate, and generally does not recruit in water depths deeper than 20 m to 30 m due to depth attenuation of ambient light, particularly along high-latitude, high-energy coastlines. The National Oceanic and Atmospheric Administration (NOAA) charts generally confirm the observations of kelp beds along the east and west shorelines of the bay extending offshore to the 30 m isobath, with patches of shells, sands, and gravels in the areas further offshore (Jones and Israel, 2002). Detailed surveys of the sediment cover have not been attempted in the offshore areas of Andrew Bay, nor are any grain size distributions of offshore sedimentary deposits known to exist.

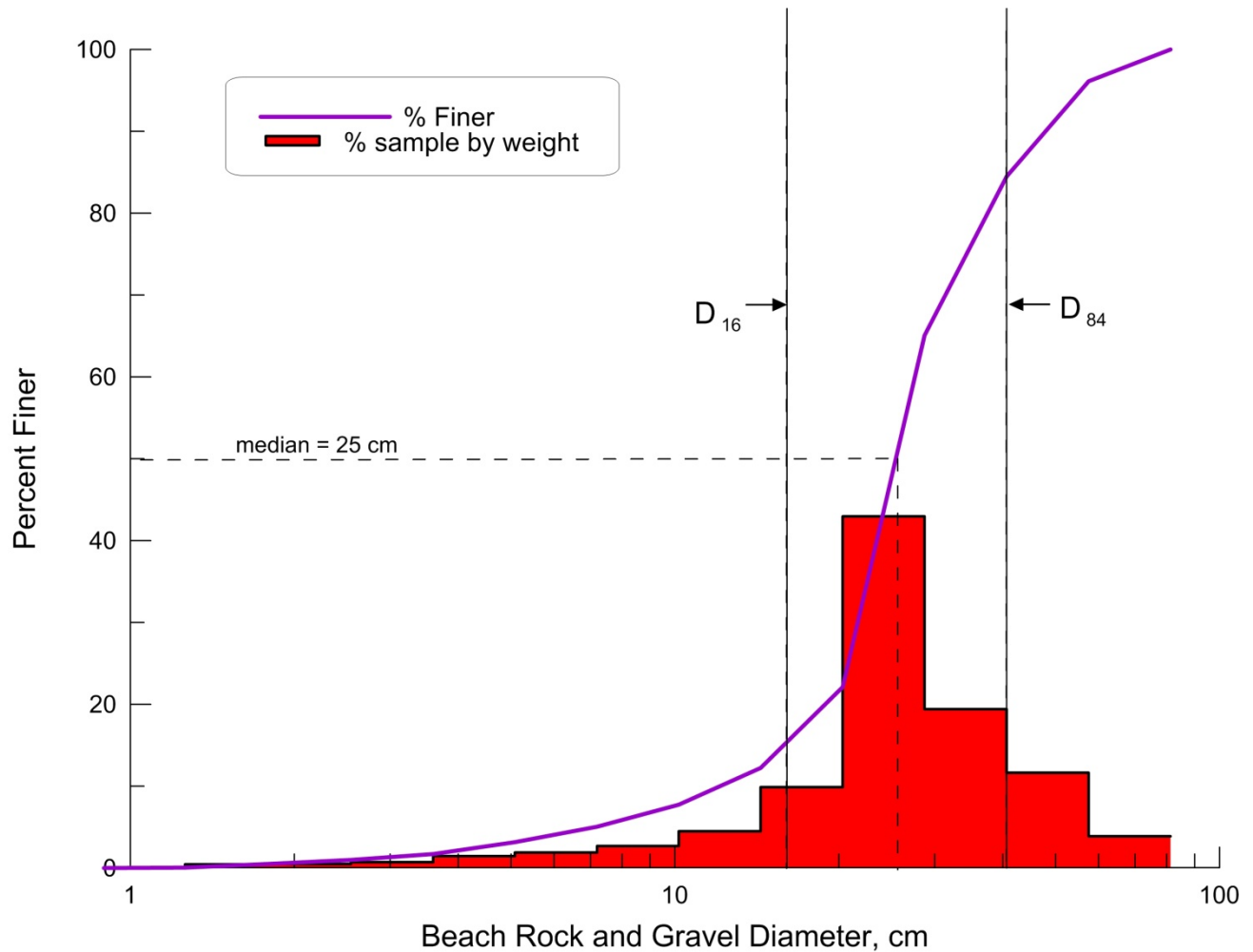


**Figure 2-3. Size Distribution of Beach Rock, Cobble and Gravels Found on the Barrier Spit of Andrew Bay** (derived from Carignan et al., 2009)  
 (Probability density in red, cumulative probability in purple based on one composite beach sample.)

Based on this limited information, the initialization of the UXO mobility model is confronted with a conundrum, namely, choosing a *moveable bottom* formulation based on sedimentary bottom deposits everywhere versus a *rigid bottom* formulation where the bottom is assumed to be bare bedrock offshore of the beach deposits of the barrier spit. The initialization of the UXO mobility model is based on the choice of bottom composition that separately maximizes risk and seeks the most plausible outcome by either of these two hypotheses. When evaluating risk associated with the beach churn hypothesis, it is assumed that the size distribution of the beach rock, cobble and gravel in Figure 2-3 and Table 2-1 persists between the beach of the barrier spit and the 30 m depth contour; the estimated seaward limit of barrier spit deposits is based on EOD communications of visual surveys during UXO sweeps reported in Jones and Israel (2002; Section 2.0 and Figure 2-2, blue dashed line).

**Table 2-1. Size Distribution of Beach Rock, Cobble and Gravels from a Composite Sample of the Beach of Barrier Spit of Andrew Bay**

Bin #	Size Range (cm)	Mass (kg)
1	0.5 – 0.9	0
2	0.9 – 1.3	0
3	1.3 – 1.8	102
4	1.8 – 2.5	102
5	2.5 – 3.6	136
6	3.6 – 5.1	272
7	5.1 – 7.2	374
8	7.2 – 10.2	510
9	10.2 – 14.4	850
10	14.4 – 20.3	1,903
11	20.3 – 28.7	8,292
12	28.7 – 40.7	3,738
13	40.7 – 57.5	2,243
14	57.5 – 81.3	748

(Carignan et al., 2009)

Sample mass inferred from percent weight statistics assuming dry bulk density for granitic rock and cobble specimens.

Bottom roughness in this inshore domain is taken as half the median size fraction of the beach deposits on the barrier spit, from bin #7 in Table 2-1, or 0 (12 cm). Offshore of the 30 m depth contour, it is assumed under the beach churn hypothesis that a coarse-sand and gravel bottom type exists based on a proxy grain size distribution adopted from a high energy coast at Ocean Shores, WA (Figure 2-4), where sediment deposits consisted of “shells, sands, and gravels” and where the first UXO mobility experiments were conducted in 2005 (Wilson and Jenkins, 2005). Median grain size of this proxy grain size distribution in Figure 2-4 is 384 microns (according to percent by weight), and roughness is based on scour bedform parameters 0 (5 cm). This assumption (*movable bottom* formulation) maximizes comingling of offshore UXO with the deposits of the barrier spit by sorting mechanisms. In evaluating risk associated with the bottom wind hypothesis, the same bottom composition assumption is made inshore of the 30 m depth contour, but a barren, bedrock bottom seaward of the 30 m depth contour is assumed. This assumption (the *rigid bottom* formulation) maximizes shoreward transport of UXO due to the hydrodynamic forces of shoaling waves and currents acting directly on UXO that are always exposed on solid bedrock in the offshore domain. Under the rigid bottom formulation, bottom roughness in the offshore domain consists of faceted plane surfaces defined by the resolution of the digital bathymetry data base, 0 (30 m), in the horizontal for each facet.

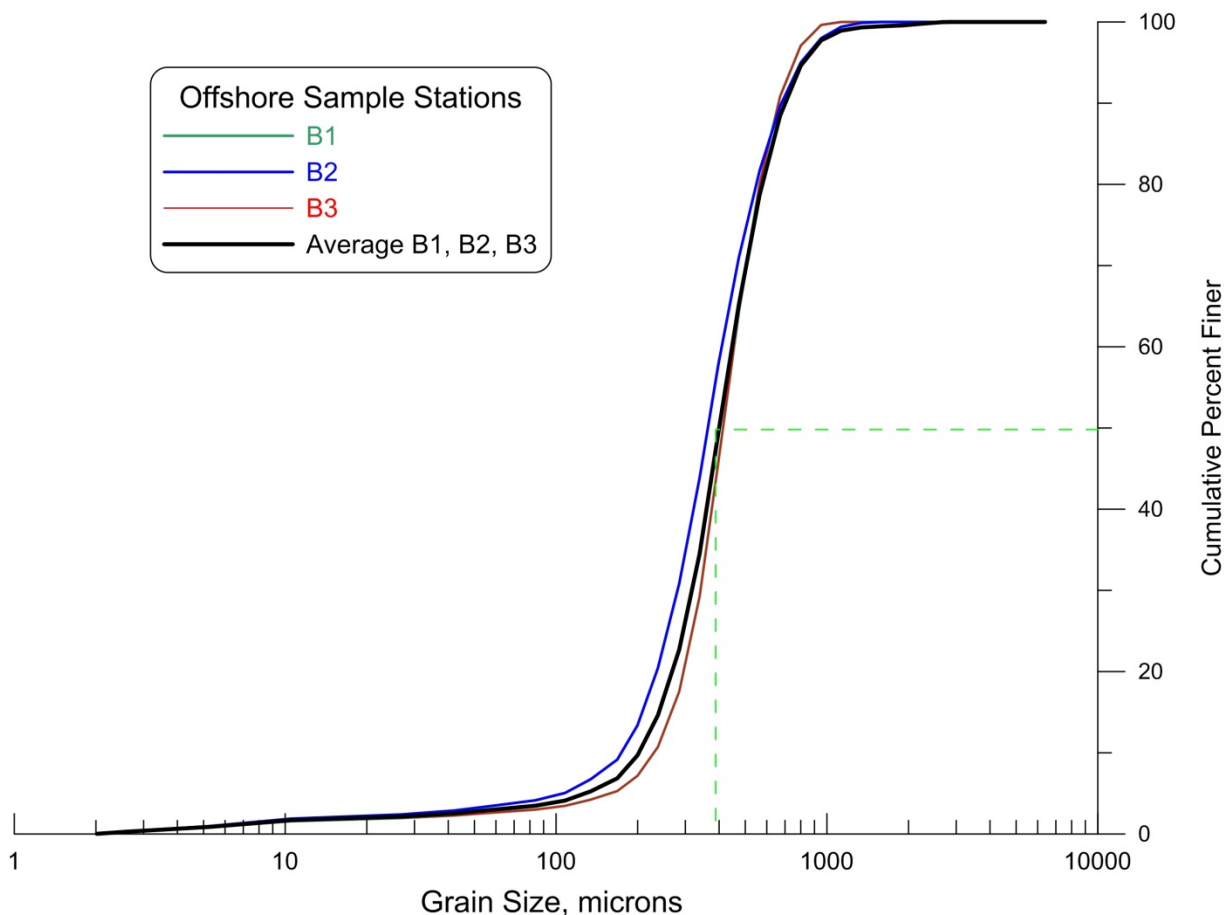


**Figure 2-4. Proxy Offshore Grain Size Distribution of Shells, Sands, and Gravels from UXO Mobility Experiments Conducted at Ocean Shores, WA**  
(after Wilson and Jenkins, 2005)

### 2.3 Tides and Currents

Andrew Bay is a north-facing coastal embayment, exposed to the full range of ocean tides, currents, and waves. Steady winds and thermal mixing can influence minor, temporary currents in Andrew Bay. However, the major influence on the dynamic environment at Andrew Bay is from wind-driven waves that are generated in the Bering Sea. There are data available on tides at Sweeper Cove, and predicted currents in the area of Adak Strait, however there are no data available of the tides and currents around Andrew Bay.

### 2.4 Wave Climate

Waves generally approach Andrew Bay from the north-northwest (Figure 2-5 obtained from NOAA/National Centers for Environmental Prediction Wave Watch III model). There were no data available on wave conditions at Andrew Bay for the UXO modeling effort. Wave data were available from NOAA Buoy Stations #46073 and #46035, (Figure 2-5). While Buoy #46035 has the longest period of record accounting for 10% of the total record length, seven of those data gaps are longer than 1 month, and three of these data gaps are a half-year or more in length.

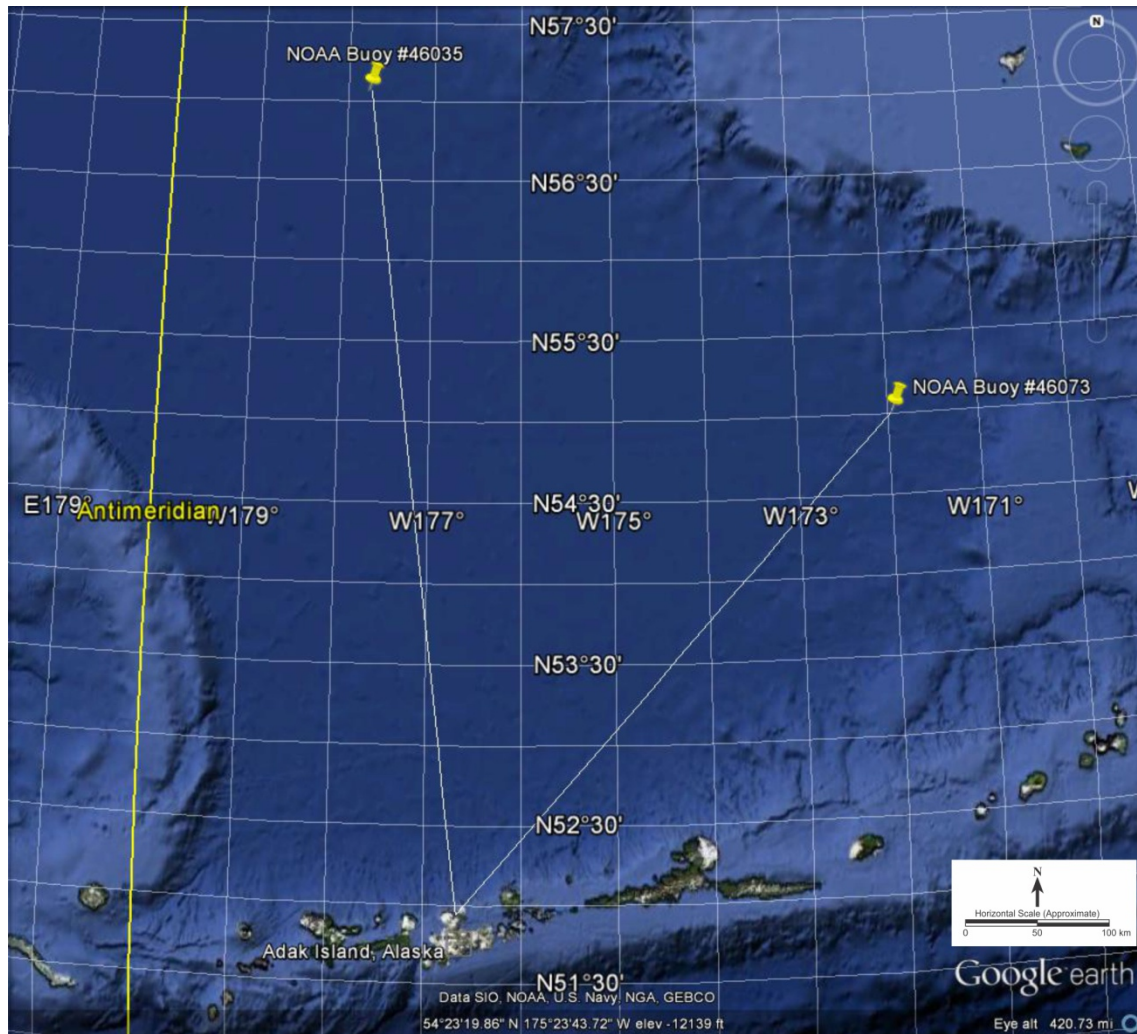


**Figure 2-5. Location of NOAA Wave Buoys for Developing Wave Forcing Records for Andrew Bay UXO Mobility Modeling**

**2.4.1 Modeling Choices Related to Wave Climate.** Data gaps are a serious problem when modeling time-stepped, time-evolving processes such as UXO migration, introducing significant uncertainty related to what occurred during the time period that the model is forced to stop and re-start across a data gap. Consequently, Buoy #46073 was selected to drive the UXO mobility model, as it provided an unbroken record of deep water wave height, period and direction at hourly sampling intervals over a period of 4 years from 2005 to 2009. Buoy #46073 is located in the southeast Bering Sea at  $56^{\circ}56'30''$  N;  $172^{\circ}01'44''$  W, in 3,000 meters of water depth, and is the closest wave monitoring station to Andrew Bay (Figure 2-5). Data from Buoy #46073 were used as the offshore forcing conditions for the UXO mobility and beach profile change modeling at Andrew Bay. Figure 2-6 plots the wave heights in black and the wave periods in red over this period of record. To obtain a continuous 20-year forcing record, it was necessary to loop this 4-year wave record five times. This simulated 20-year wave record was then used to provide time-stepped forcing on the deep water boundary condition of the UXO mobility model.

Figure 2-7 provides histograms of wave height and periods to assess the statistical fidelity of the wave forcing derived from looping the 2005 to 2009 period of record from Buoy #46073 (red) versus the data fragments from the 1985 to 2011 period of record for NOAA Buoy #46035 (green). Probability densities and cumulative probabilities for wave heights in Figure 2-7a show about a 1% difference between these two buoy records in the occurrence of waves greater than 6 m in height, and less than a 0.5% difference in occurrence of the largest waves. The largest wave height in the 4-year unbroken wave data block from Buoy #46073 was 11 m; the largest wave in the 27 years of data fragments from Buoy #46035 was 12 m. Since UXO migration is generally episodic, with the largest movements occurring during extreme event waves, these small differences between the two records do not appear significant for the risk assessment problem at hand. The largest difference occurs for small to intermediate waves, those with heights less than 3.5 m, with the 4-year data block from Buoy #46073 indicating about a 5% higher cumulative wave height occurrence probability than found among 27 years of data fragments from Buoy #46035. Median wave height is 1.9 m in the 4-year data block from Buoy #46073 and 2 m in the 27 years of data fragments from Buoy #46035. So generally, the longer, fragmented record from Buoy #46035 gives wave heights that on average are about 5% higher than the 4-year unbroken record from Buoy #46073, and waves that are 1% higher or less for extreme events. The cumulative probability curves for wave period in Figure 2-7b show virtually no significant difference in the wave period data between the two records. However, 10% of the data from Buoy #46035 are missing and Figure 2-8 emphasizes the significance of this missing data during the concurrent 2005 to 2009 period of record. Since there is no apparent modeling work-around for the missing data from Buoy #46035, and because the statistical difference between the two records is small, the choice was made to use the looped 4-year unbroken record from Buoy #46073 to drive the UXO mobility model.

By any standard, both wave records (Buoy #46035 and Buoy #46073 ) indicate an enormous dynamic range in the interannual wave climate variability, with maximum wave heights of 11 to 12 m during the high energy winter months, and minimum wave heights of only 0.3 m during the summer doldrums.

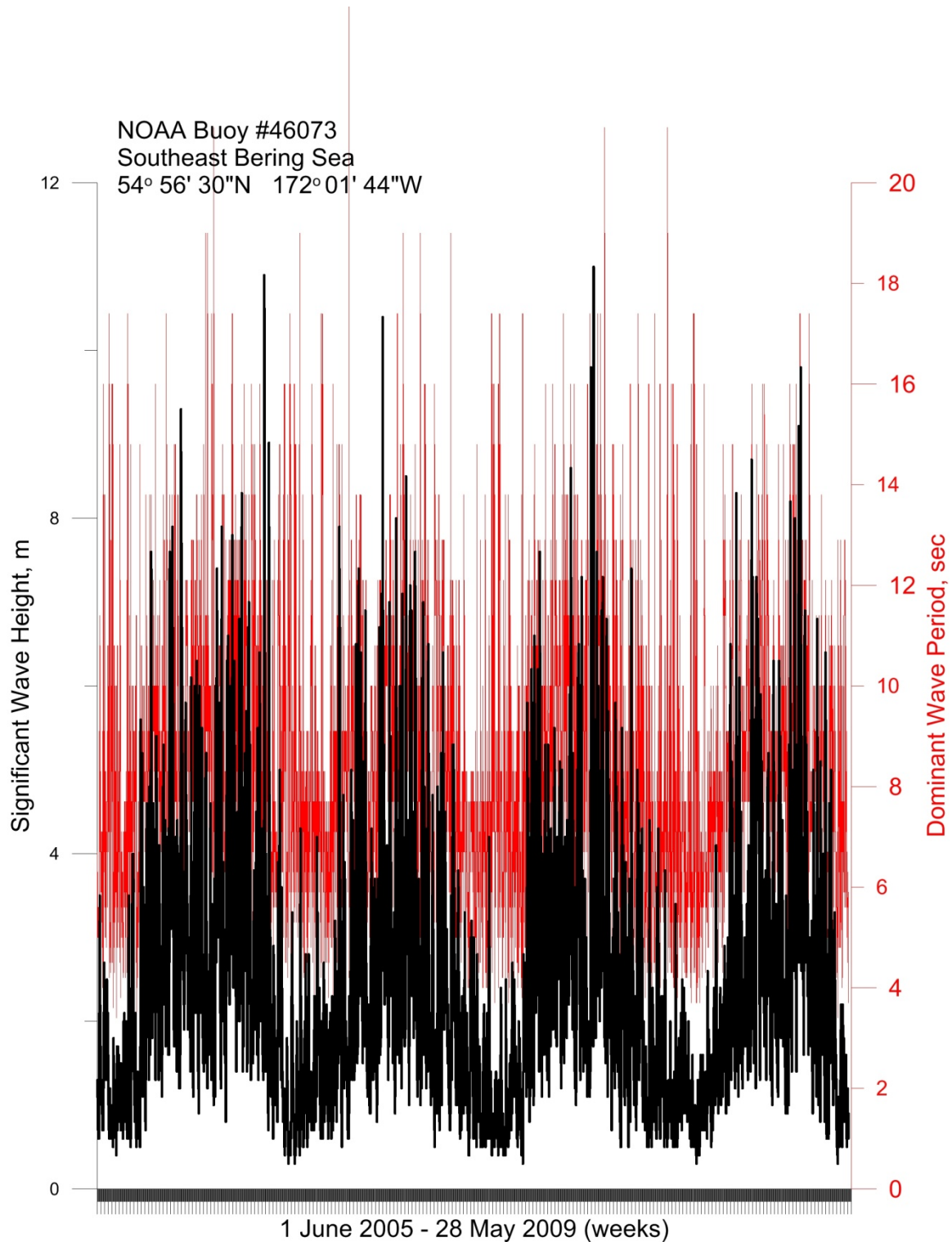


**Figure 2-6. Historic Wave Record Measured by NOAA Buoy #46073 in the Southeast Bering Sea (2005-2009)**

(This wave record was used to provide time-stepped forcing on the deep water boundary condition of the UXO mobility model; wave heights plotted in black; wave periods plotted in red.)

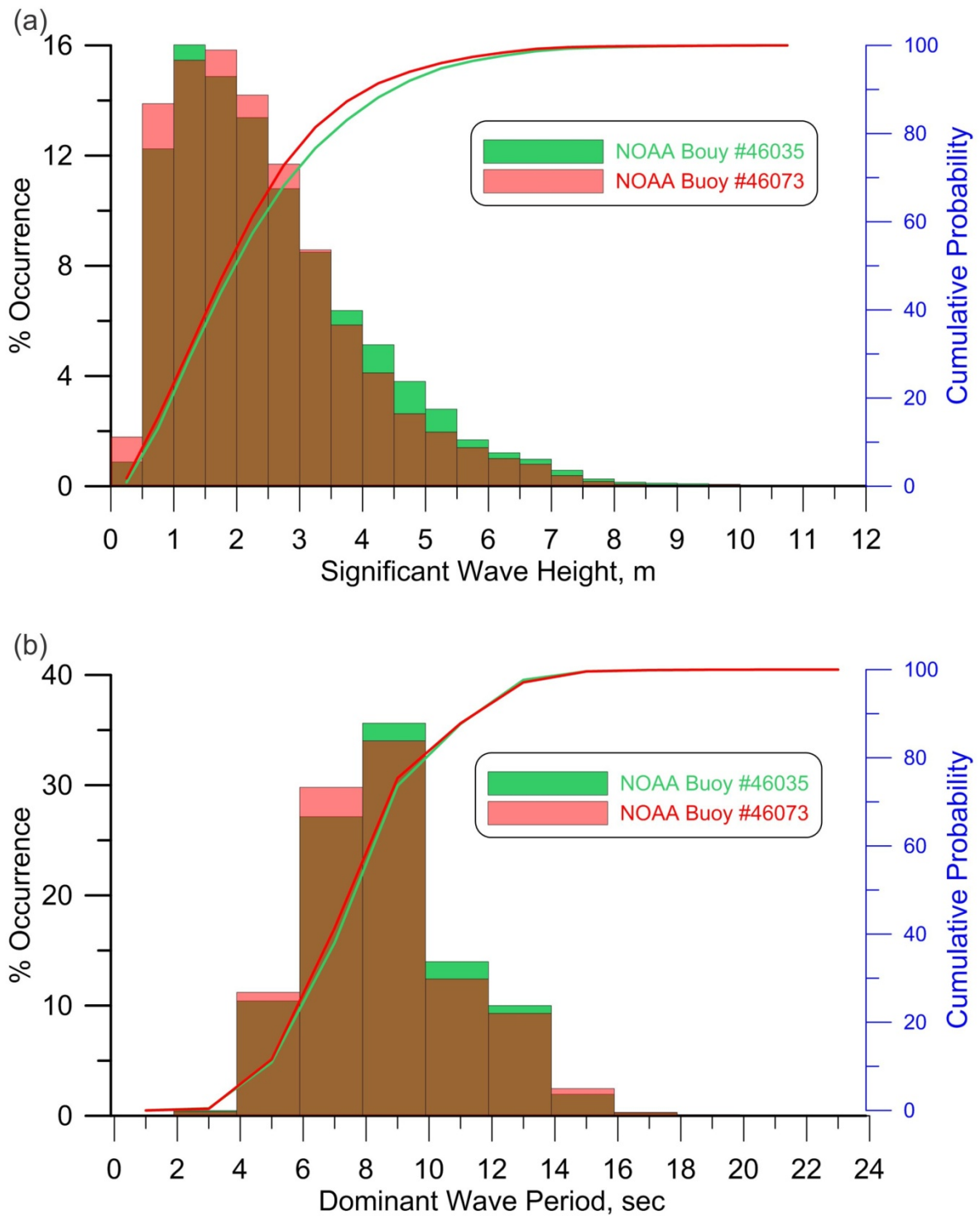


**Figure 2-7. Histograms and Cumulative Probability: (a) Wave Height; (b) Wave Period as Derived from the 1985-2011 Period of Record for NOAA Buoy #46035 (green) Compared with the 2005-2009 Period of Record for NOAA Buoy #46073 (pink) (Overlapping values shown in brown.)**

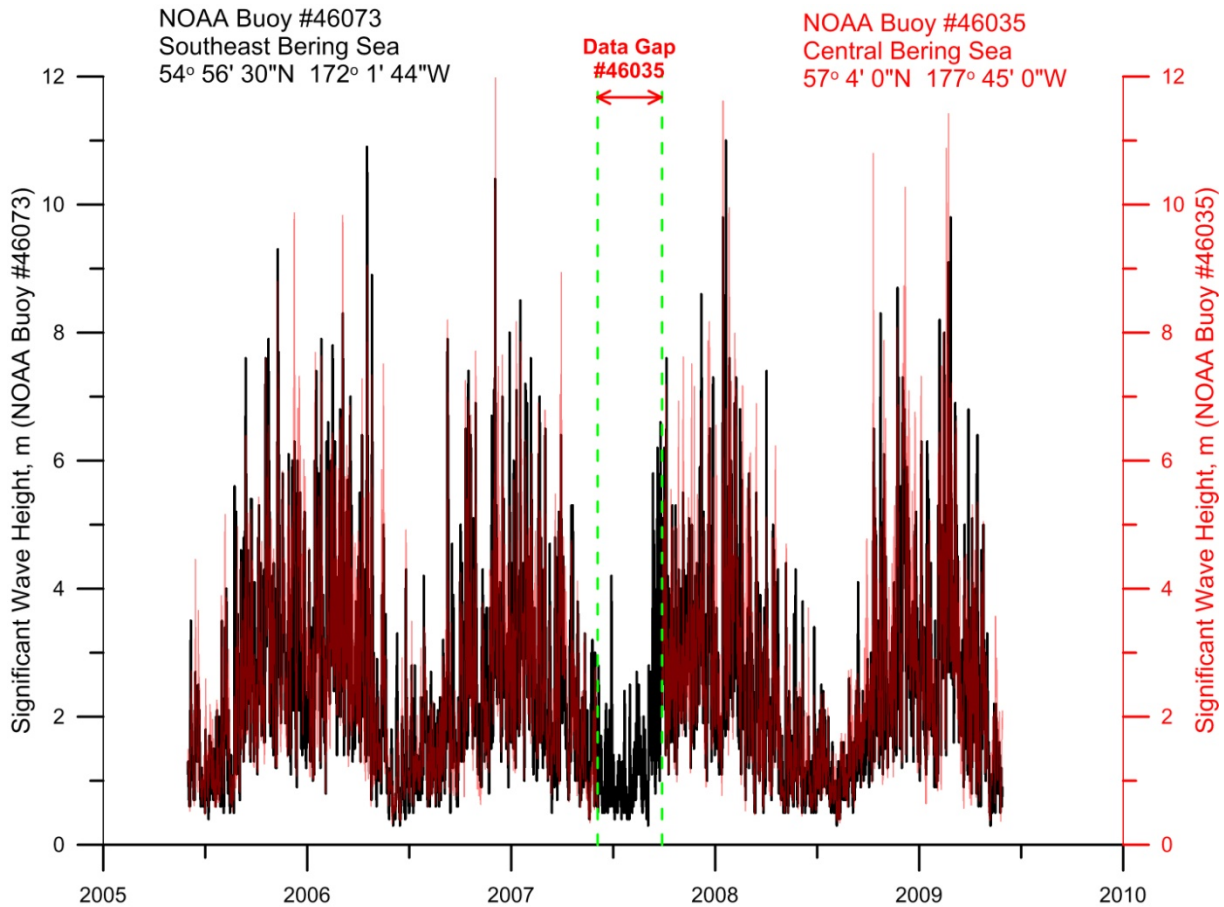


**Figure 2-8. Historic Wave Record Measured by NOAA Buoys #46073 and #46035 in the Southeast Bering Sea (2005-2009)**

(This wave record was used to provide time-stepped forcing on the deep water boundary condition of the UXO mobility model; wave heights plotted in black for NOAA Buoy #46073; wave heights plotted in red for NOAA Buoy #46035. Data gap in record for Bouy#46035 shown in green.)

The high-energy winter waves also have very long periods of as much as 23 seconds, while the summer waves have typical wind wave periods of only 3.2 seconds. This broad dynamic range in heights and periods tends to promote several modes of UXO transport, with onshore, upslope transport occurring under the influence of long period, high-energy waves, and offshore transport occurring during action of the shorter period waves. The long-term mean wave height at Andrew Bay is 0 (2 m), which definitely classifies this as a high-energy site.

## 2.5 UXO Types in Andrew Bay

A complete listing of possible UXO types at Andrew Bay is listed in Appendix A. The numbers of UXO types in Appendix A are too numerous to study each particular type in hydrodynamic simulation. Therefore, a short list of canonical types was constructed in Table 2-2 that not only represents UXO types actually recovered by EOD at Andrew Bay, but also spans the size and weight distribution of the potential list in Appendix A. Appendix B provides photographs and engineering drawings of each ordnance type found in the canonical listing in Table 2-2.

**Table 2-2. Canonical Listing of Ordnance Recovered on the Beach at Andrew Bay**

Ordnance Type	Diameter (cm)	Length (cm)	Weight (kg)
81 mm Mortar	8.1	28.2	4.89
75 mm HE M41A1	7.5	24.816	6.24
60 mm Mortar M721	6	36.1	2
60 mm Mortar	6.1	12.2	2.01
Grenade Rifle M17	5.7	5.7	0.667
40 mm APFSDS PGU-31/B	4	28.4	0.372
40 mm HEI PGU-9/B	4	18	0.966
20 mm HE M97	2	8.3	0.13154
2,000 LB Bomb	47.2	177	909.03

(from Jones and Israel, 2002)

Communications with the Officer in Charge, EOD Mobile Unit Eleven Detachment North West as reported in Jones and Israel (2002), revealed that underwater surveys found only small amounts, approximately 40 to 50 UXO, on the bottom. These surveys were conducted during the summer months and were limited to the area inshore of the dashed blue line in Figure 2-2, which corresponds approximately to the 30 m depth contour. EOD personnel reported that most of the UXO were generally recovered on the beach after severe storms. The green shaded area in Figure 2-2 was the general location in which most UXO were recovered, and later destroyed, during 1962-1964 by EOD personnel. This area of the Andrew Lake Seawall was searched repeatedly during this period.

Three general types of UXO were selected from Table 2-2 for analysis herein. The 60 mm and 81 mm mortar rounds were selected for size matching with native beach rock and for relative ease of potential mobility and comparable size (Section 2-2); the 20 mm and 40 mm rounds were selected to represent the high mobility UXO types due to their relative small size and size similarity with the gravels and smaller cobble fractions found at Andrew Bay (Section 2.2), and the 2000 lb bomb was chosen due to its high critical shear stress value (i.e., low potential for mobility) and size similarity with the largest fractions of beach rock found at Andrew Bay (Figure 2-9). These three example categories represent the range mobility characteristics of the typical UXO found in Andrew Bay. For each of these three example categories, whole, intact rounds were gridded and modeled when evaluating both the bottom wind hypothesis as well as the beach churn hypothesis. This was done in spite of visual evidence that the UXO recovered during the EOD sweeps were often degraded or fragmented by corrosion and abrasion (Figure 2-9). The choice to model intact rounds was not only based on the practical requirement to have standardized and known shapes in the model gridding exercise, but also to ensure the model analysis was maximizing risk in the risk assessment and seeking the most plausible outcome by the two operative hypotheses. The inclusion of guidance fins, propellant charges and charge casings in the modeled UXO shapes (in spite of the fact these features are typically obliterated over time in this high energy environment) increases the wetted area and hydrodynamic drag on these shapes, while reducing net density and rendering the UXO more mobile to any given fluid forcing.

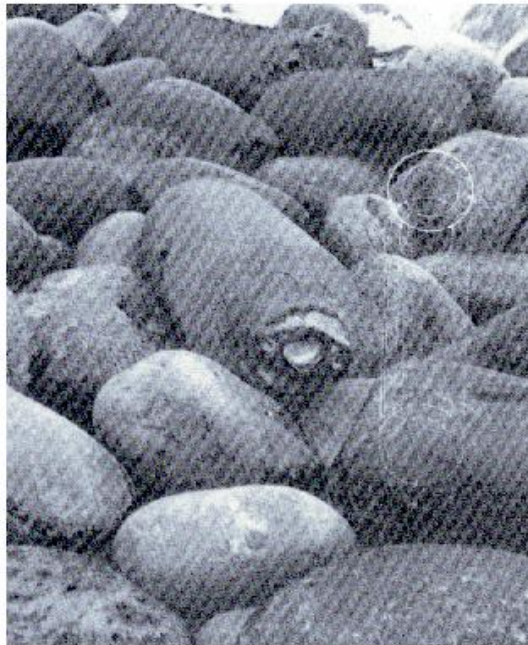


**Figure 2-9. EOD Personnel with Recovered UXO on the Beach at Andrew Bay circa 1962**  
(from Jones and Israel, 2002)

### Section 3.0: UXO MOBILITY MODELING

This section details the vortex lattice mobility model used in the determination of UXO mobility in Andrew Bay.

#### 3.1 Technology

The vortex lattice mobility model is a three-dimensional, time-stepped, process-based model for the prediction of exhumation, migration, and subsequent burial of UXO by general bed erosion and local vortex scour. Details of the UXO mobility model and the model code are provided in Wilson et al. (2008).

#### 3.2 Technology Description

The UXO mobility model is a process-based model that uses vortex lattice computational methods to generate three-dimensional simulations of subsequent burial, exposure and migration of complex UXO shapes. In these simulations it accounts for effects of large-scale erosion or accretion of the seabed (farfield processes) and fine-scale vortex shedding, scour and bedform evolution around the UXO shape (nearfield processes). Farfield processes are those that alter the seabed elevation over length scales that are comparatively large with respect to the size of an individual UXO round. Nearfield processes are due to the flow disturbance caused by the UXO and affect the seabed elevation by local scour, as well as induce hydrodynamic forces that cause the UXO to move. The present UXO mobility model software was validated in two ESTCP-funded field tests, where it correctly predicted all the basic behaviors of UXO test surrogates with high quantitative predictive skill factors.

Migration and burial processes consist of two distinct types: nearfield and farfield (Jenkins et al., 2007). These operate on significantly different length and time scales. Nearfield processes occur over length scales the order of the body dimensions and on time scales of a wave period, primarily governed by scour mechanics. In contrast, farfield processes involve changes in the elevation of the seabed with cross-shore distances of hundreds of meters that may extend along the coast for kilometers. Farfield time scales are typically seasonal with longer periods due to variations in climate and travel time of longshore sediment fluxes associated with accretion/erosion waves. These processes are coupled together in an architecture diagrammed by the flow chart shown in Figure 3-1 and referred to as the *vortex lattice (VORTEX) scour and burial model* (Jenkins et al., 2007). The farfield processes and inputs are found above the orange line in Figure 2-1, while the nearfield processes and inputs are below the green line.

As with any boundary value problem, the solution follows from specifying initial conditions, forcing functions and the boundary conditions, from which the response is computed using a set of process-based algorithms. This computational sequence proceeds in Figure 3-1 from the top down, with the set of forcing functions and initial conditions bundled together in a *module* shown by the box at the top of the flow chart, while boundary conditions and response modules of the farfield are found in the pathways below that. The farfield response modules are upstream of the nearfield modules in the computational flow chart because the farfield processes determine the fluid forcing and elevation of the sand bed around the object, essential to specifying the nearfield boundary value problem.

Farfield processes provide the broad-scale forcing leading to general seabed erosion and/or accretion. Seabed erosion can exhume buried UXO, while seabed accretion can result in deeper entombment of buried UXO, or can lead to the subsequent re-burial of exhumed UXO. These farfield processes involve changes in the elevation of the seabed with cross-shore distances of hundreds of meters

that may extend along the coast for kilometers. The domain of such regional scale variation is the littoral cell. Farfield time scales are typically seasonal with longer periods due to variations in climate. Farfield exhumation and burial mechanics are associated with large-scale processes including changes in beach profile, deposition from rivers, sediment loss by turbidity currents, and bottom modification by ice push. These processes vary with many time scales, including diurnal oscillations associated with tides and sea breeze, inter-annual oscillations associated with summer/winter seasonal change, multi-annual variability associated with short-term global climate oscillations such as the El Nino-Southern Oscillation and multi-decadal differences due to long-term climate variability associated with the Pacific Decadal and North Atlantic Oscillations. Because the farfield processes determine the elevation and slope of the seabed on which the nearfield processes operate, the farfield exerts a controlling influence on the nearfield. Hence, farfield processes form the basis of the model and are shown as the top half of the UXO mobility model architecture in Figure 3-1.

Farfield processes are controlled by the balance between the amount of sediment entering the farfield and the amount leaving. This balance, known as the sediment budget, requires the identification of sediment sources and sinks, which will vary with the type of coastline. Some basic types of coastlines have been identified. The Geomorphic Coastal Classification module in Figure 3-1 (highlighted in orange) is used to select the relative scaling and assigns the sediment sources and sinks to which a particular UXO site belongs. The classification includes three general tectonic types of coasts with their morphologic equivalents and two types associated with latitudinal extremes: 1) collision coasts with narrow shelves and steep coastal topography resulting from collisions between two or more tectonic plates, 2) trailing edge coasts that are on the stable, passive margins of continents with broad shelves and low inland relief, 3) marginal sea coasts that are semi-enclosed by island arcs and thereby fetch limited, and, 4) biogenic coasts that are formed by fringing coral reefs or mangroves.

Although the relative importance of transport processes varies among coastal type, two processes are always important to UXO exhumation and burial. These are seasonal changes in the beach profile (Figure 3-2c) and fluxes of sediment into and out of the UXO environment by accretion/erosion waves (Figure 3-2a).

The forcing functions that drive the far field processes are developed by the module indicated by the top box in Figure 3-1 and provide time series of waves (#2), currents (#3) and sediment flux (#4). Waves and currents are derived from direct observations by means of NOAA buoys and/or acoustic Doppler current profilers (ADCPs).

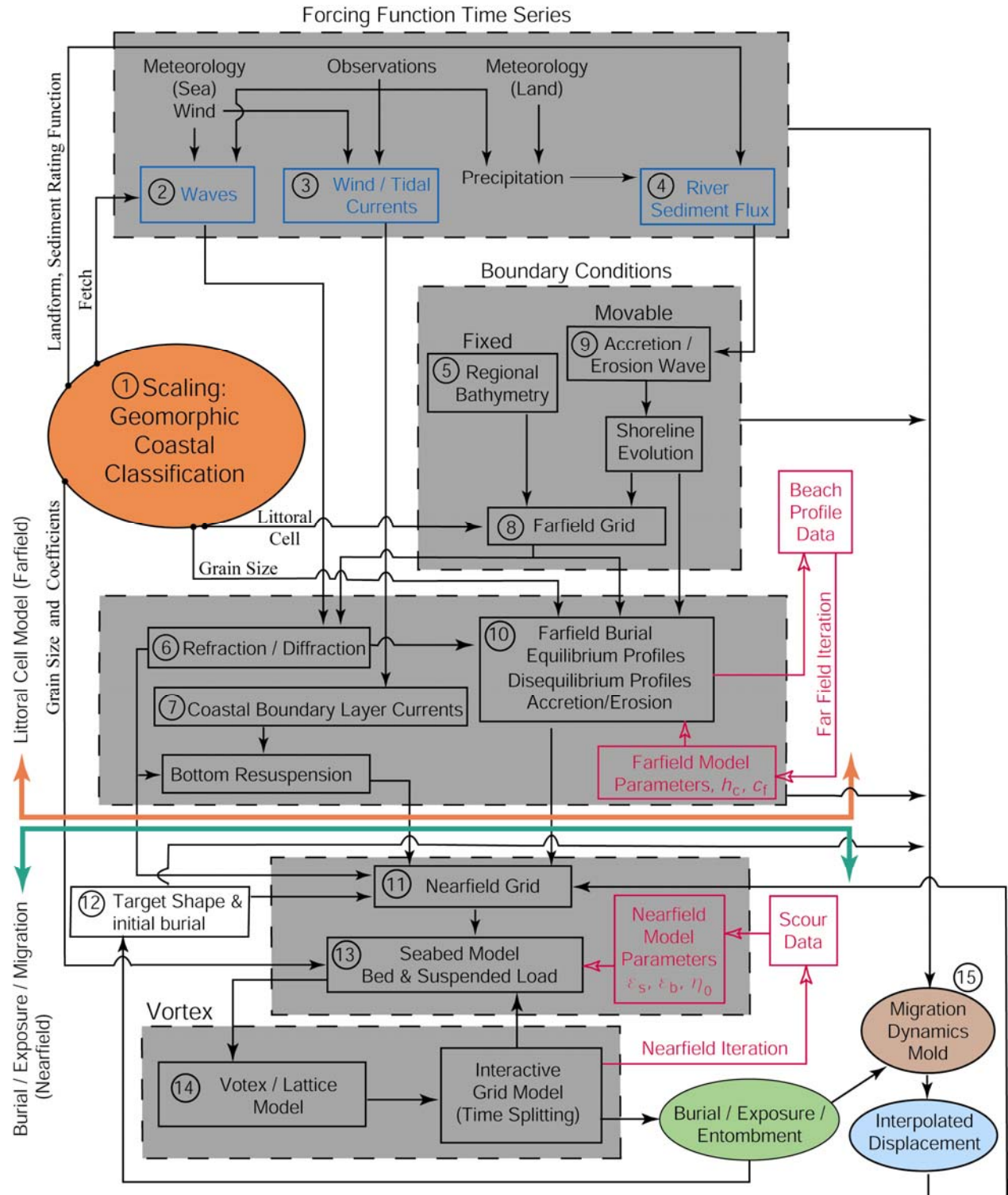
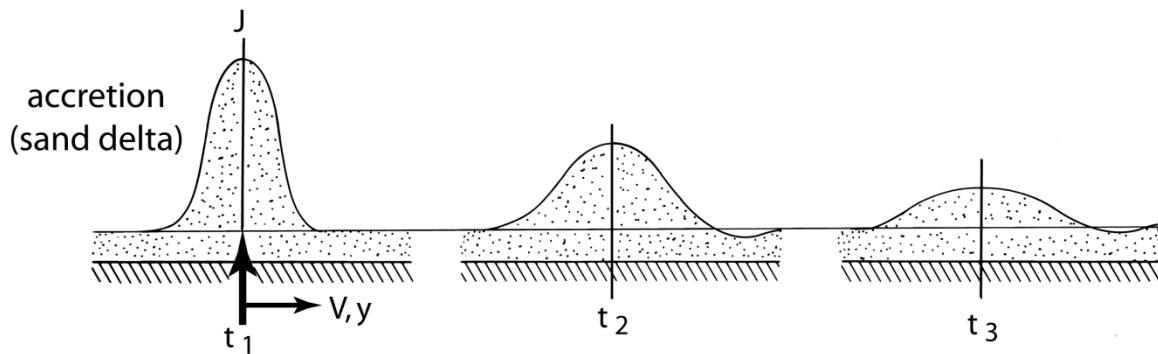
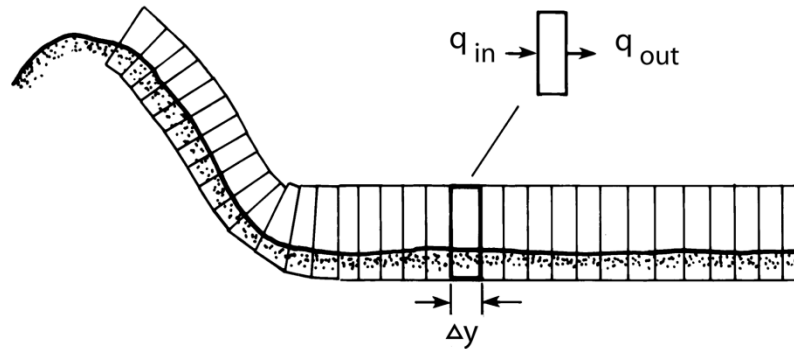


Figure 3-1. Architecture to the Vortex Lattice UXO Mobility Model

### a) Accretion / Erosion Wave



### b) Coupled Control Cells



### c) Profile Changes

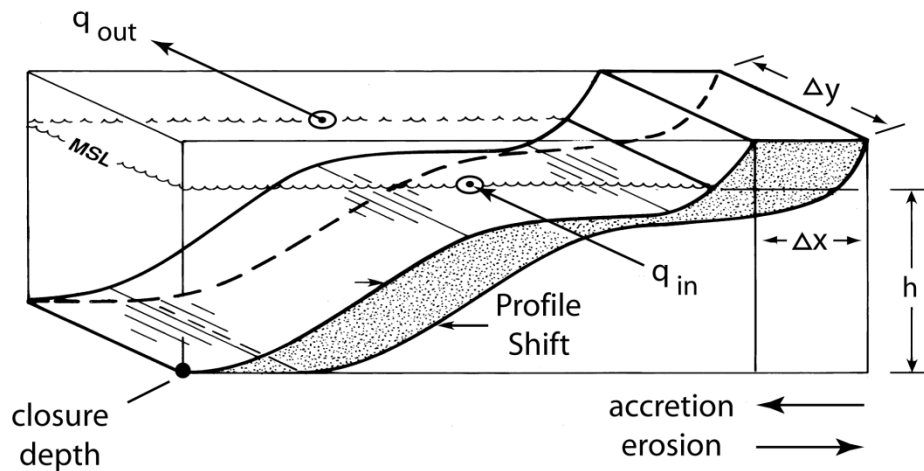


**Figure 3-2. Computational Control Cells and Farfield Movable Boundary Conditions Used in the Vortex Lattice Computational Methodology: (a) Accretion/Erosion Wave; (b) Coupled Control Cells; and (c) Profile Changes**

Fluxes of river sediment are neglected as explicit boundary conditions in the Andrew Bay model problem, but the presence of those sediments are accounted for in the grain size distributions of the beach and offshore sediments, cobble and basal conglomerates. The wave and current forcing provides excitation applied to the deep water boundary of the farfield computational domain. These boundaries are specified in the boundary conditions module (beige box) in Figure 3-1, where the farfield computational domain is assembled from a series of boundary-conforming control cells (Figure 3-2b), using a combination of bathymetric data obtained from Carignan et al. (2009) to assemble the digital bathymetry in Figures 1-2 and 1-3.

With these forcing functions and boundary conditions, the farfield response module (blue box) computes the spatial and temporal evolution of the fluid forcing and bottom elevation along cross-shore profiles of a control cell (Figures 3-2 and 3-3a). These cross-shore profiles have three matching segments: 1) the stationary profile that extends from the deep water boundary inshore to closure depth  $h_c$ , where profile changes become vanishingly small; 2) the shore rise profile that continues from closure depth to the wave break point; and 3) the bar-berm profile that begins at the break point and ends at the berm crest. The stationary profile is invariant with time and is given by the regional bathymetry. Bottom elevation changes along the non-stationary profiles of the shore rise and bar-berm (Figure 3-3a) are computed by (#10) in the farfield response module (blue box) using equilibrium profile algorithms (Jenkins and Inman, 2006). The stationary and non-stationary profiles are interpolated to create a Cartesian depth grid within each control cell on which simultaneous refraction and diffraction patterns are computed by (#6) using algorithms from Kirby (1986) and Dalrymple et al. (1983), to specify fluid forcing by shoaling waves. Fluid forcing by currents in the farfield are computed in (#7) where wave induced streaming and mass transport are based on algorithms and shallow water tidal currents follow from algorithms.

Fluid forcing time series and bottom elevations computed in the farfield response module are through-put to the nearfield response modules shown below the green line in Figure 3-1. Nearfield processes occur over length scales on the order of the UXO dimensions and on time scales of a few seconds to hours, primarily governed by local hydrodynamic forces and scour mechanics arising from the disturbance which the UXO creates in the flow.

The UXO and adjacent seabed is subdivided into a set of panels to form a lattice (Figure 3-4a). The vortex field induced by the UXO is constructed from an assemblage of horseshoe vortices, with a horseshoe vortex prescribed for each panel. This computational technique is known as the vortex lattice method and has been widely used in aerodynamics and naval architecture. The strength of the vortices is derived from the pressure change over each panel associated with the local wave and current velocity. The release of trailing vortex filaments from each panel causes scour of the neighboring seabed. This action is portrayed in nature in Figure 3-4b and schematically in Figure 3-5. When viewed in any cross-wake plane (Figure 3-5b), each pair of filaments induces a flow across the seabed that results in scour proportional to the cube of the vortex strength and inversely proportional to the cube of the sediment grain size. This sensitivity of scour to grain size selectively removes the finer grained fraction of the bed material and leaves behind the coarser grained fraction in the scour depression. The coarse material that remains in the scour hole armors the bed against further scour, thereby slowing the rate of scour burial.

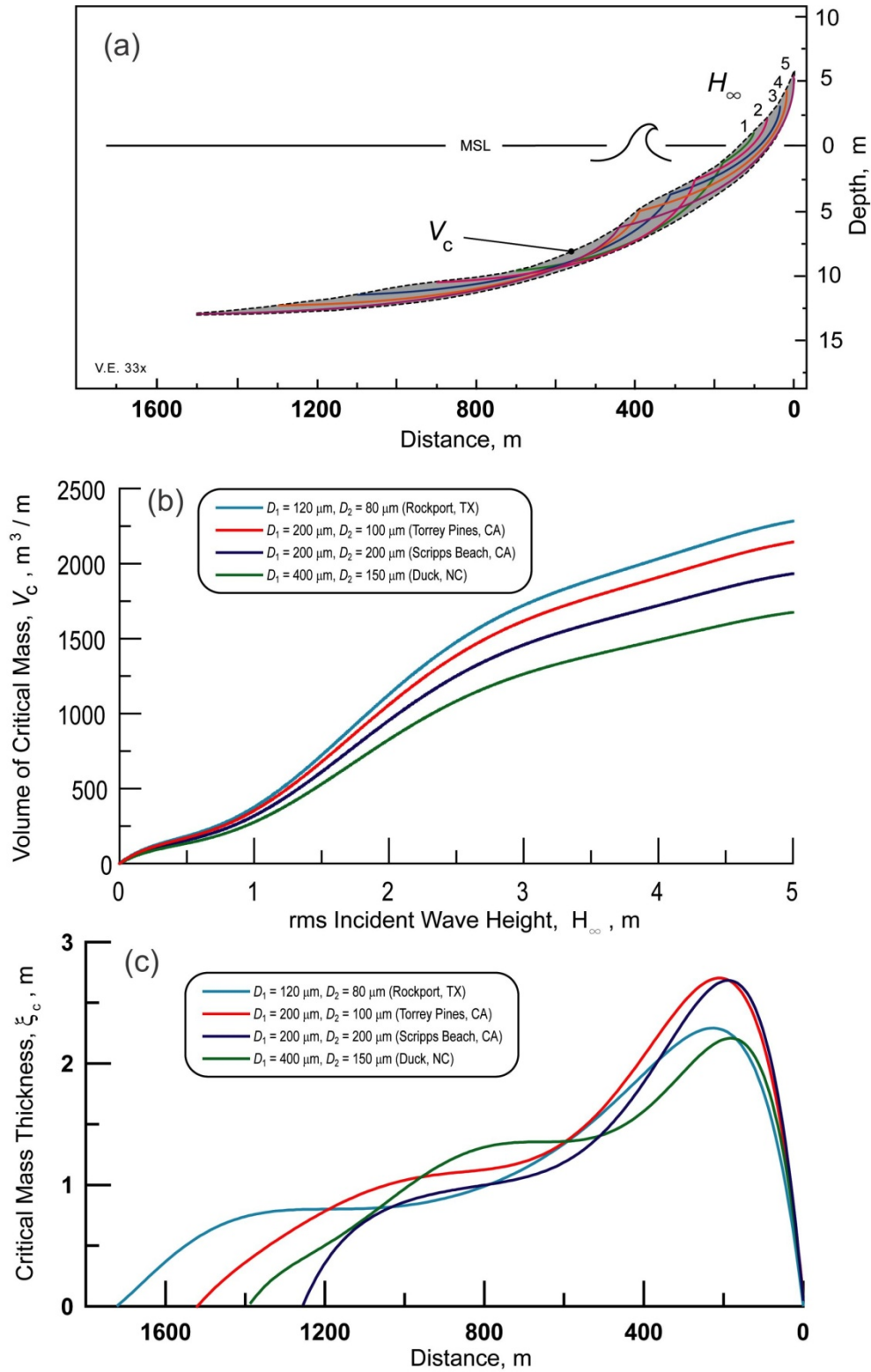


**Figure 3-3. Mechanics of Farfield Burial: (a) Envelope of Profile Change Gives Critical Mass; (b) Volume of Critical Mass from Elliptic Cycloids; and (c) Cross Shore Variation in Critical Mass Thickness**

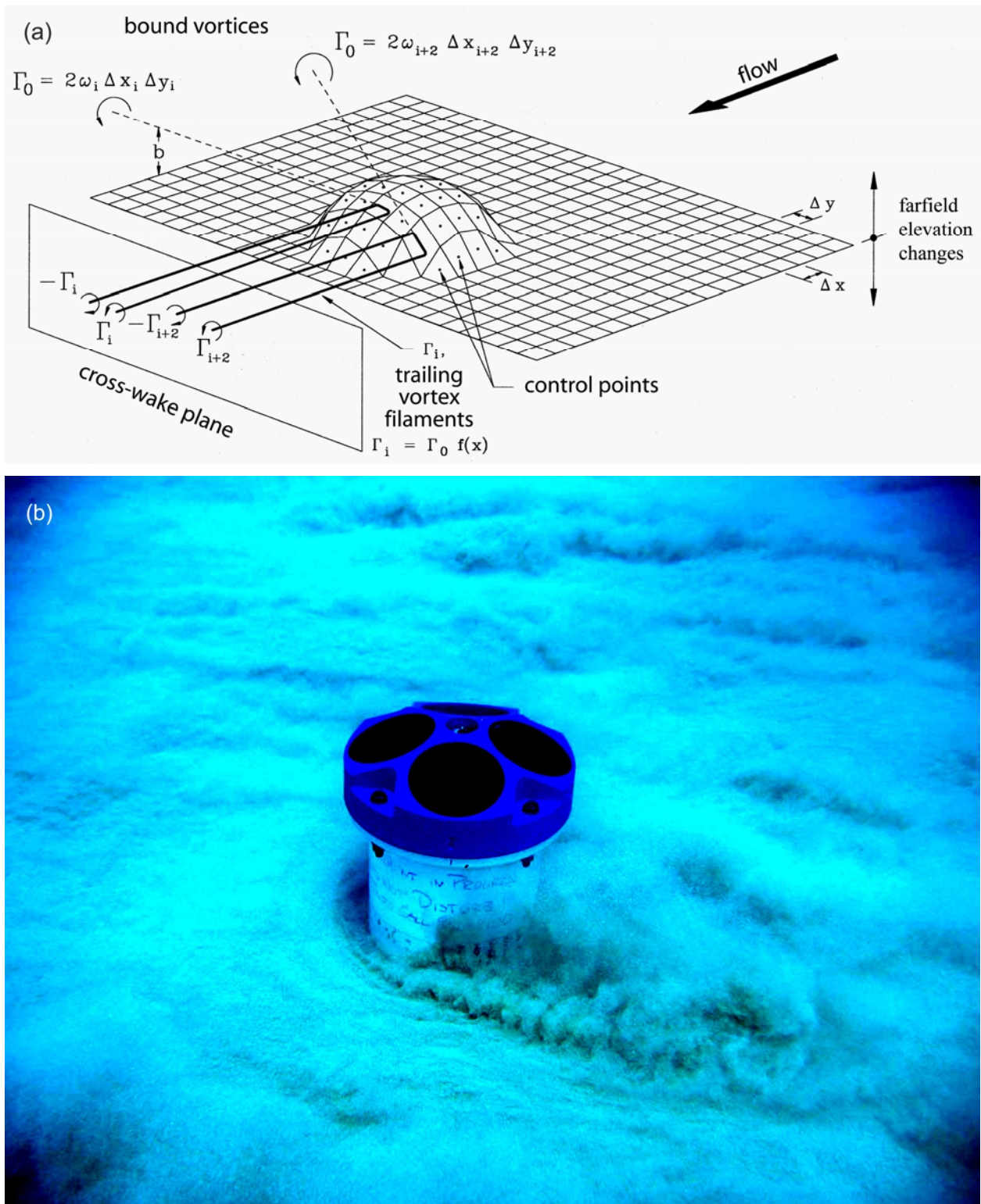


**Figure 3-4. Vortex Lattice Method: (a) Lattice and Horseshoe Vortex System; (b) Horseshoe Vortices Inducing Sediment Transport in Nature**  
(from Jenkins et al., 2007)

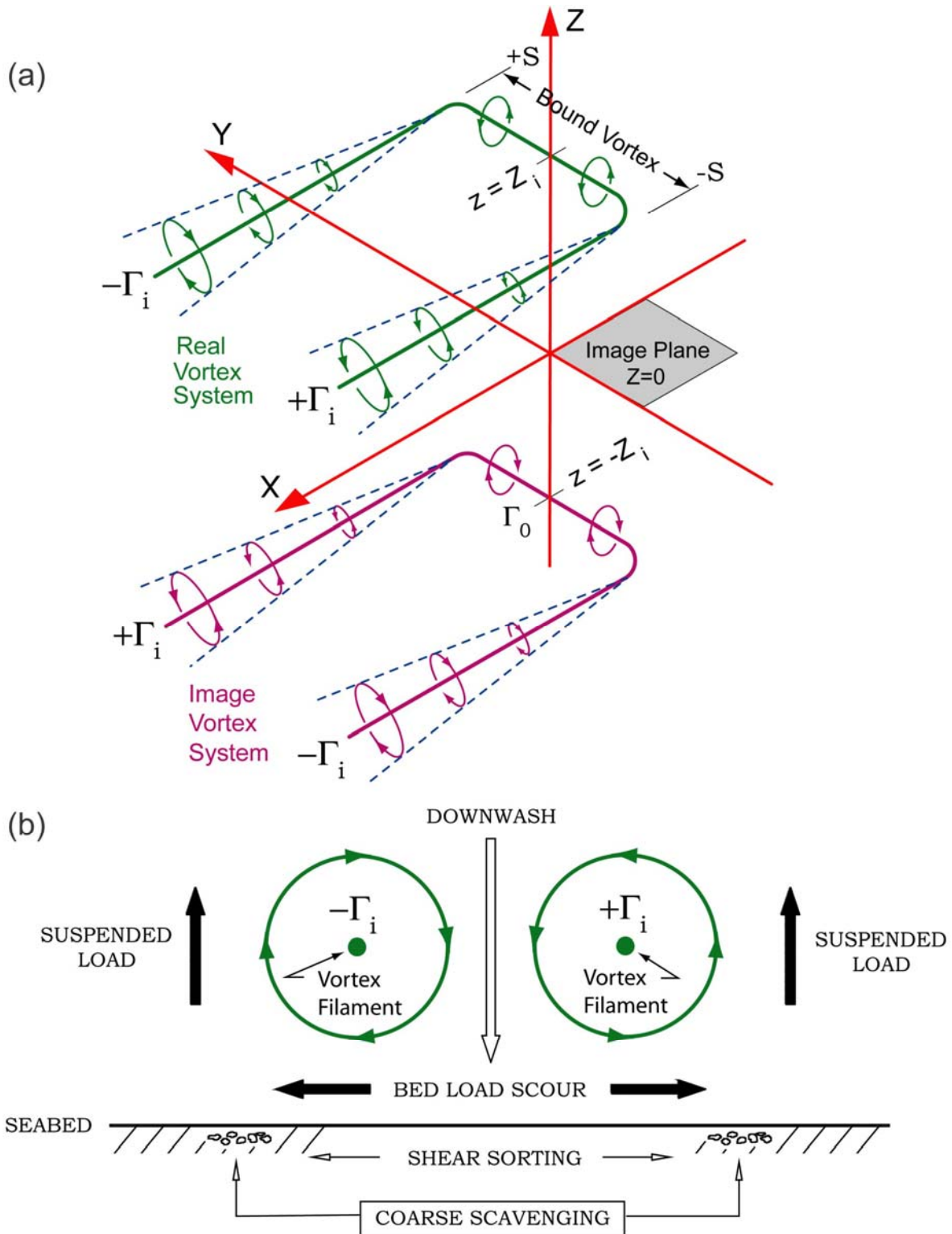
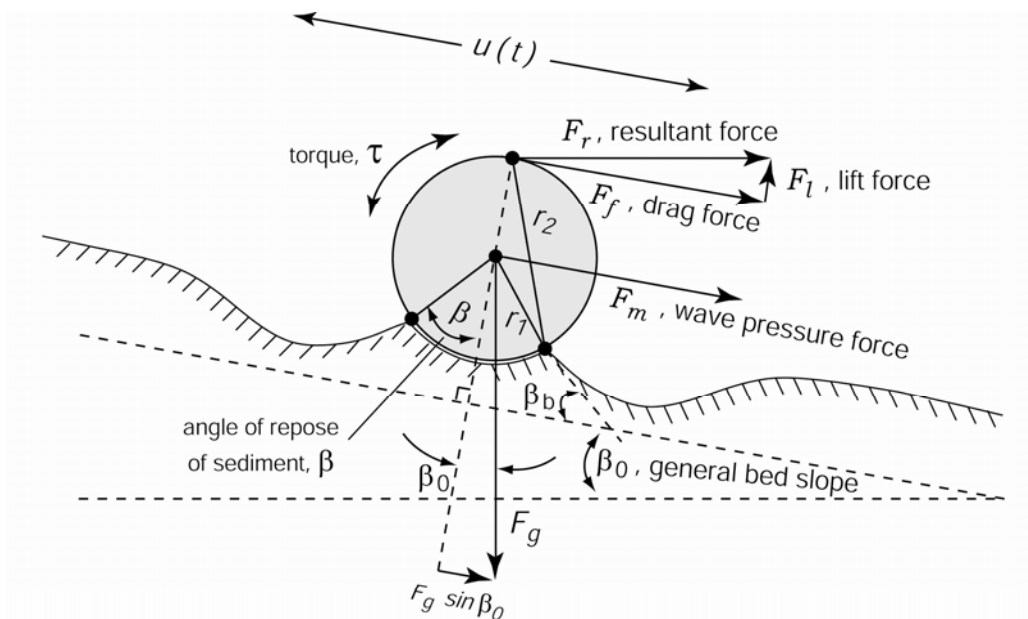


**Figure 3-5. (a) Image Method for Vortex Induced Velocity at any Point near the Bed (image plane) Due to Horseshoe Vortex System of an Arbitrary Lattice Panel; (b) Schematic in the Cross-wake Plane of a Pair of Vortex Filaments Trailing out of the Page (Figure 3-4a)**  
 (The real vortex of the lattice panel is shown in green; the image vortex is in magenta).



Threshold of migration criteria:  $\Sigma \text{ moments} = 0$

$$\vec{F}_g \times \vec{r}_1 = \vec{F}_m \times \vec{r}_1 + \vec{F}_r \times \vec{r}_2 + \vec{\tau}$$

**Figure 3-6. Moment Balance for Threshold of UXO Movement in Response to Reaction Forces Generated by Trailing Vortex Filaments**

The farfield throughput to the nearfield process modules is initially applied to the local seabed boundary conditions module (gray box in Figure 3-1). These local boundary conditions include two types: 1) the slope and elevation of the seabed plane around the object base derived by (#11) from location in the farfield control cell; and 2) the shape file of the body in question (#12). These two local boundary conditions are used to generate lattice panels by (#13) that define the object and bedform of the surrounding seabed (Figure 3-4a). The lattice is the computational domain of the nearfield scour-burial processes in which the method of embedded vortex singularities (vortex lattice method) is applied in (#14) using algorithms after Jenkins and Wasyl (1990), and Jenkins et al. (2007). This method employs horseshoe vortices embedded in the near-bottom potential wave oscillation to drive local sediment transport in (#13) based on ideal granular bed load and suspended load equations after Bagnold (1956; 1963). A horseshoe vortex is specified by (#14) for each lattice panel during every half-cycle of the wave oscillation as shown schematically in Figure 3-4a. The horseshoe vortices release trailing pairs of vortex filaments into the local potential flow field that induce downwash on the neighboring seabed (Figure 3-5b), causing scour with associated bed and suspended load transport as computed by (#13). This scour action by trailing vortex filaments can be seen occurring in nature in Figure 3-4b. The trailing vortex filaments also produce reaction forces on the UXO that induce movement at the instant the moments from these forces balance the moments of gravity associated with the immersed weight of the UXO, as shown schematically in Figure 3-6.

The lattice generation in (#14), horseshoe vortex generation in (#14) and sediment transport computations in (#13) and UXO threshold movement and migration (#15) are implemented as a leap-frog iteration in a time-stepped loop shown by the pathway arrows at the bottom of Figure 3-1. The leading

time step computes the strength of the horseshoe vortex filaments generated by the pressure gradients and shear setup over the lattice panels of the combined body-bedform geometry of the previous (lagging) time step. The bed and suspended load transport induced by these filaments results in an erosion flux from certain neighboring lattice panels on the seabed and a deposition flux on others, based on image lifting line theory (Figure 3-5a) as first applied in Jenkins and Wasyl (1990) to a mobile sedimentary boundary. The erosion and deposition fluxes of the leading time step are returned in the computational loop to the lattice generator where those fluxes are superimposed on the lattice geometry of the lagging time step. That superposition produces a new lattice geometry for implementing the next leading time step. By this leap-frog iterative technique, an interactive bedform response is achieved whereby the flow field of the leading time step modifies the bedform of the lagging time step, and that modified bedform in turn alters the flow field of the next leading time step. This lead and lag arrangement is based on the fact that the inertial forces of granular bed near incipient motion are large compared to those of the fluid, hence the flow field responds faster to a change in bedform than the bedform can respond to a change in flow field.

Because most UXO are bodies of revolution, the burial mechanism proceeds by a series of scour and roll events on a fine sand bottom, whereby the UXO successively scours a depression and then rolls into that depression. In contrast, flat bottom, mine-like objects (e.g., MANTA, ROCKAN, etc.) or UXO resting flat-side down buried by scour and slip sequences involving episodic shear failures (avalanches) of the slopes of the scoured depression (Jenkins and Inman, 2002). During these shear failures, the UXO is in a state of sliding friction with the bed and is easily moved by the hydrodynamic forces of waves and currents.

Both of these mechanisms (scour and roll or scour and slip) may be arrested by large-scale changes in the bed elevation due to either seasonal profile changes or influx of material by accretion/erosion waves. Both of these mechanisms (scour and roll and scour and slip) involve movement of the UXO during the burial sequence. Over erosion-resistant beds, waves and currents may cause UXOs to migrate large distances before scour and burial arrests further UXO migration. During lower energy summer conditions, sand and rock cobbles move onshore from the shore rise, shifting the bottom profile shoreward, potentially exposing the UXOs and inducing migration.

### **3.3 Wave Refraction/Diffraction Analysis**

No current data are available in the vicinity of Andrew Bay. However, waves rather than currents dominate the particle mobilization in the coastal environment (Madsen and Wikramanayake, 1991), particularly nearshore and on the barrier spit where the preponderance of UXO remediation efforts have focused to date. By analyzing the wave environment in the region, areas of UXO mobilization can be identified. Therefore, the focus of fluid forcing analysis will be on modeling the wave environment present in Andrew Bay.

Deep wave data from NOAA Buoy Station #46073 are shoaled into Andrew Bay and onto the adjacent beaches and headlands using the UXO mobility model numerical refraction-diffraction computer code. The primitive equations and codes of the UXO mobility model appear in Jenkins and Wasyl (2005) were beta tested by Garood (2008) and ESTCP-certified in Naval Facilities Engineering Service Center (2008). These codes calculate the simultaneous refraction and diffraction patterns propagating over a Cartesian depth grid. The UXO mobility model uses the parabolic equation method (PEM) (Radder, 1979), applied to the mild-slope equation (Berkhoff, 1972). To account for very wide-angle refraction and diffraction relative to the principle wave direction, the UXO mobility model also incorporates the high order PEM Pade approximate corrections modified from those developed by Kirby and Dalrymple (1994). Unlike the recently developed refraction/diffraction model due to Dalrymple et al. (1984), the Pade approximates in the UXO mobility model are written in tesseral harmonics, per Jenkins and Inman

(1985); in some instances improving resolution of diffraction patterns associated with steep, highly variable bathymetry along steeply sloping shelf breaks, as found in the Cartesian grid used for this analysis in Figure 1-3. These refinements allow calculation of the evolution and propagation of directional modes from a single incident wave direction, which is a distinct advantage over the more conventional directionally integrated ray methods that are prone to caustics (crossing rays) and other singularities in the solution domain where bathymetry varies rapidly over several wavelengths.

Examples of the refraction/diffraction calculation of the deep water wave data overlaid on the depth contours in meters is shown in Figures 3-7 through 3-11 for the five largest storms during the 2005 to 2009 period of record in Figure 2-5. Wave heights are contoured in meters according to the color bar scale and represent 1 hour averages, not an instantaneous snapshot of the sea surface elevation. Irregularities in the shelf off Andrew Bay refract the incoming waves into a complex pattern of *shadows* and *bright spots* in the shoaling wave heights. Bright spots are localized areas where incident wave energy is focused or concentrated (red areas in Figures 3-7 through 3-11) producing locally higher waves. Shadows are areas where wave energy is locally less concentrated and wave heights locally smaller (dark areas shown in blue in Figures 3-7 through 3-11). When the pattern of shadows and bright spots is repeatable among different wave events (as is the case with the five biggest storm waves in Figures 3-7 through 3-11), the repeated pattern can have consequences on the fate and transport of UXO. UXO tend to be more mobile in bright spots, and immobile in shadows. Furthermore, wave-driven currents flow away from regions of high waves and towards regions of low waves. Consequently populations of UXO will tend to decline over time in areas of repeated bright spots, and will tend to accumulate in areas of repeated shadows. In the case of the five biggest storms at Andrew Bay in Figures 3-7 through 3-11, there is a persistent shadow in the middle of the barrier spit separating Andrew Cove from Andrew Bay, and in general the waves are focused into very strong bright spots along the flanking headlands of the bay. The fact that the barrier spit exists at all is evidence that it is an accretion zone for beach rock due to the generally smaller waves in the middle of the Bay and the larger waves along the flanking headlands. This causes wave induced circulation with longshore currents flowing away from the headlands and converging in the middle of the bay where the barrier spit has formed. This circulation pattern would also cause similarly sized UXO to accumulate on the barrier spit over time, especially in the area of the persistent shadow in the middle of the spit.

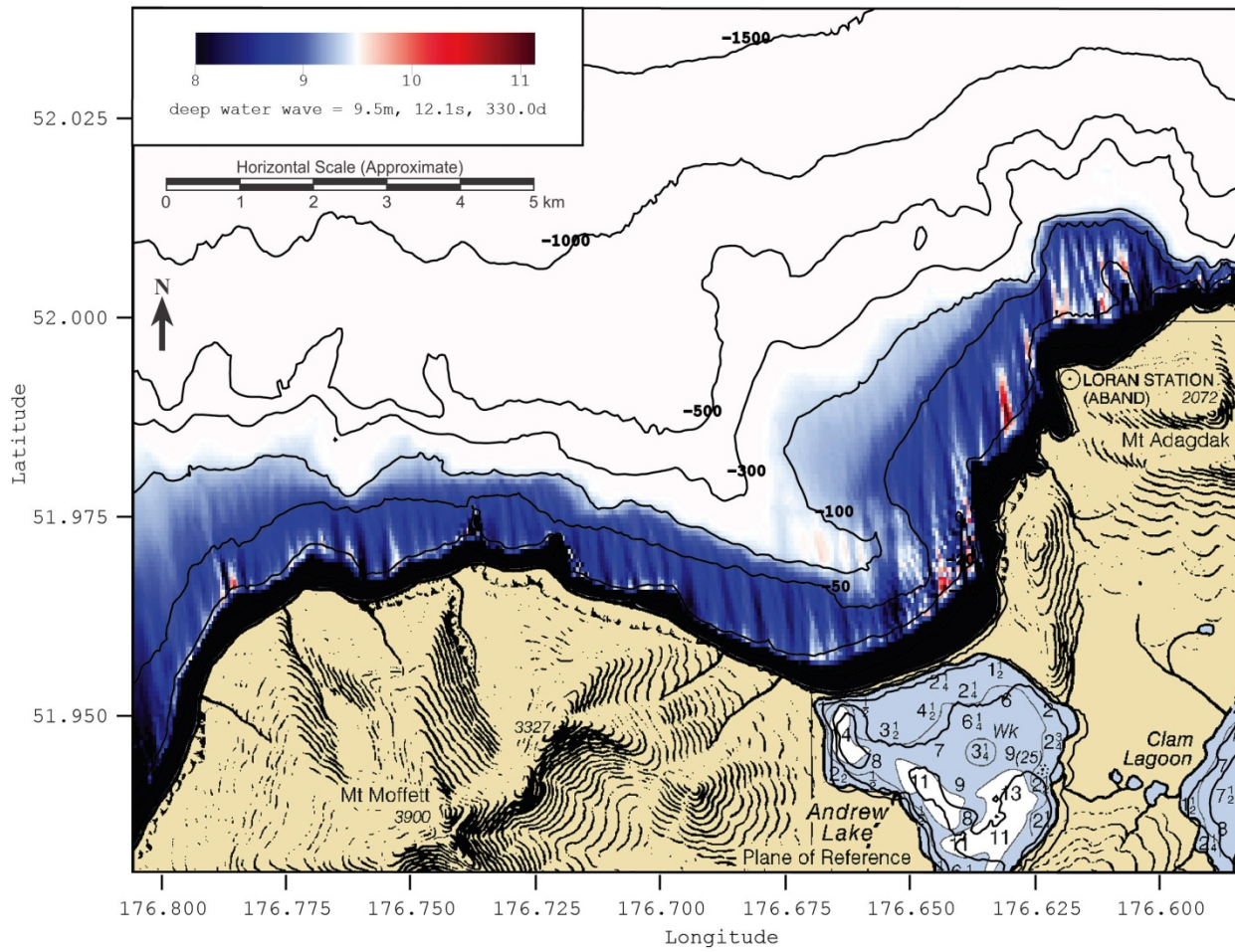


**Figure 3-7. Refraction/Diffraction Pattern of the Five Largest Storms at Andrew Bay (2005-2009)**  
(Wave height = 9.8 m; wave period = 12.1 seconds)

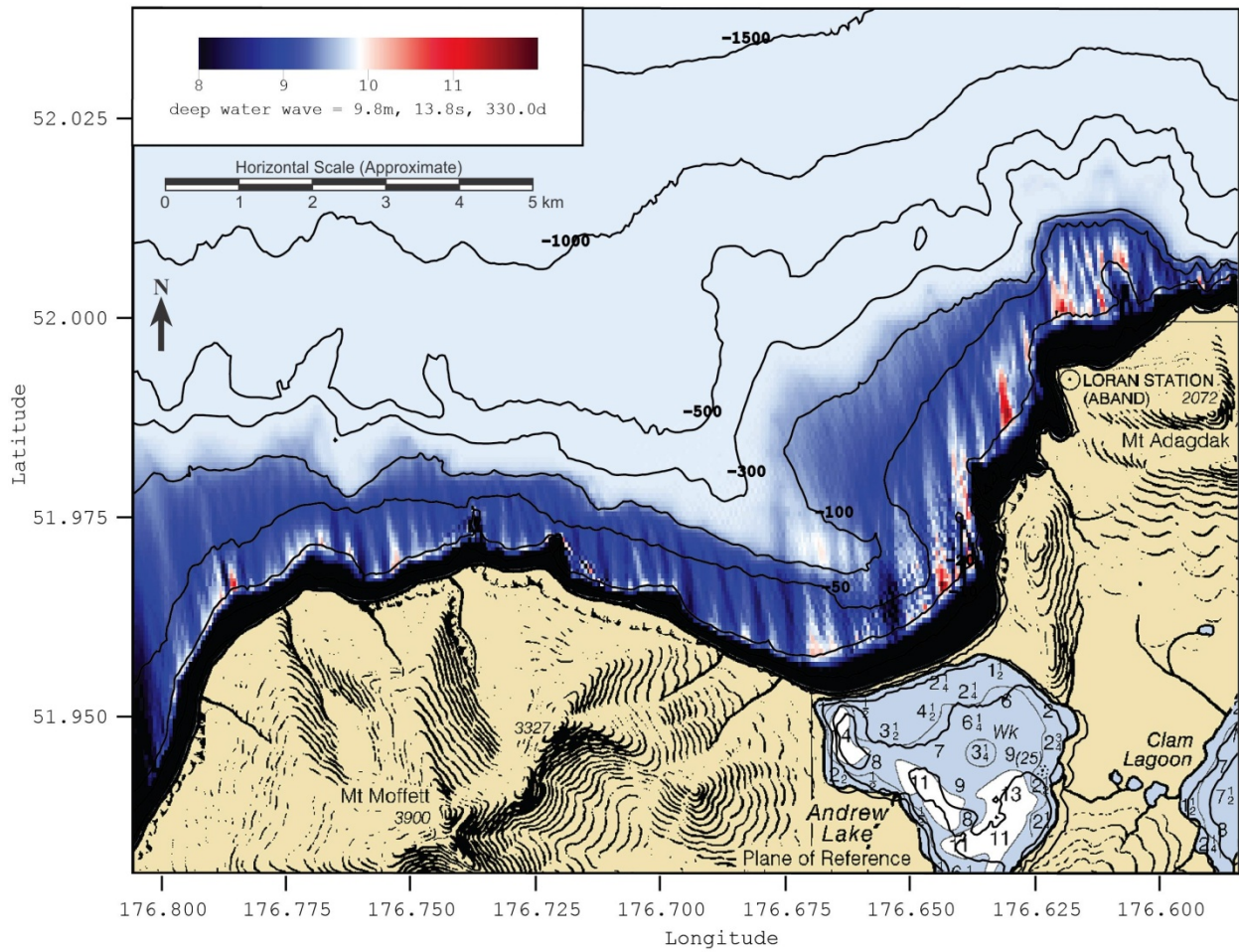


**Figure 3-8. Refraction/Diffraction Pattern of the Five Largest Storms at Andrew Bay (2005-2009)**  
(Wave height = 9.8 m; wave period = 13.8 seconds)

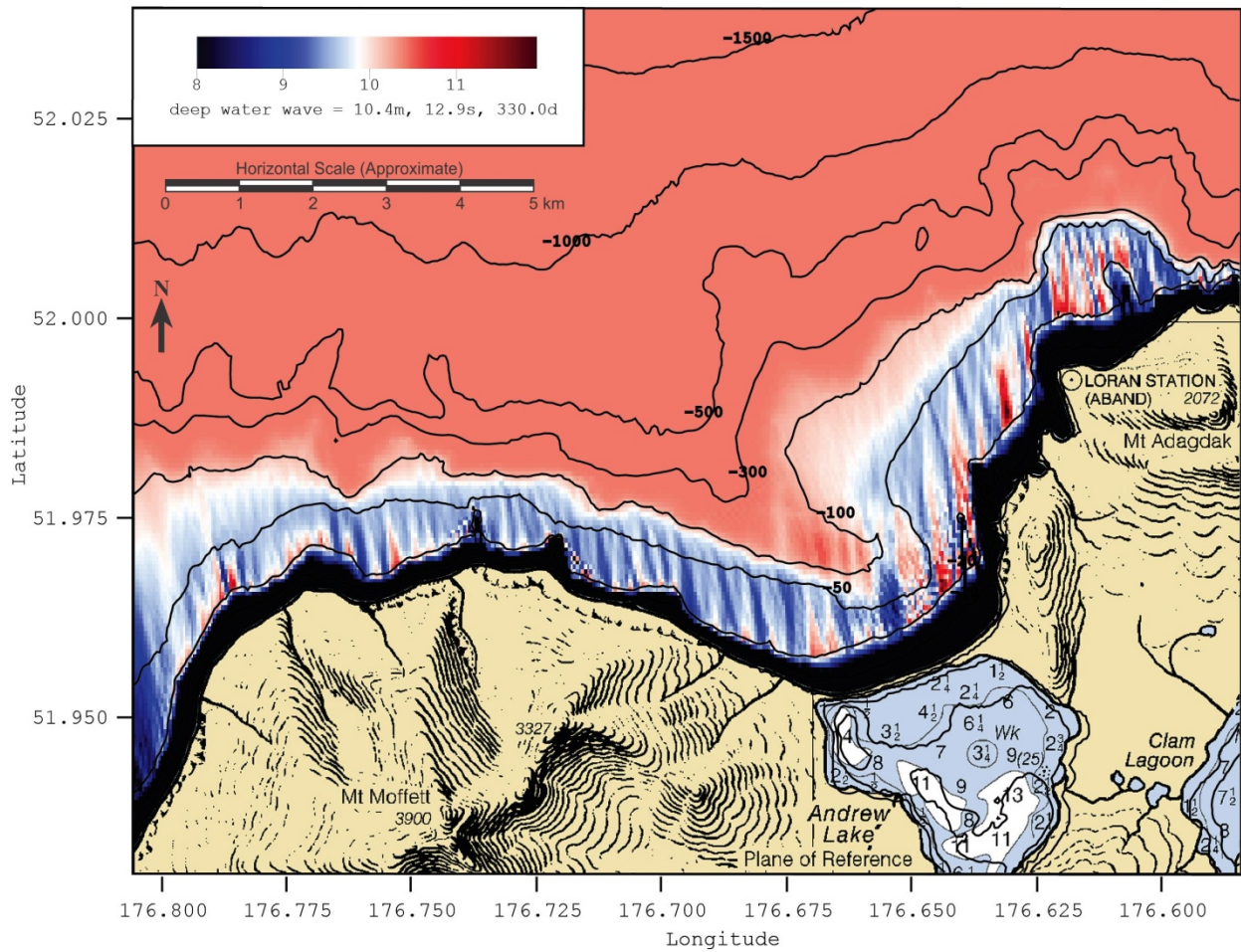


**Figure 3-9. Refraction/Diffraction Pattern of the Five Largest Storms at Andrew Bay (2005-2009)**  
(Wave height = 10.4 m; wave period = 12.9 seconds)

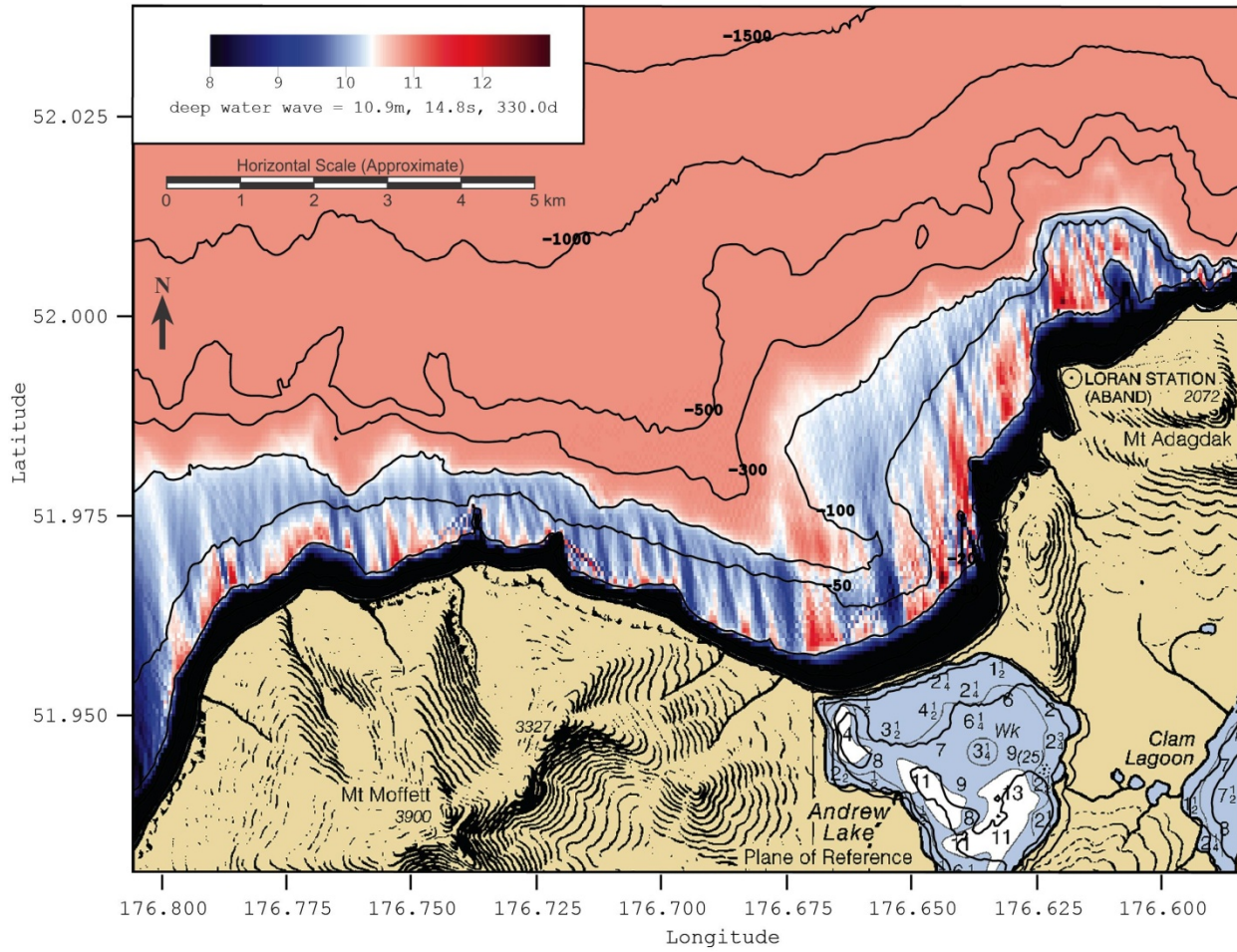


**Figure 3-10. Refraction/Diffraction Pattern of the Five Largest Storms at Andrew Bay (2005-2009)**  
(Wave height = 10.9 m; wave period = 14.8 seconds)

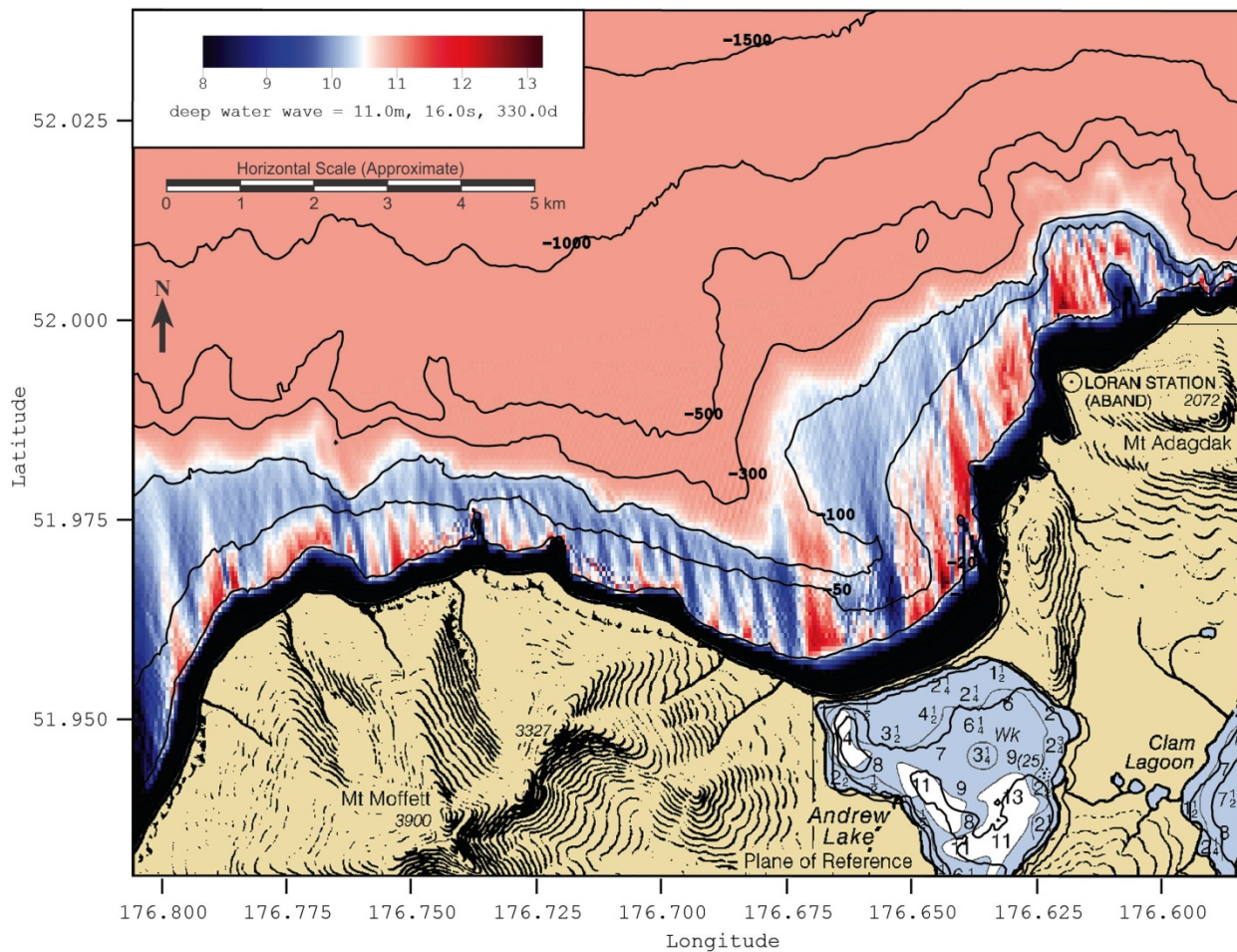


**Figure 3-11. Refraction/Diffraction Pattern of the Five Largest Storms at Andrew Bay (2005-2009)**  
 (Wave height = 11.0 m; wave period = 16.0 seconds)

### 3.4 Bar-Berm and Shore Rise Profile Modeling

The equilibrium bar-berm and shore rise cross-sectional profiles of beaches in general, or in this case, the barrier spit at Andrew Bay, are determined by the extreme events and native grain size distribution (Jenkins and Inman, 2006). In Section 2.2, the size distribution of native gravels, cobble and beach rock on the barrier spit was presented; in Section 3.3 the local wave heights along the barrier spit were computed for the five largest storms in the period of record using refraction/diffraction analysis. Here, those results and similar results from lesser waves in the 2004-2009 period of record are used to compute the envelope of variability of the bar-berm and shore rise profiles of the spit. The equilibrium profiles were calculated using the algorithms published in Jenkins and Inman (2006).

Figure 3-12 presents the simulated shore rise/bar-berm cross sectional profiles of the barrier spit at Andrew Bay. Analytically, these profiles belong to the mathematical class of *type-b elliptic cycloids* (Jenkins and Inman, 2006). Summer equilibrium profiles due to low energy, short period summer waves are plotted in black. Typical winter profiles arising from the long-period, high-energy winter waves are plotted in blue for 8 m high waves, red for 7 m high waves, green for 6 m high waves and gray for 5 m high waves. The blue profile corresponds to the extreme event waves in Figure 3-11. The summer

profile (black) is less steep on the upper bar-berm face of the barrier spit, and has a pronounced offshore bar and trough in the shore-rise section of the profile. The high energy winter waves cause the upper bar-berm face to erode and become steeper, while the shore rise bar and trough are filled in by deposition from the material eroded from the bar-berm section. Beyond a certain depth offshore, referred to as *closure depth*, the beach profile remains invariant, and on the barrier spit at Andrew Bay, closure depth appears in Figure 3-12 to occur at a depth of 28 m, or about 1200 m offshore of the mean sea level contour. These kinds of summer/winter changes in the equilibrium profile are quite typical of sandy beaches (Jenkins and Inman, 2006), but are seen here on the barrier spit of Andrew Bay occurring on a rubble beach formation comprised predominately of rounded beach rock on the order of 25 cm diameter each. The vertical change in elevation of this beach rock profile between the summer and winter equilibrium states is on the order of 2 m. Therefore, it is highly plausible that UXO of comparable size to the native beach rock (e.g., 60 mm and 81 mm mortar, Table 2-1) that are either blended among this beach rock, or sorted down into lower portions of the profile, could be exposed by the winter erosion of the bar berm face, or transported onto the bar-berm face from offshore deposits during transitions from the winter to summer equilibrium profiles. Figure 3-12 suggests that the deepest depths from which this onshore summer migration of UXO could occur is on the order of 28 m. This equilibrium profile response supports the *beach churn hypothesis* from Section 1; namely, UXO are mixed among the beach deposits of gravels, cobbles, and beach rock, and become episodically exposed by sorting, erosion and realignment of the beach profile in response to wave climate variation. For greater resolution of the second hypothesis, and dimensions of the nearshore region affected by seasonal profile change, beach and nearshore profile measurements are needed on a minimum of three range lines along the length of the barrier spit, extending from the seawall to beyond closure depth (a depth of at least 30 m).

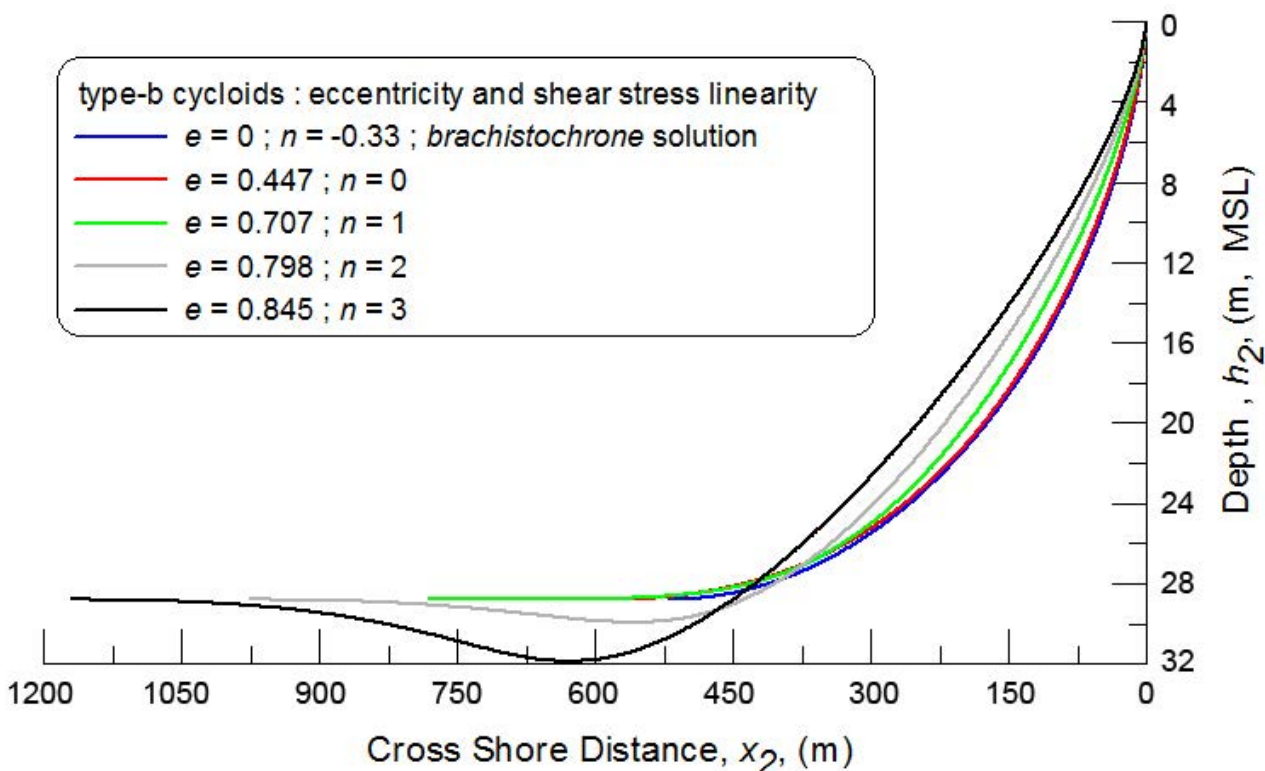


**Figure 3-12. Simulated Shore Rise/Bar-berm Cross Sectional Profile of the Barrier Spit at Andrew Bay**

(Low-energy summer equilibrium profiles plotted in black, high-energy winter profiles plotted in blue, red, green and gray. The blue profile corresponds to waves in Figure 3-11.)

### 3.5 Hydrodynamic UXO Mobility Simulation

In this section, the upgraded UXO mobility model from ESTCP Project # MM-201003 (Jenkins et al., 2011) was implemented in a modified mode-2 fate and transport assessment of the bottom wind hypothesis at Andrew Bay based on micro-bathymetry generated by the 1-arc second resolution digital data base provided by Carignan et. al. (2009), see Figure 1-3. The goal of the mobility analysis was to determine when and where the types of UXO typically found at Andrew Bay would most likely mobilize and in which direction they are likely to move. Three general types of UXO were selected for analysis herein. The 60 mm and 81 mm mortar rounds were selected for size matching with native beach rock and for relative ease of potential mobility and comparable size (Section 2.2); the 20 mm and 40 mm rounds were selected to represent the high mobility UXO types due to their relative small size and size similarity with the gravels and smaller cobble fractions found at Andrew Bay (Section 2.2), and the 2000 lb bomb was chosen due to its high critical shear stress value (i.e., low potential for mobility) and size similarity with the largest fractions of beach rock found at Andrew Bay (Section 2.2). These three example categories represent the range mobility characteristics of the typical UXO found in Andrew Bay. An additional objective of this implementation is to demonstrate how the increased computational efficiency and numerical stability afforded by this UXO mobility model upgrade allows simultaneous computations of the potential migration of large numbers of UXO over large areas. Through this implementation effort, it will also be shown that a natural sorting mechanism of the UXO occurs in response to long-term wave climate interacting with the unique features of the Andrew Bay bathymetry,

which has important implications for remediation planning and in assessing potential risk of human contact with underwater UXO.

For each of these three UXO size classes, a numerical experiment was conducted, 20 years in duration, by looping the wave record in Figure 2-6 through five repetitive cycles. This ensures stability and convergence in any of the mobility tendencies that occur in the simulation. For each of these 20-year simulations, the Andrew Bay bathymetry in Figure 1-3 was populated with a hypothetical, uniformly distributed ensemble of 500 each of a given UXO type. The uniform distribution was limited from the 300 m depth contour into the shore, and confined between the headlands of the Bay.

Two biogenic site features are neglected in these simulations: kelp and bio-fouling. The kelp only grows shoreward of the 30 m depth due to depth attenuation of ambient light (consistent with notations in NOAA charts; Section 2.0 and 2.2.1). In these nearshore locations kelp stands are uprooted during the high-energy winter months by shoaling, long-period waves, 6 m and higher, and this is when most of the UXO mobility occurs. The kelp grows back rapidly during the long, arctic summer days, but the waves are generally very small at this time (Figure 2-8), whence not much UXO mobility would occur. Because of this seasonality, it is unconvincing that kelp is a direct factor on predominant UXO transport processes. The biofouling is neglected under the premise that the model analysis is being conducted under a set of simplifying assumptions that maximizes risk in the risk assessment and seeks the most plausible outcome by the two operative hypotheses. Biofouling would impede mobility by creating angularity on otherwise smooth, rounded UXO shapes and by cementing the UXO to hard bottom substrate.

Figure 3-13 shows the general flow pattern over a subset of the initial 60 mm mortar UXO population, as rendered by a sheet of instantaneous streamlines under a wave crest (shoreward transport from right to left). The simulation is based on the rigid bottom formulation that assumes bare bedrock seaward of the 30 m depth contour. The wave used in this simulation is incident from  $330^{\circ}$  N, has a 4 m wave height and 12 second period (typical of a moderate size swell propagating into the Bay from the Bering Sea). Under the wave crest the general circulation is onshore producing both bathymetric divergence and large-scale eddying over portions of the bedrock shelf slope having either expansion or contraction sections in bottom features or which exhibit longshore turning in the axis of the bottom depressions. These types of non-uniformities in the general flow field create significant variation in the intensity of the nearfield flow disturbances acting on any given UXO (and hence differences in onset of motion among individual UXO). Vertical divergence of the flow field over a hummock or bottom depression promote sub-critical flow conditions over the UXO that retard migration while promoting burial if sufficient sediment cover is present. On a high spot (Figure 3-14) near bottom flow is intensified, promoting large hydrodynamic forces on the UXO round and inducing migration when threshold of motion criteria (Figure 3-6) are exceeded. However, it is likely that these bathymetric-induced flow variations tend to average out in over a large randomly distributed UXO population; and over a long-term (20-year) simulation with variable wave direction. The eddying and flow divergence over the 500 individual UXO distributed across Andrew Bay is highly directionally dependent.

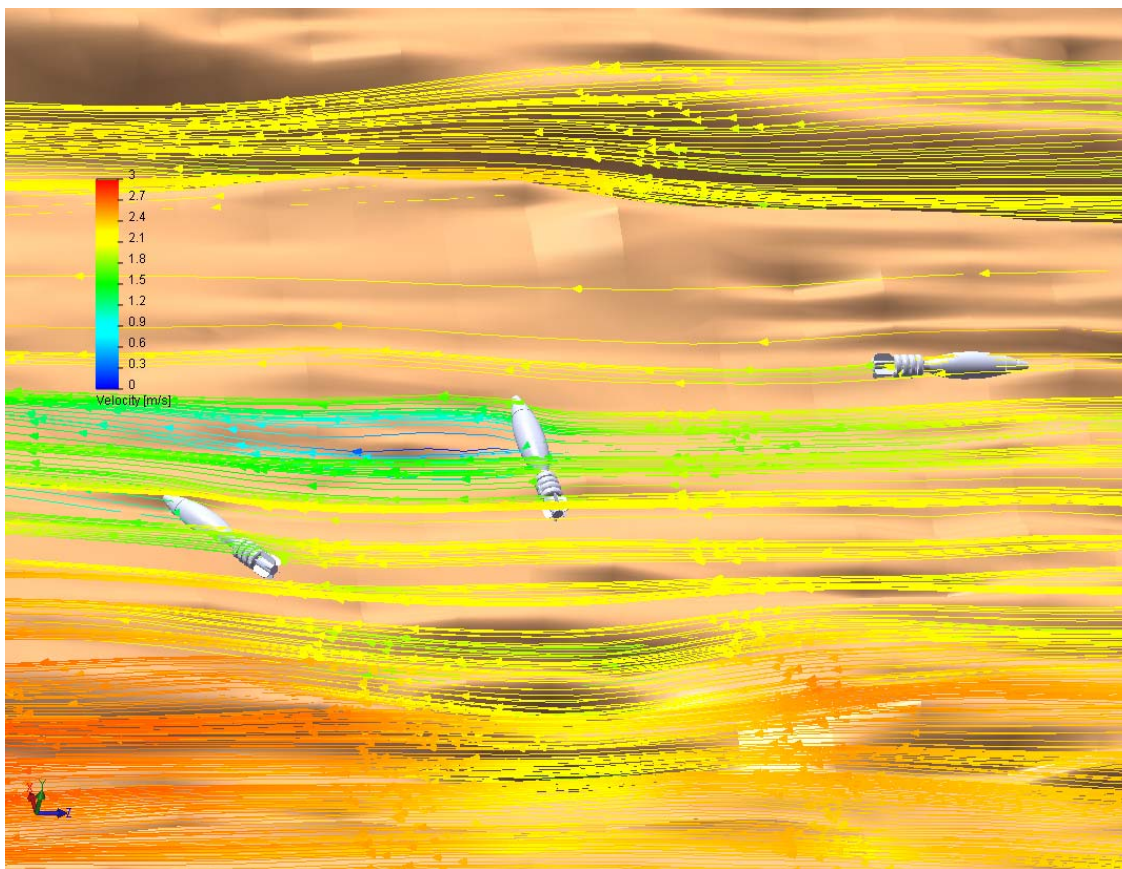


**Figure 3-13. Simulation of Flow Divergence Induced over 60 mm Mortar UXO by the Expansion and Contraction of Near Bed Flow Field over High and Low Spots in the Bottom Micro-bathymetry of Andrew Bay**

(This simulation is based on the rigid bottom formulation.)

Figure 3-14 shows the instantaneous vertical velocity profile over a 60 mm mortar in a plane oriented in the on/off shore direction. For comparison, this figure uses the same incident waves as Figure 3-13, but with a movable bottom formulation. The occurrence of flow separation over a UXO positioned on a high spot on the bottom exerts large pressure and shear stress on that round (Figures 3-15 and 3-16) that promote migration. Pressure and shear stress distributions like those in Figure 3-16 integrate over the body of the UXO round to produce the net hydrodynamic forces that overcome gravity and induce motion (Figure 3-6). The forces required to move UXO upslope against gravity under a wave crest are significantly larger than the forces required to move UXO downslope under a wave trough, when gravity augments hydrodynamic forces in moving the round. Therefore, the mobility of a large number of UXO in a complex area such as Andrew Bay has significant stochastic factors associated with that mobility. As these examples indicate, the presence of bottom irregularity associated with micro-bathymetry has a strong bearing on whether hydrodynamic forces on the UXO are locally intensified or diminished by local flow convergences (over high spots) or local flow divergences (over divergences). In addition, location factors related to whether a given UXO is in a bright spot or a shadow of the regional refraction/diffraction pattern will obviously exert a strong influence on the propensity for a given UXO to become mobile. The nature of the bottom substrate also affects UXO mobility.

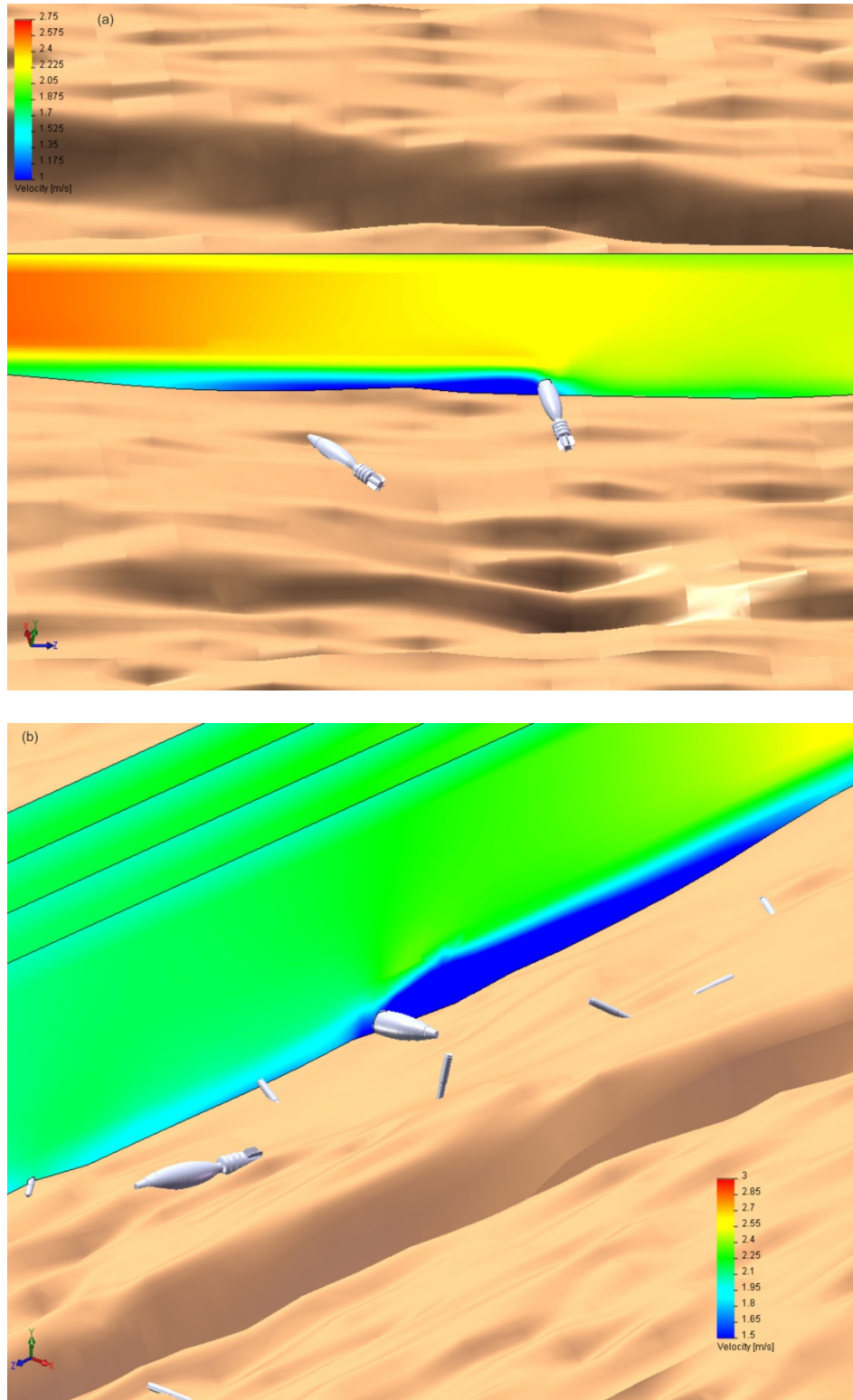


**Figure 3-14. Vertical Velocity Profile over a 60 mm Mortar Round Resting on an Irregular Sloping Bottom at Andrew Bay**  
(This simulation is based on the movable bottom formulation.)

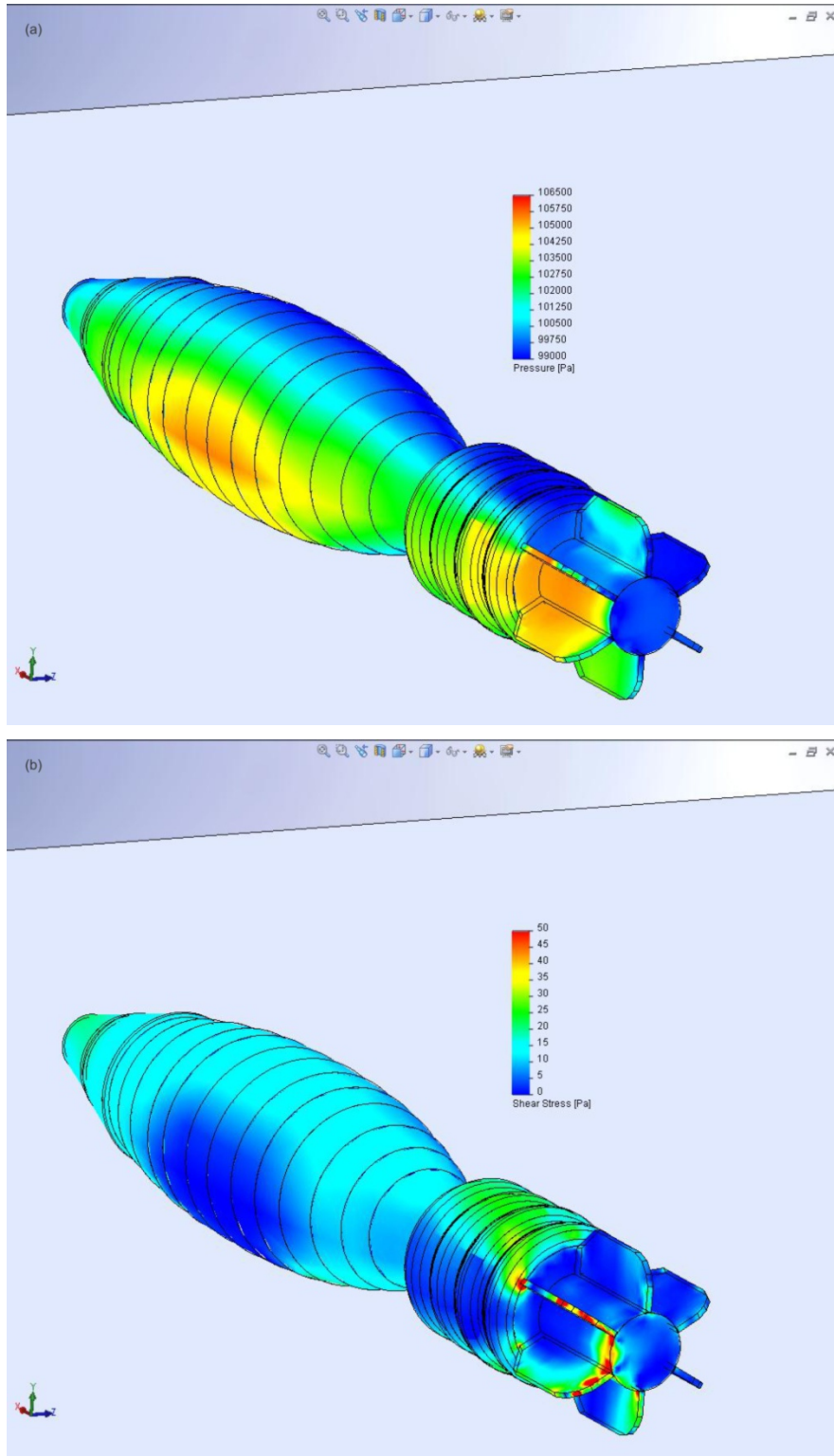


**Figure 3-15. 60 mm Mortar Round Resting on an Irregular Sloping Bottom at Andrew Bay: (a) Pressure Distribution; and (b) Shear Stress Distribution**  
(Wave and flow conditions from Figures 3-13 and 3-14.)

Bottom substrate type drives the sorting mechanism by increasing the mobility of UXO on hard, rocky or gravel bottom types and reducing their mobility on sandy or silty bottom types. That mechanism is due to the differences in rolling resistance for UXO on hard bottom vs. soft bottom types. On a sandy or silty soft bottom, onset of motion and migration is constrained by partial burial. As a result, there is resistance to motion by the gravitational and granular force moments in Figure 3-6 associated with the burial depth. These rolling resistance forces require additional drag and added mass forces from the fluid motion to both raise the UXO out of its scour hole and then push it against the granular shearing forces and dispersive pressures of the soft sedimentary bed. However, for UXO perched on a hard bottom, there are no such rolling resistance forces because there is no burial, as the UXO rests on hard substrate. Without burial, the fluid motion is able to get under the UXO, as shown in Figure 3-16 for a 2000 lb bomb, that produce lift forces, and consequently larger fluid dynamic drag associated with those lift forces (induced drag). (The induced drag is associated with the complex vortex structure in the lower panel of Figure 3-16). With no rolling resistance and enhanced fluid dynamic forces, UXO becomes more mobile on hard substrate. This enhanced mobility on hard substrate also allows the UXO to migrate under the influence of even the most mild slope gradients. Figure 3-17 shows an upgraded UXO mobility model simulation of a UXO migration pathway following a local slope gradient. While a rolling cone would roll in a closed circle on a flat plane surface, a paraboloid of revolution such as a UXO will roll in a series of J-shaped trajectories directed down-slope, with each J-shaped trajectory (numbered 1 through 8 in Figure 3-17) resembling elliptic cycloids of varying eccentricity depending on the local slope (Jenkins and Inman, 2006). This rolling behavior was observed in the field as reported in Wilson and Jenkins (2005). Rocky crags and crevices acting to wedge the UXO in place on a hard bottom were neglected in the model initialization and physics. This is another example of how the model analysis is being conducted under a set of simplifying assumptions that maximizes risk in the risk assessment and seeks the most plausible outcome by the two operative hypotheses. However, these dynamics indicate the future need for better mapping of bottom type, sediment cover and micro-bathymetry at Andrew Bay to better account for the stochastic influences of bottom detail on the simulation results.

The hydrodynamic influences of stochastic features related to UXO location, bottom type, bathymetric roughness and directional wave variability underscore the need for large ensemble, long-term simulations to assess UXO mobility. Because of these stochastic factors, there is no single quantitative measure of what mobility is. For that reason, the results are presented in terms of probability density functions, cumulative probability curves of UXO migration distance, and dividing those mobilities into three directional categories: onshore, longshore and offshore. In all cases, the rigid bottom formulation is used in the offshore domain (seaward of the 30 m depth contour) to estimate the most plausible outcome for these probability density functions and cumulative probability curves (Section 2.2.1). Figures 3-18 and 3-19 give the probability density functions and cumulative probability curves of UXO migration distance for onshore transport of the 60 mm and 81 mm UXO size class at Andrew Bay onshore, longshore and off shore transport directions, respectively. The cumulative probability curves show that the UXO migration after 20 years is predominately downslope and offshore, with only 1.5% of the mid-sized UXO population migrating onshore (as compared with 88% migrating offshore), while 10.5% migrate alongshore, moving from areas of high waves near the headlands towards areas of low waves, principally abeam the mid-point of the barrier spit dividing Andrew Cove from Andrew Bay.

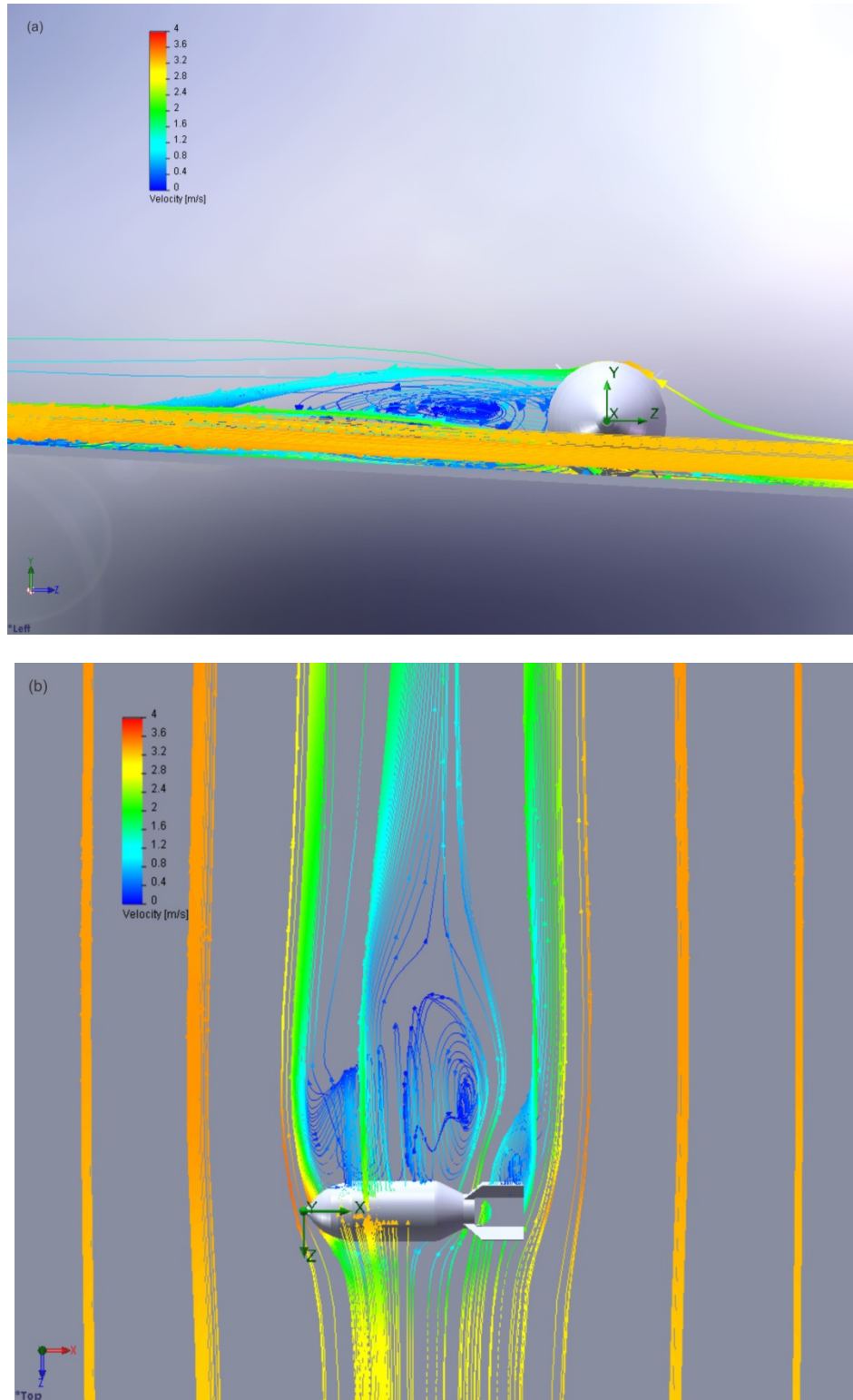


**Figure 3-16. Upgraded UXO Mobility Model Simulation of Local Flow Field around a 2000 lb Bomb UXO Resting on Hard Sloping Substrate with no Burial (rigid bottom formulation)**

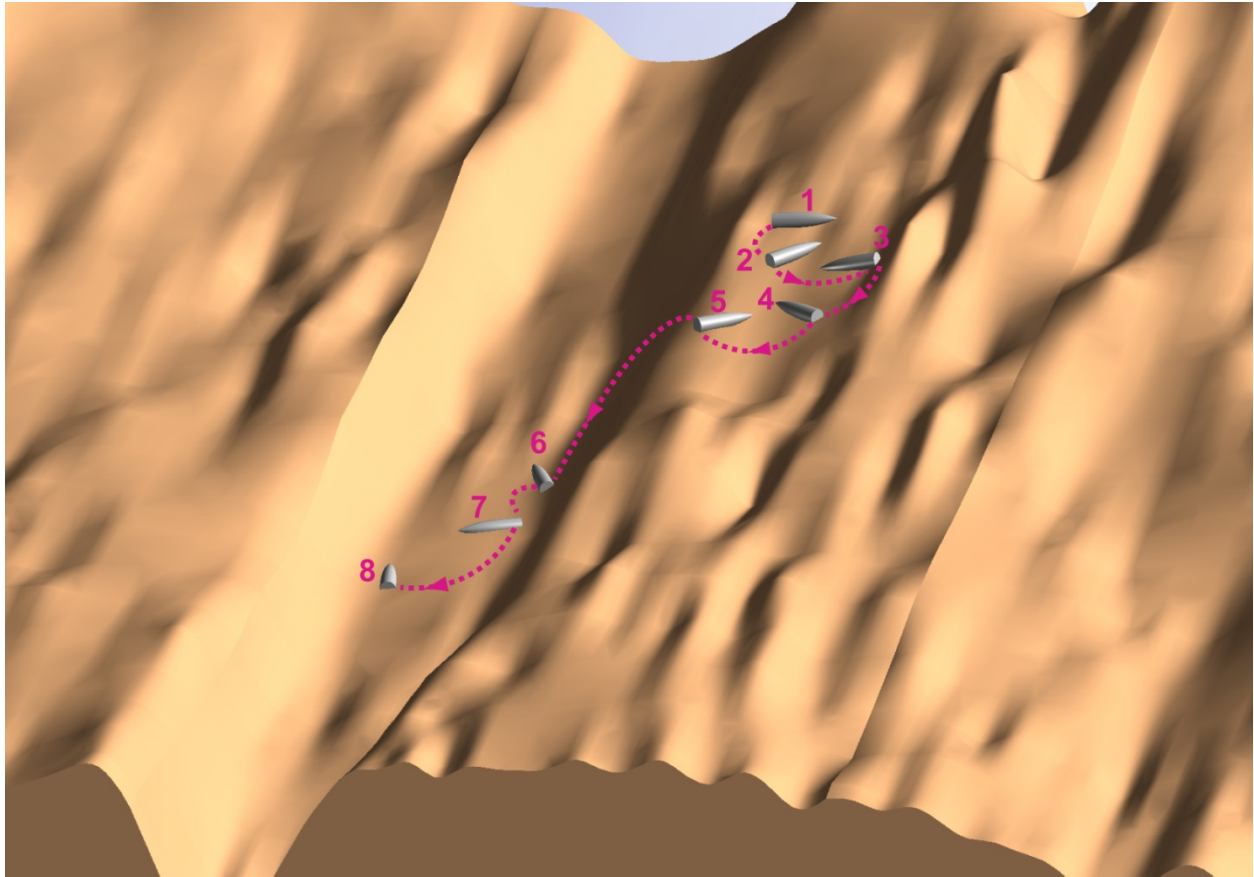


**Figure 3-17. Mechanics of UXO Downslope Migration Progression**

(Bathymetric roughness features rendered in brown; UXO rendered in silver [from Jenkins et al., 2012].)

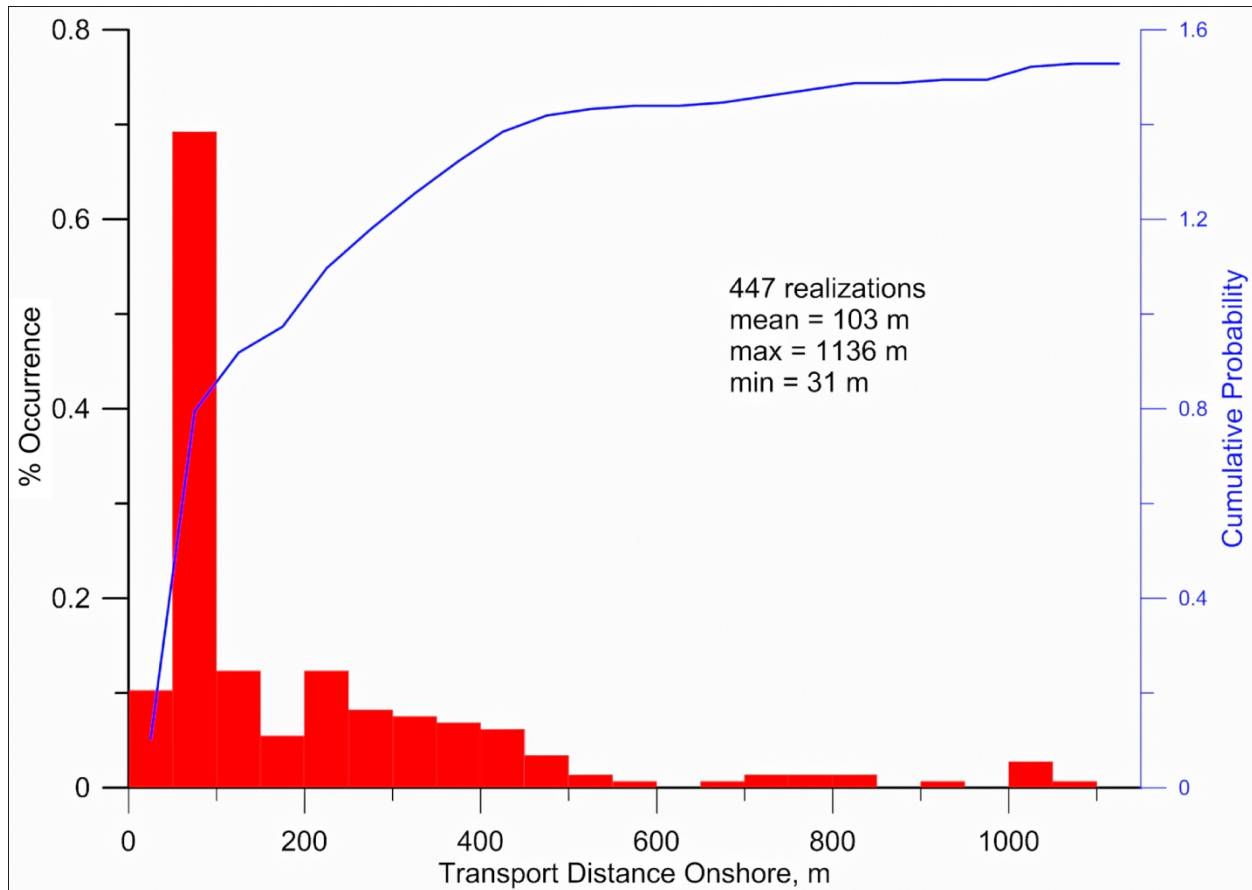


**Figure 3-18. Probability Density Function (red) and Cumulative Probability (blue) for Onshore Transport of 60 mm and 81 mm UXO at Andrew Bay; Based on Rigid Bottom Formulation in the Offshore Domain (seaward of the 30 m depth contour)**

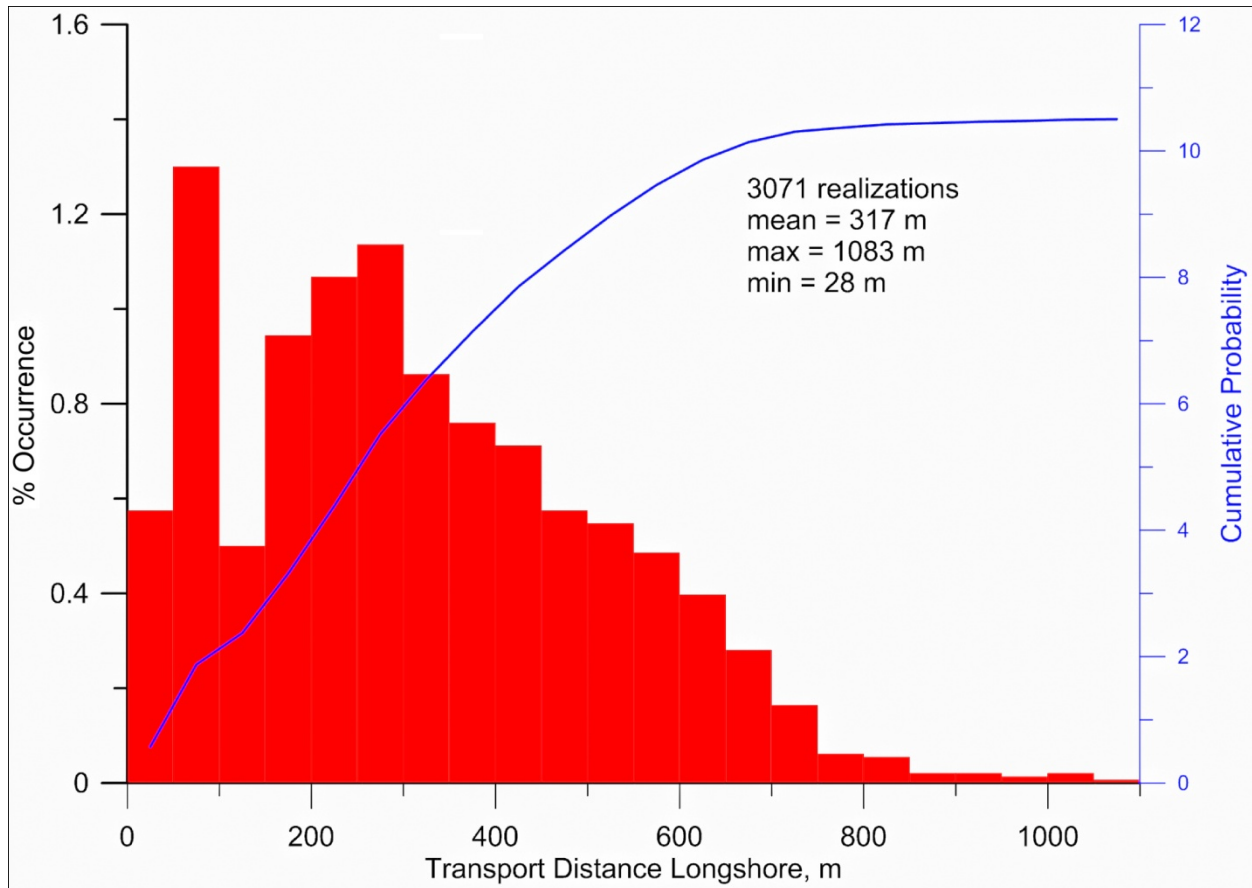


**Figure 3-19. Probability Density Function (red) and Cumulative Probability (blue) for Longshore Transport of 60 mm and 81 mm UXO at Andrew Bay; Based on Rigid Bottom Formulation in the Offshore Domain (seaward of the 30 m depth contour)**

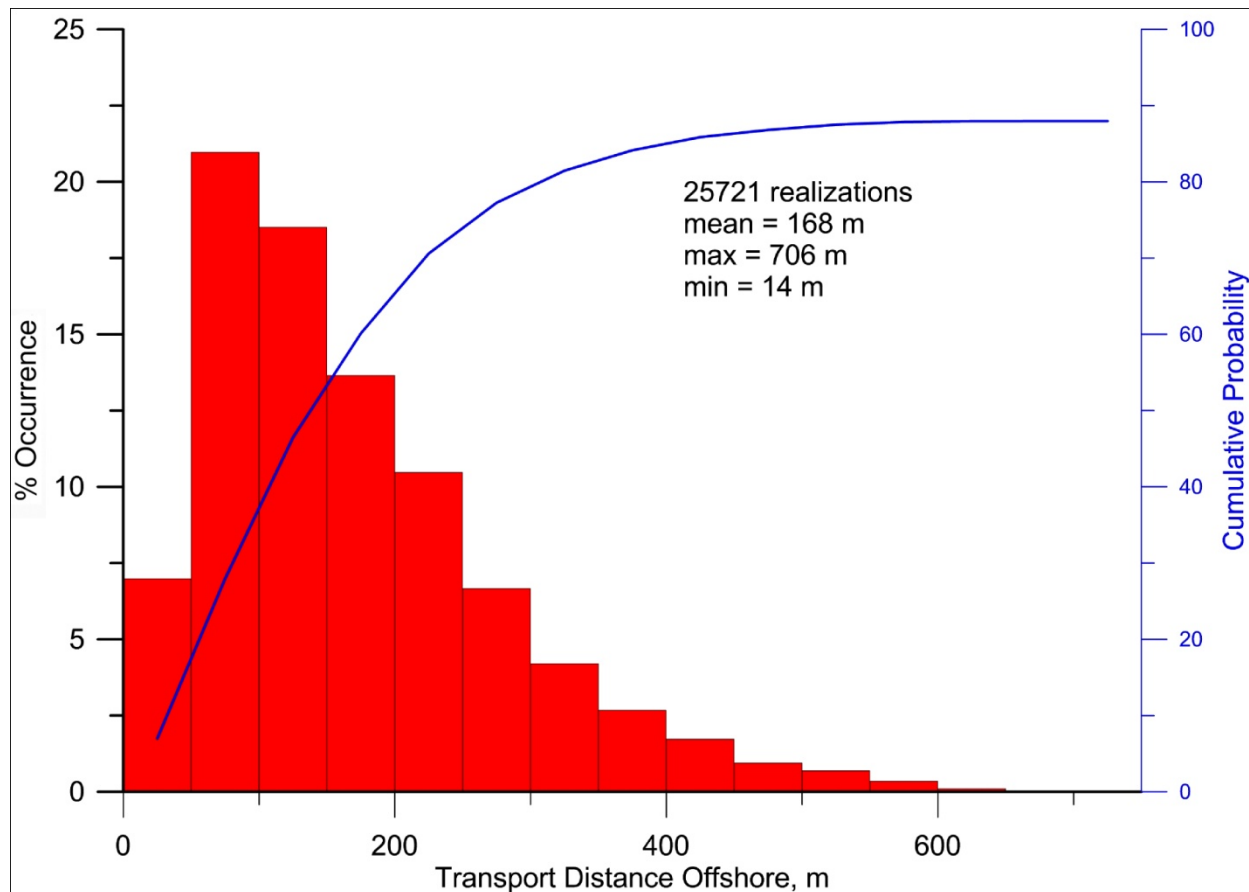


**Figure 3-20. Probability Density Function (red) and Cumulative Probability (blue) for Offshore Transport of 60 mm and 81 mm UXO at Andrew Bay; Based on Rigid Bottom Formulation in the Offshore Domain (seaward of the 30 m depth contour)**

This transport pattern for the mid-sized UXO population is representative of all size classes of UXO at Andrew Bay, and is the outcome of about 30,000 combinations of wave height, period and direction and UXO location initially spread uniformly across Andrew Bay. On closer inspection of Figure 3-18, the average onshore transport distance of 60 mm and 81 mm UXO is 317 m, while the maximum onshore migration distance of the 60 mm and 81 mm mortar rounds is 1,136 m, in rough agreement with the maximum distance seaward from the barrier spit where seasonal equilibrium profile adjustments still occur (i.e., distance to closure depth, Figure 3-3). This supports the fate and transport of the bottom wind hypothesis that implies this UXO size class behaves similarly to the comparatively sized native beach rock. Onshore transport is typically the result of the longer period high energy waves, and the minimum onshore migration distance of the 60 mm and 81 mm mortar is 31 m, roughly the width of the portion of barrier beach between the mean higher high water level and the mean tide line (based on the winter profiles in Figure 3-3). The preponderance of migration of the 60 mm and 81 mm mortar rounds at Andrew Bay is offshore (Figure 3-20), in the direction of the action of the downslope gravitational component (Figure 3-6). The average offshore movement of this size class of UXO is 168 m, while the maximum excursions are 706 m and the minimums are 14 m. Maximum offshore displacements are less than the onshore movements for several reasons: 1) offshore movement of the UXO places them in deeper water where maximum wave induced velocities and pressure gradients are less; and 2) offshore movement follows bottom slope gradients that result in the UXO finding resting places in bottom

depressions where flow divergence produces smaller hydrodynamic forces on the rounds. The longshore migration distances of 60 mm and 81 mm UXO in Figure 3-19 (when bottom slope gradients are diminishing small), show the largest average displacements, 317 m. Maximum longshore displacements are 1,083 m (comparable to maximum onshore displacements), and occur in bright spots of the local refraction patterns where wave heights and wave induced velocities are highest. Minimum longshore transport distances are 28 m, occurring in and around shadow zones of the local refraction patterns.

Figure 3-21 shows the flow pattern over a subset of the initial 20 mm and 40 mm UXO population due to a sheet of instantaneous streamlines under a wave crest (shoreward transport from right to left). The wave used in this simulation is the same as in Figures 3-13 and 3-14. Again, the general circulation is onshore and displays bathymetric divergence and convergence over the bottom depressions and high spots. Due to the low profile of these small rounds above the native bottom, the non-uniformities in the general flow field that arise from bottom roughness create significant variation in the intensity of the nearfield flow disturbances acting on any given UXO; thereby magnifying differences in the distributions of pressure and shear stress acting to induce motion of that round (Figures 3-22 and 3-23). In particular, small caliber rounds such as those that rest in a low spot can become virtually sheltered from the effects of the general flow field that separates over the bottom depression, leaving the UXO at rest in what might be termed a “wind shadow”. On the other hand, small caliber rounds resting on a high spot become exposed to super critical flow speeds in relatively moderate wave climate, and are induced to move relatively early, potentially travelling great distances unless a bottom depression is encountered. The small caliber rounds behave much like the native gravels and are capable of movement in both bed load and suspended load transport states.

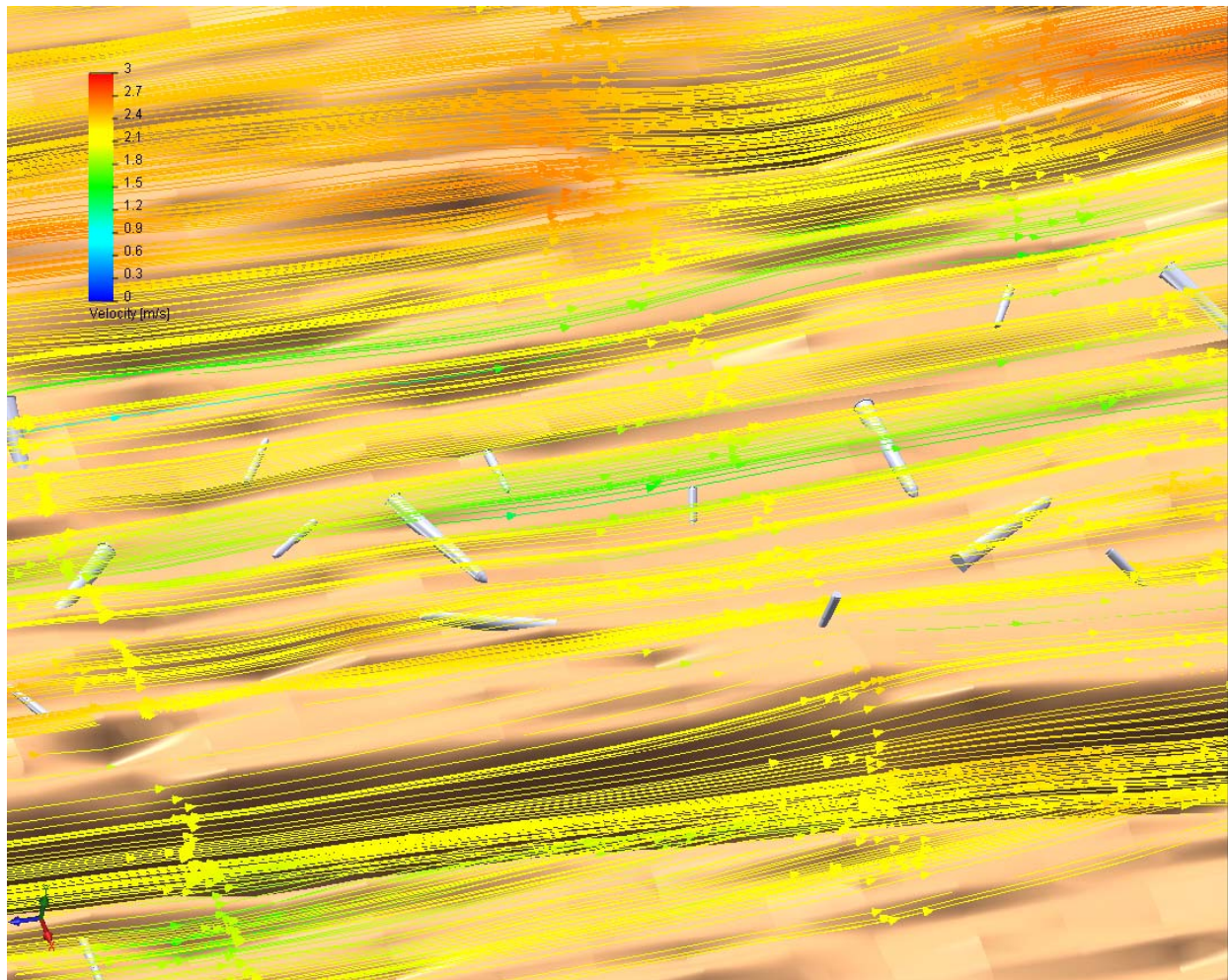


**Figure 3-21. A Simulation of Flow Divergence Induced over 20 mm and 40 mm UXO by the Expansion and Contraction of near Bed Flow Field over High and Low Spots in the Bottom Micro-bathymetry of Andrew Bay**  
(Simulation based on movable bottom formulation.)

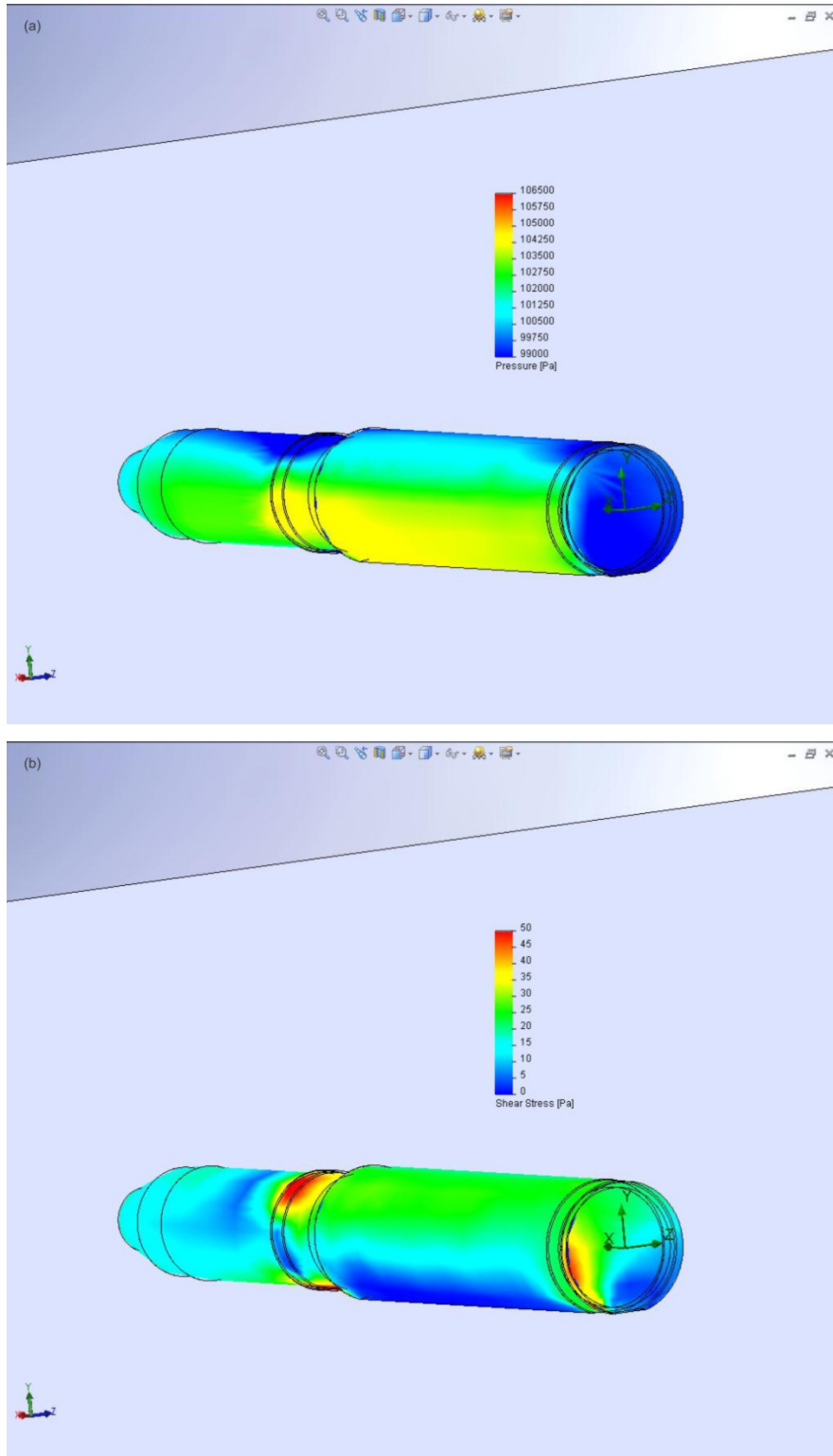


**Figure 3-22. 20 mm UXO Resting on an Irregular Sloping Bottom at Andrew Bay: (a) Pressure Distribution; and (b) Shear Stress Distribution**  
(Wave and flow conditions from Figures 3-13 and 3-14.)

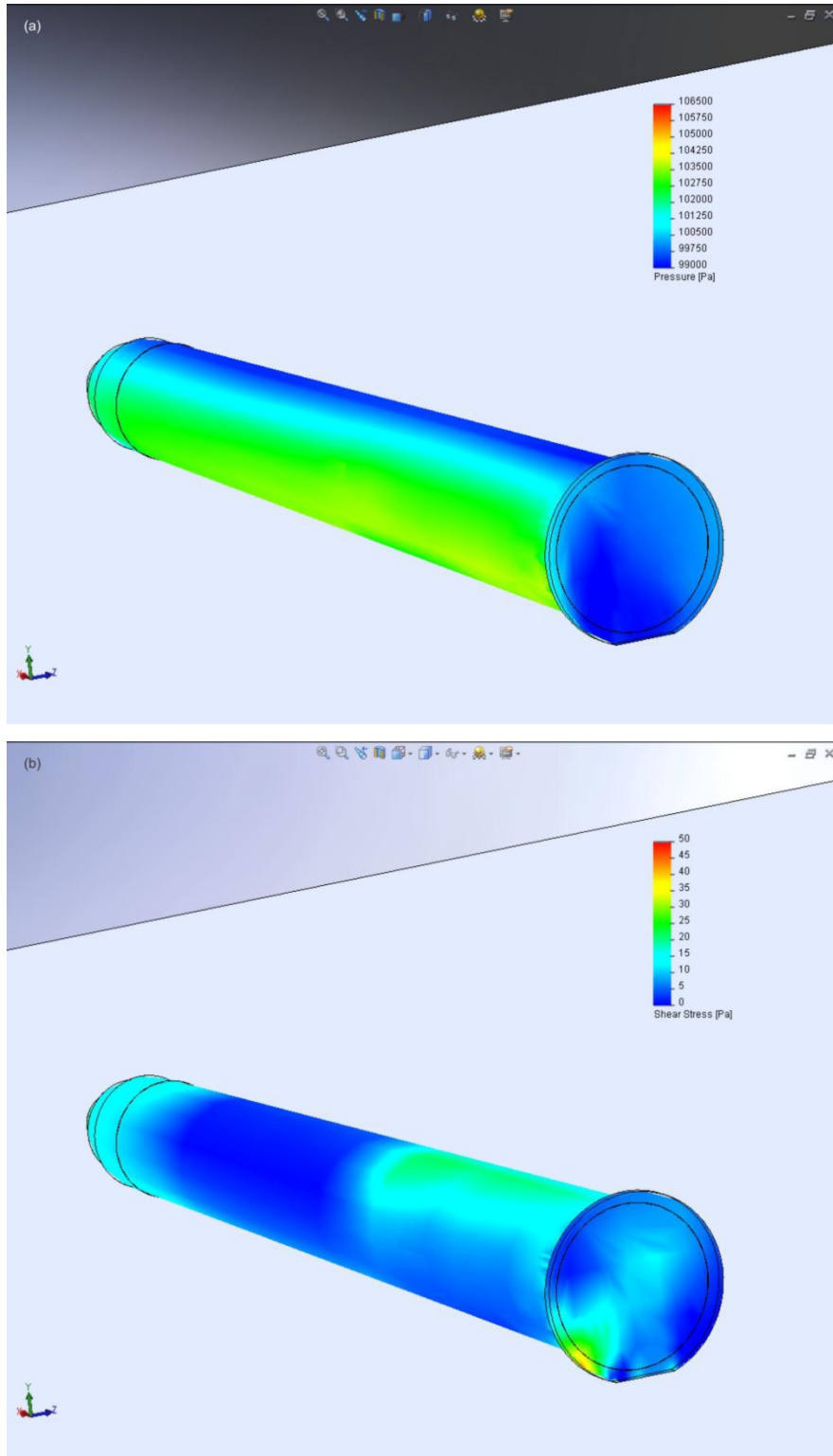


**Figure 3-23. 40 mm UXO Resting on an Irregular Sloping Bottom at Andrew Bay: (a) Pressure Distribution; and (b) Shear Stress Distribution**  
(Wave and flow conditions from Figures 3-13 and 3-14.)

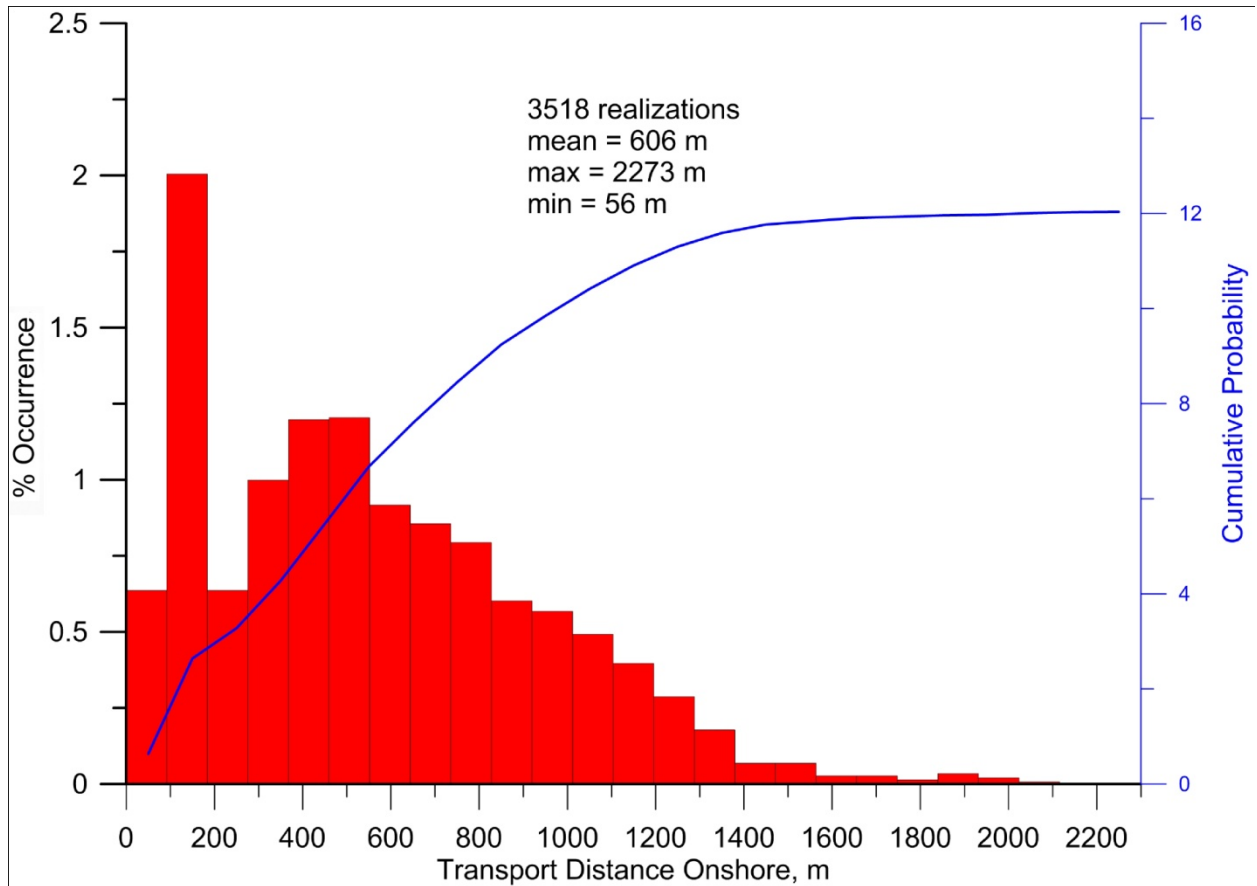


**Figure 3-24. Probability Density Function (red) and Cumulative Probability (blue) for Onshore Transport of 20 mm and 40 mm UXO at Andrew Bay; Based on Rigid Bottom Formulation in the Offshore Domain (seaward of the 30 m depth contour)**

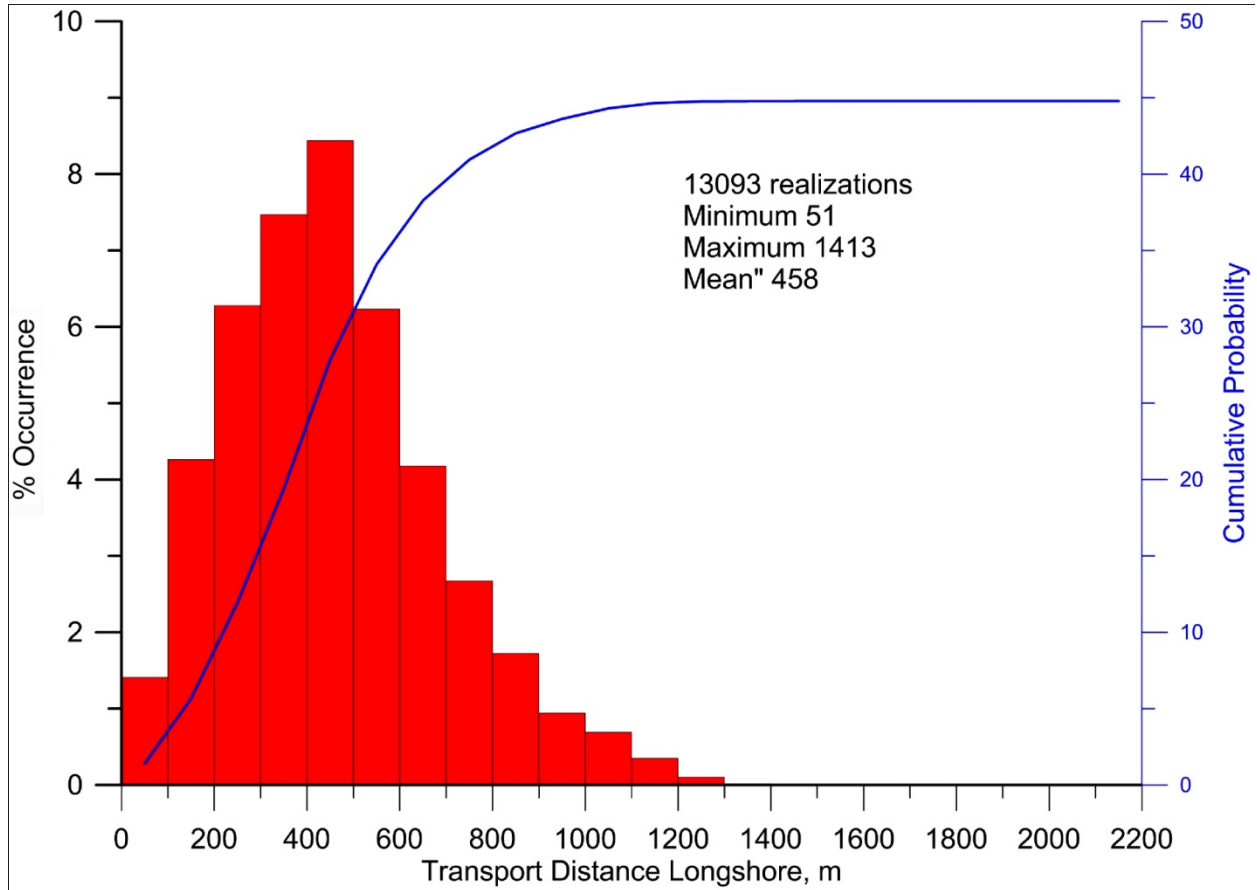


**Figure 3-25. Probability Density Function (red) and Cumulative Probability (blue) for Longshore Transport of 20 mm and 40 mm UXO at Andrew Bay; Based on Rigid Bottom Formulation in the Offshore Domain (seaward of the 30 m depth contour)**

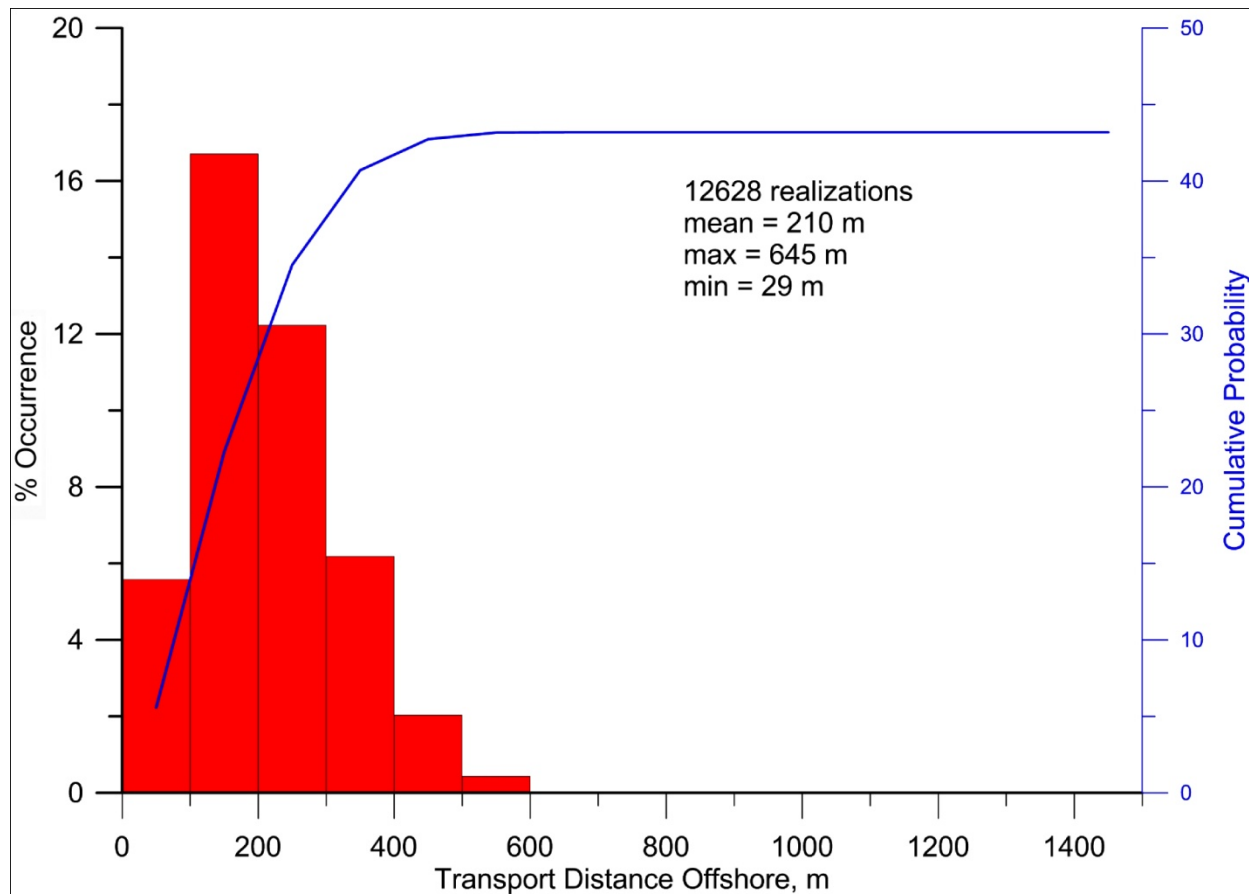


**Figure 3-26. Probability Density Function (red) and Cumulative Probability (blue) for Offshore Transport of 20 mm and 40 mm UXO at Andrew Bay; Based on Rigid Bottom Formulation in the Offshore Domain (seaward of the 30 m depth contour)**

Figures 3-24 through 3-26 give the probability density functions and cumulative probability curves of UXO migration distance for onshore transport of the 20 mm and 40 mm UXO size class at Andrew Bay onshore, longshore and offshore transport directions, respectively. The cumulative probability curves of the small caliber UXO show that migration after 20 years has a significantly higher likelihood of onshore transport than the larger 40 mm and 81 mm size class, but is still predominately downslope and offshore or alongshore. Twelve percent of these small caliber UXO migrate onshore (usually in response to the longer period high energy waves), while 43% migrate offshore and 45% migrate alongshore. Figure 3-24 indicates that the maximum onshore transport distance for the small caliber rounds is considerable, on the order of 2,273 m, while the average onshore migration distance of the 20 mm and 40 mm rounds is 606 m, nearly twice that as the 60 mm and 81 mm mortar rounds in Figure 3-19. Minimum onshore migration distance of the 20 mm and 40 mm rounds is 56 m. Offshore migration of the 20 mm and 40 mm mortar rounds at Andrew Bay (Figure 3-26) averages 210 m, while the maximum excursions are 645 m and the minimums are 29 m. Again, offshore displacements are less than the onshore movements because of wave attenuation in deeper water and bottom slope channeling of small caliber rounds to resting places in bottom depressions. The largest displacements of the small caliber UXO occur in the longshore direction (Figure 3-25) with average displacements of 458 m and maximum longshore displacements of 1,413 m occurring in bright spots of the local refraction patterns.

Minimum longshore transport distances are 51 m, occurring in shadow zones of the local refraction patterns.

Figure 3-27 shows the near bottom flow pattern over a 2000 lb UXO bomb as rendered by a sheet of instantaneous streamlines under a wave crest (shoreward transport from right to left). Again, the wave used in this simulation is incident from 330 degrees north, has a 4 m wave height and 12 second period. For scale comparison with Figure 3-19, two 60 mm mortars are also included in the nearfield of the bomb. The general circulation in the nearfield is dominated by the bomb shape itself, while micro-bathymetry tends to be second order bed roughness. The cross section of the bomb creates the predominant local field accelerations and large contrasts in pressure and shear stress distributions over the surface of the bomb (Figure 3-28). These pressure and shear stress distributions in turn result in large hydrodynamic reaction forces acting to move the bomb (via rolling action). However the presence of any amount of sediment cover will contribute to partial or complete burial of the bomb, and resistance to rolling motion of the bomb by the gravitational and granular force moments depicted in Figure 3-6. The extreme immersed weight of the bomb (whose specific gravity is on the order of three times that of sea water), contributes both to at rest inertia, as well as adverse potential energy that opposes upslope, onshore transport of the bomb under wave action. These inertia effects contribute to very muted mobility of the bomb, as indicated in the migration probability distributions in Figures 3-29 through 3-31.

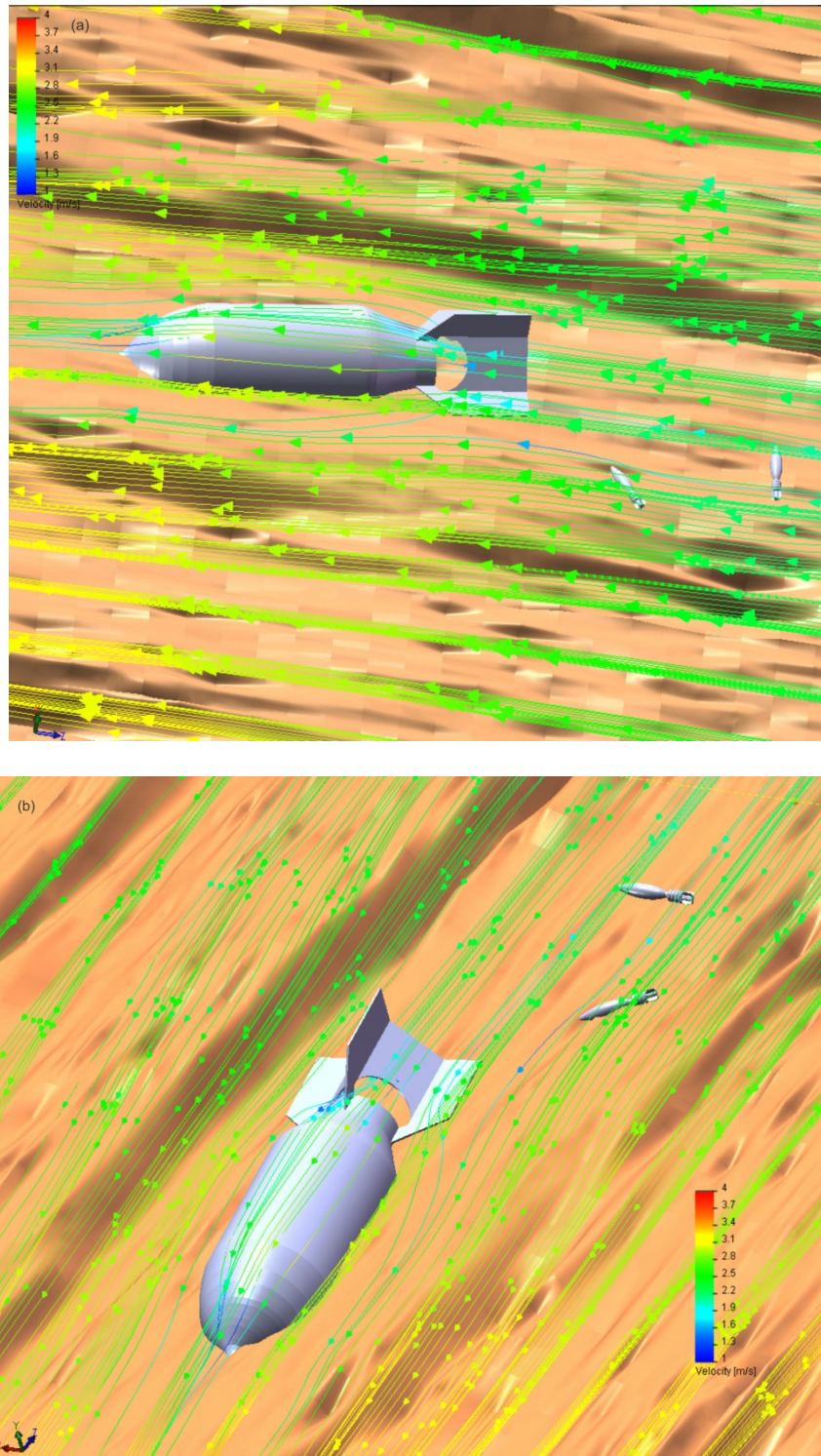


**Figure 3-27. Simulation of Nearbed Flow over a 2000 lb UXO Bomb Resting on an Irregular Sloping Bed at Andrew Bay**  
(Upper panel based on rigid bottom formulation; lower panel based on movable bottom formulation.)

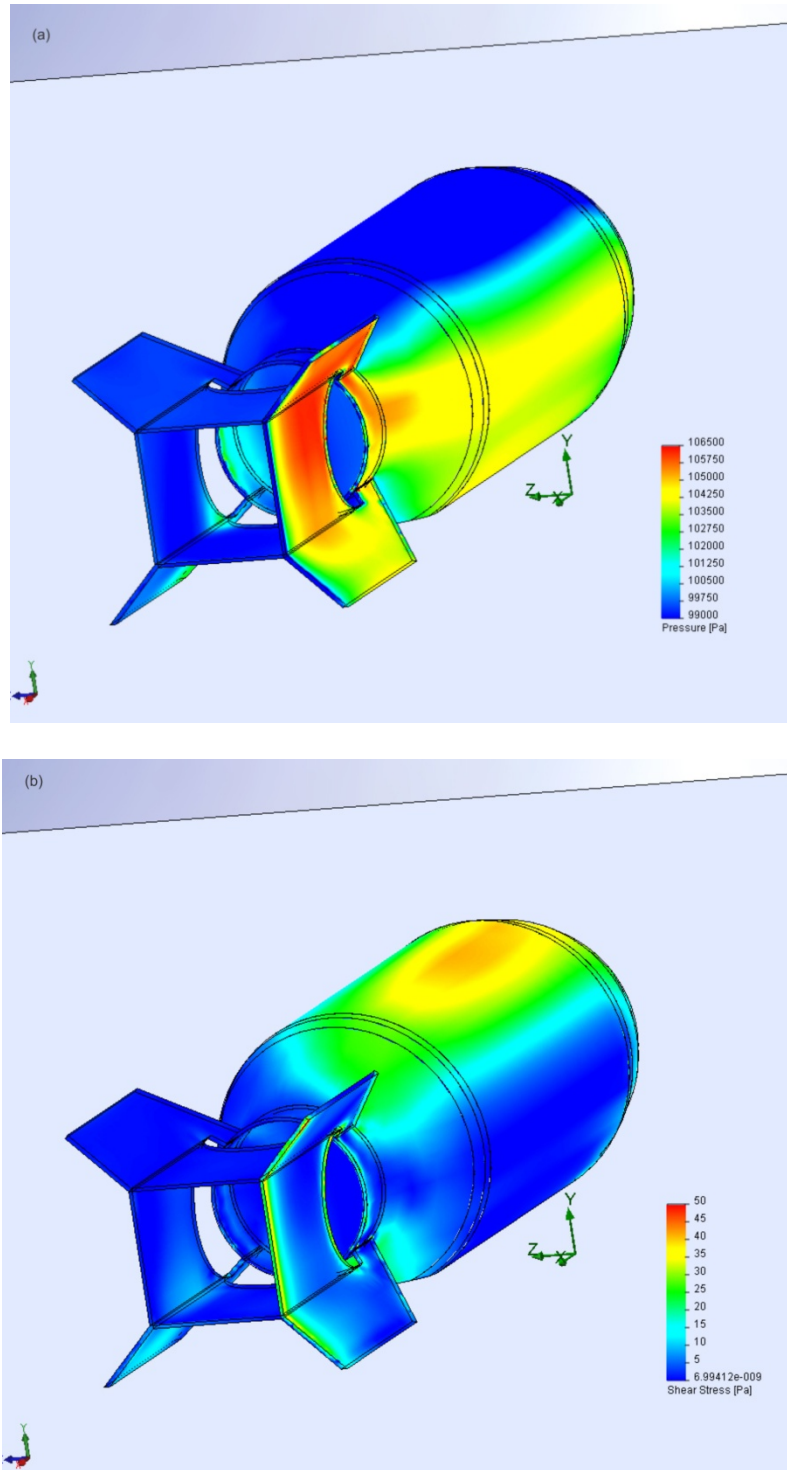


**Figure 3-28. 2000 lb UXO Bomb Resting on an Irregular Sloping Bottom at Andrew Bay: (a) Pressure Distribution; and (b) Shear Stress Distribution**  
(Wave and flow conditions from Figure 3-27.)

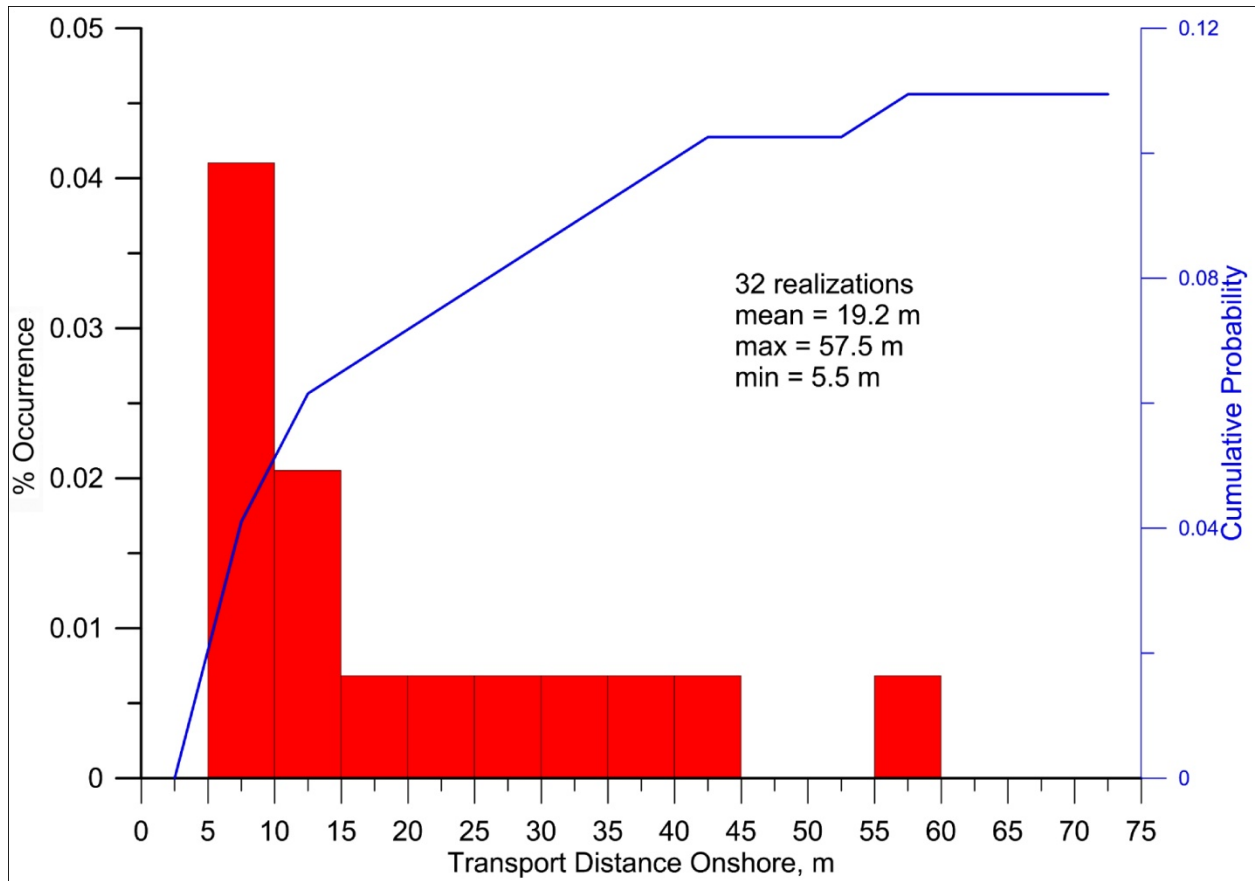


**Figure 3-29. Probability Density Function (red) and Cumulative Probability (blue) for Onshore Transport of a 2000 lb UXO Bomb at Andrew Bay; Based on Rigid Bottom Formulation in the Offshore Domain (seaward of the 30 m depth contour)**

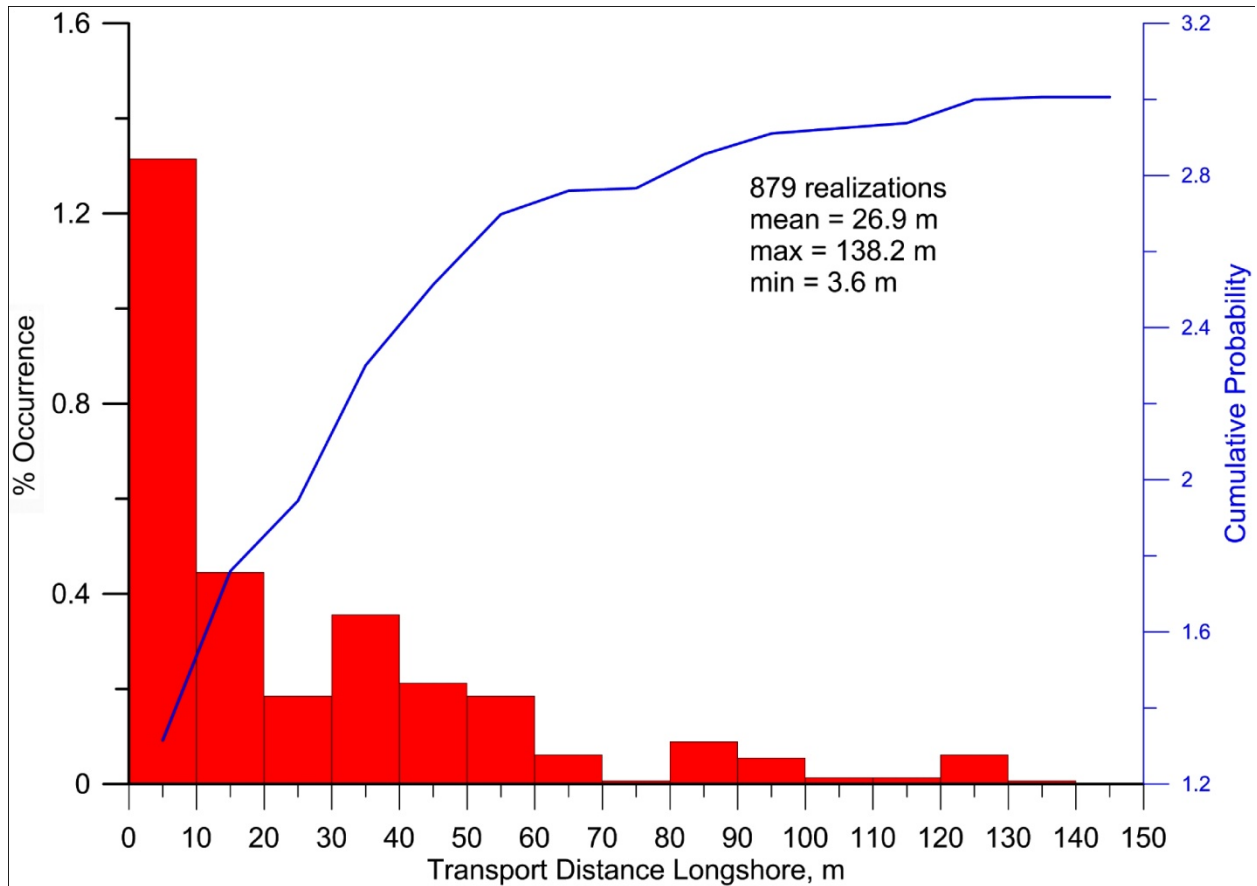


**Figure 3-30. Probability Density Function (red) and Cumulative Probability (blue) for Longshore Transport of a 2000 lb UXO Bomb at Andrew Bay; Based on Rigid Bottom Formulation in the Offshore Domain (seaward of the 30 m depth contour)**

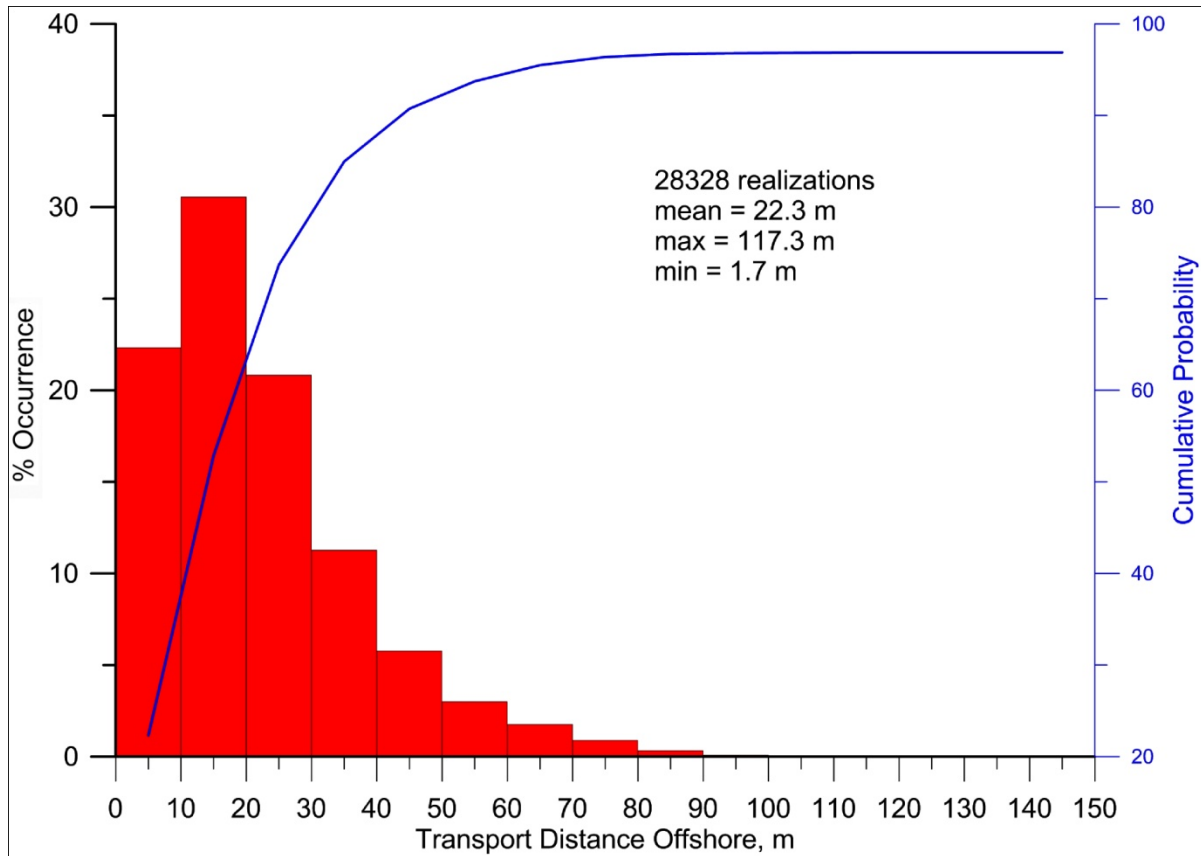


**Figure 3-31. Probability Density Function (red) and Cumulative Probability (blue) for Offshore Transport of a 2000 lb UXO Bomb at Andrew Bay; Based on Rigid Bottom Formulation in the Offshore Domain (seaward of the 30 m depth contour)**

The cumulative probability curves show that the UXO migration after 20 years is predominately downslope and offshore, with only 0.11% of the UXO bomb population migrating onshore (as compared with 96.8% migrating offshore), while 3.0% migrate alongshore, moving from areas of high waves near the headlands towards areas of low waves, principally abeam the mid-point of the barrier spit dividing Andrew Cove from Andrew Bay. The average onshore transport distance of the 2000 lb UXO bomb is only 19.2 m, while the maximum onshore migration distance of the bombs is 57.5 m. Onshore transport is typically the result of the longer period high energy waves. The minimum shoreward migration distance of the bomb is 5.5 m. As expected from size and weight considerations, the preponderance of migration of the 2000 lb bombs is offshore (Figure 3-31), in the direction of the action of the downslope gravitational component (Figure 3-6). The average offshore movement of UXO bombs is 26.9 m, while the maximum seaward excursions are 138.2 m and the minimums are 3.6 m. Generally, the bombs have a very limited watch circle of movement, even after 20 years of forcing by the high energy Adak wave climate.

## Section 4.0: RISK ASSESSMENT

Evidence is found in the hydrodynamic simulations for two operative hypotheses of fate and transport of UXO at Andrew Bay: 1) bottom wind hypothesis, UXO are being transported onto the beach from offshore deposits due to wave and wave-induced current action, usually resulting from the action of long period high energy waves; or 2) beach churn hypothesis, UXO are mixed among the beach deposits of gravels, cobbles, rock and basal conglomerate, and become episodically exposed by sorting, erosion and realignment of the beach profile in response to wave climate variation. It is also possible that the mechanisms of these two hypotheses are coupled, and that the bottom wind mechanism moves UXO close enough to the beach to enter the zone of active beach profile change (shoreward of closure depth), whence the beach churn mechanism ultimately exposes these UXO on the beach (barrier spit). A risk model based on the likelihood of UXO appearing on the beach of the barrier spit is adopted in response to either of these two mechanisms. Since repeated UXO sweeps of the Andrew Bay barrier spit by EOD continually discover new ordnance, it is already known that the likelihood is non-zero. Some quantitative probability estimates are assigned for the likelihood of appearance of new UXO on the beach in response to each of these transport mechanisms, given the assumption that UXO are still present in offshore deposits. The extent of offshore waters from which UXO can conceivably reach the beach in the future (referred here as *critical zone*) is estimated based on the notion that those areas define the domain where future monitoring efforts should focus search and detection assets.

In assessing risk and estimating the size of the critical zone, the most plausible outcome is pursued for either of the two operative hypotheses, given the site uncertainties, particularly in regard to the unknown bottom composition in the offshore domain. As detailed in Section 2.2.1, the most plausible outcome is derived from the rigid bottom formulation in the offshore domain when evaluating the bottom wind hypothesis, and from the movable bottom formulation in the offshore domain when evaluating the beach churn hypothesis.

### 4.1 Risk Assessment of Bottom Wind Hypothesis

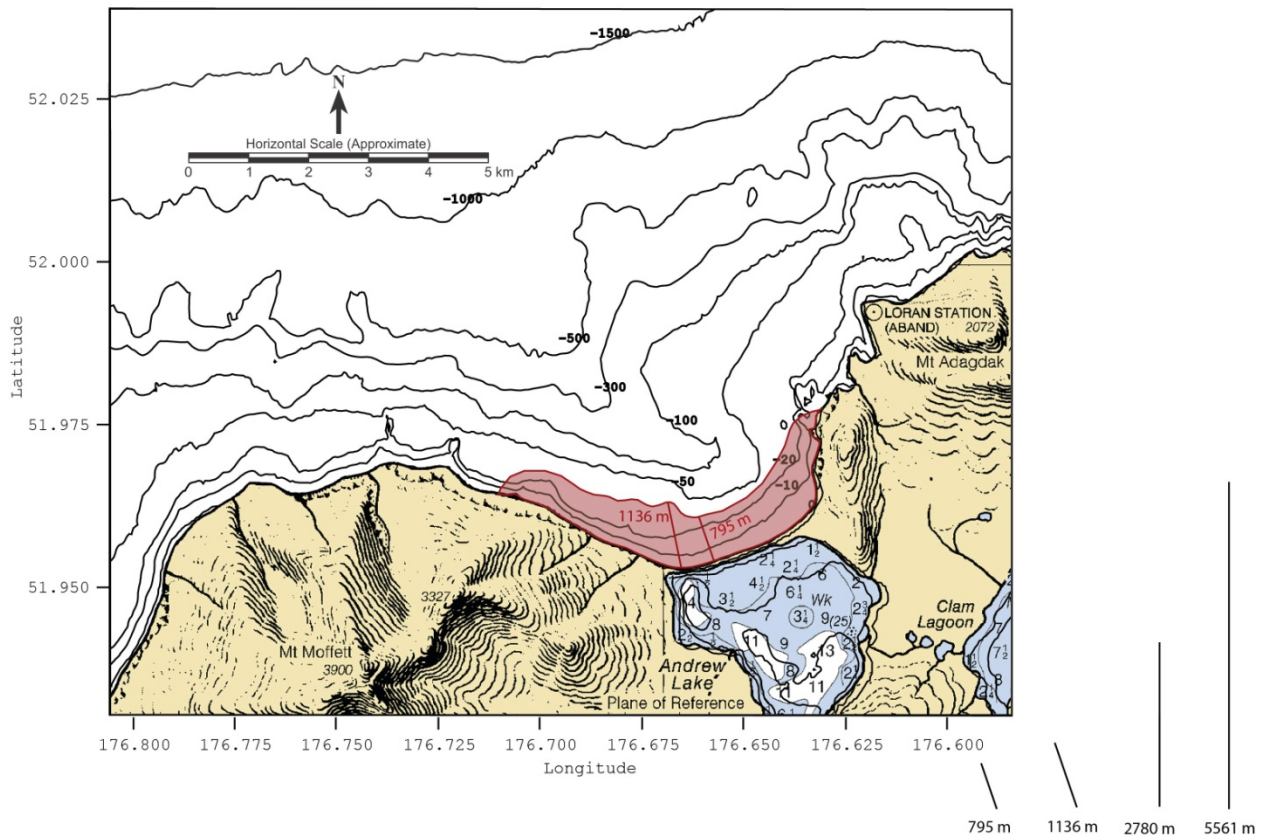
Risk will be assessed separately for the three distinct size classes of UXO for which quantitative transport modeling has been performed: namely, the 60 mm and 81 mm mortar rounds, the 20 mm and 40 mm rounds, the 2000 lb UXO bombs. Onshore transport of these ordnances is most likely during the occurrence of the long period (wave period greater than 14 to 16 seconds) high-energy waves. The shorter period waves generally result in longshore or down-slope, offshore movement of these UXO types.

Figure 3-18 shows that only 1.5% of the mid-sized UXO population of 60 mm and 81 mm mortar rounds migrates onshore. (This is the size class that most closely matches the beach rock comprising the barrier spit). Only half of that very small percentage moves more than a distance of 103 m upslope and toward the beach during a period of 20 years of simulation. However, Figure 3-18 shows there is a 0.01% probability of occurrence that a 60 mm and 81 mm mortar round might reach the beach over a 20-year period from as far offshore as 1,136 m. Figure 4-1 maps the critical zone in red for the 60 mm and 81 mm mortar UXO based on the area around the barrier spit where onshore transport of this size class of UXO has a non-zero likelihood of reaching and being exposed on the beach. Within this red area there is a 1.5% probability that at least one of the 60 mm or 81 mm mortar rounds reaches the beach in a 20-year period. (This is a conditional probability based on the assumption that population of 60 mm and 81 mm mortar rounds is spread uniformly across Andrew Bay. If these UXO are concentrated in patches closer to shore, the probability of beaching would be higher). For the purpose of future monitoring of

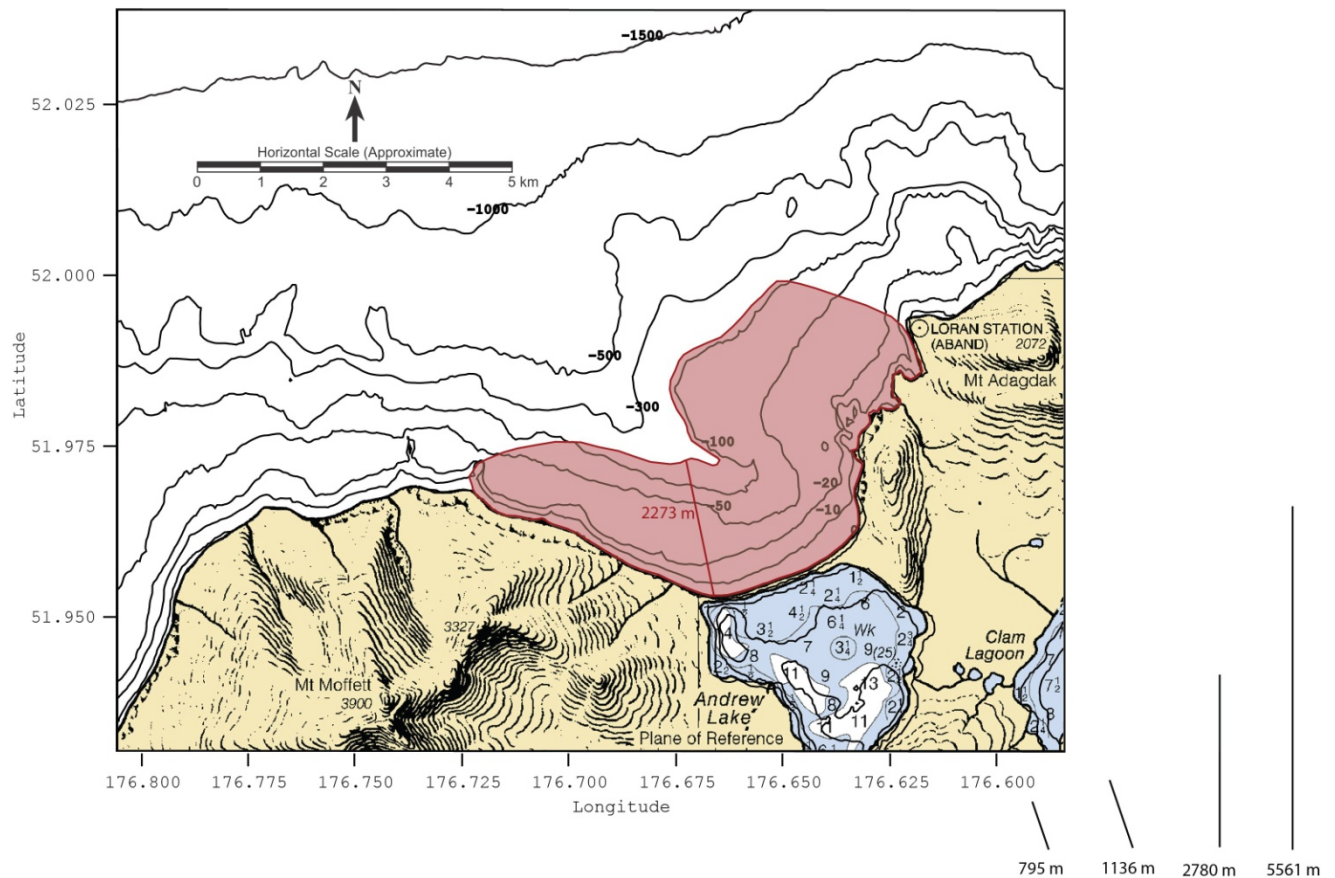
offshore deposits of this UXO type, the area delineated in red in Figure 4-1 is where search and detection assets should be focused.

Figure 3-24 shows that 12% of the small-sized UXO population of 20 mm and 40 mm UXO migrates onshore, and only 6% move more than a distance of 606 m upslope and toward the beach over a 20-year period. This UXO size class matches most closely with the small cobble and large gravels that comprise a minor fraction (about 2%) of the barrier spit beach material (Figure 2-3) Figure 3-24 also shows that there is a 0.05% probability of occurrence that a 20 mm or 40 mm round might reach the beach over a 20-year period from as far offshore as 2,273 m. Figure 4-2 maps the critical zone in red for the 20 mm and 40 mm UXO. Within the red area of Figure 4-2 there is a 12% probability that at least one of the 20 mm or 40 mm rounds reaches the beach in a 20-year period. (This is a conditional probability based on the assumption that the population of 20 mm and 40 mm UXO is spread uniformly across Andrew Bay.) If these UXO are concentrated in patches closer to shore, the probability of beaching would be higher). Because of small size, the 20 mm and 40 mm UXO are not likely to be retained on the beach for long periods of time, as evidenced by the very small percentage of comparable sized native cobble and gravel found on the barrier spit beach (Figure 2-3). The critical zone for the 20 mm and 40 mm rounds in Figure 4-2 is the most extensive of any UXO type, and could be used to delineate the outer boundary of the offshore UXO search area for future monitoring and remediation planning for all UXO at Andrew Bay.

Figure 3-29 shows that only 0.11% of the large-sized UXO population of 2000 lb bombs migrates onshore, and only 0.05% moves more than a distance of 19.2 m upslope and toward the beach over a 20-year period of time. This UXO size class matches most closely with the largest beach rock that comprises a very minor fraction (about 4%) of the barrier spit beach material (Figure 2-3) Figure 3-29 also shows that the maximum distance a 2000 lb can move onshore and upslope against gravity is only 57.5 m, and the probability of occurrence is only 0.06%. Figure 4-3 maps the critical zone in red for the 2000 lb bombs. Within the critical zone there is a 0.11% probability of a 2000 lb bomb moving further onshore over a 20-year period. (This is a conditional probability based on the assumption that a population of 2000 lb bombs is spread uniformly across Andrew Bay. If these UXO are concentrated in patches closer to shore, the probability of beaching would be higher). The critical zone of the 2000 lb bomb is within the zone of active seasonal beach profile change, and would be covered by a beach profile monitoring program of the barrier spit beach for future monitoring and remediation planning under the beach churn hypothesis.



**Figure 4-1. Critical Zone Mapping (red) for the 60 mm and 81 mm Mortar Rounds**  
(Within the critical zone, a 1.5% probability exists of at least one of the 60 mm or 81 mm mortar rounds reaching the beach in a 20-year period. This mapping is also a proxy for the critical zone of the beach churn hypothesis [Section 4.2]. Distance markers shown in the lower right hand corner.)



**Figure 4-2. Critical Zone Mapping (red) for the 20 mm and 40 mm Rounds**

(Within the critical zone, a 12% probability exists of at least one of the 20 mm or 40 mm rounds reaching the beach in a 20-year period. The area in red could be used to delineate the outer boundary of the UXO search area for future monitoring and remediation planning for all UXO at Andrew Bay. Distance markers shown in the lower right hand corner.)

#### 4.2 Risk Assessment of Beach Churn Hypothesis

The previous section established probabilities that various UXO size classes could be transported onshore and arrive at the beach zone of the barrier spit from offshore deposits, due to shoreward transport by hydrodynamic forces of long period waves. Here, the probability that those UXO or UXO already blended into the beach aggregate could be exposed by erosion or over-turning action (churning) due to seasonal beach profile change is evaluated.

There are two parts to the calculation. The first is the probability that UXO of a particular size class are resident among the existing beach aggregate. That estimate is based upon the retention of that size class when subjected to the long term sorting action by waves that has produced the size distribution of resident gravel, cobble and beach rock in Figure 2-3. Using shear stress considerations of establishing effective diameter of UXO, the values listed in Table 4-1 are obtained.

**Table 4-1. Residence Probability from Native Size Distribution and Effective Diameter of UXO**

Type	Diameter (cm)	Length (cm)	Density (g/cm <sup>3</sup> )	Effective Diameter (cm)	Residence Probability	Joint Probability
81 mm Mortar	8.1	28.2	3.37	14.053	12%	1.11%
75 mm HE M41A1	7.5	24.8	5.65	12.793	10%	.925%
60 mm Mortar M721	6.0	36.1	1.96	12.492	10%	.925%
60 mm Mortar	6.1	12.2	5.61	8.798	7%	.647%
Grenade Rifle M17	5.7	5.7	4.81	6.525	5%	.462%
40 mm APFSDS	4.0	28.4	1.12	8.800	7%	.647%
40 mm HEI	4.0	18.0	4.42	7.559	2.5%	.231%
20 mm HE M97	2.0	8.3	3.84	3.679	2%	0.18%
2,000 LB Bomb	47.2	177.0	2.93	83.940	4%	0.37%

The second part of the risk assessment of the beach churn hypothesis is the probability of occurrence of large waves that will erode and overturn the beach profile of the barrier spit. Figure 2-5 shows the probability of occurrence of waves over 5 m in height is 9.25%. These are the height of waves required to make as much as 2 m of vertical over-turning and erosion of the beach profile of the barrier spit in Figure 3-12. Multiplying the residence probabilities in Table 4-1 by the probability of occurrence of erosion-inducing waves gives a joint probability of 2.96% for the exposure of 81mm mortars and .925% for 60 mm M721 or .64% for 60mm mortars on the beach. Similar computations for the 20 mm and 40 mm UXO gives a joint probability of between .647 % and .185 % for the exposure on the beach of the barrier spit, and 0.37% probability of exposure of a 2000 lb bomb. These risk assessments by the beach churn mechanism are based on the assumption that these UXO types are already blended among the beach cobble and rock on the barrier spit. The distance offshore to closure depth where beach profile changes no longer occur is 1,200 m (Figure 3-12). Therefore, the critical zone of the beach churn hypothesis is similar to Figure 4-1 for the bottom wind critical zone of the 60 mm and 81 mm mortar rounds.

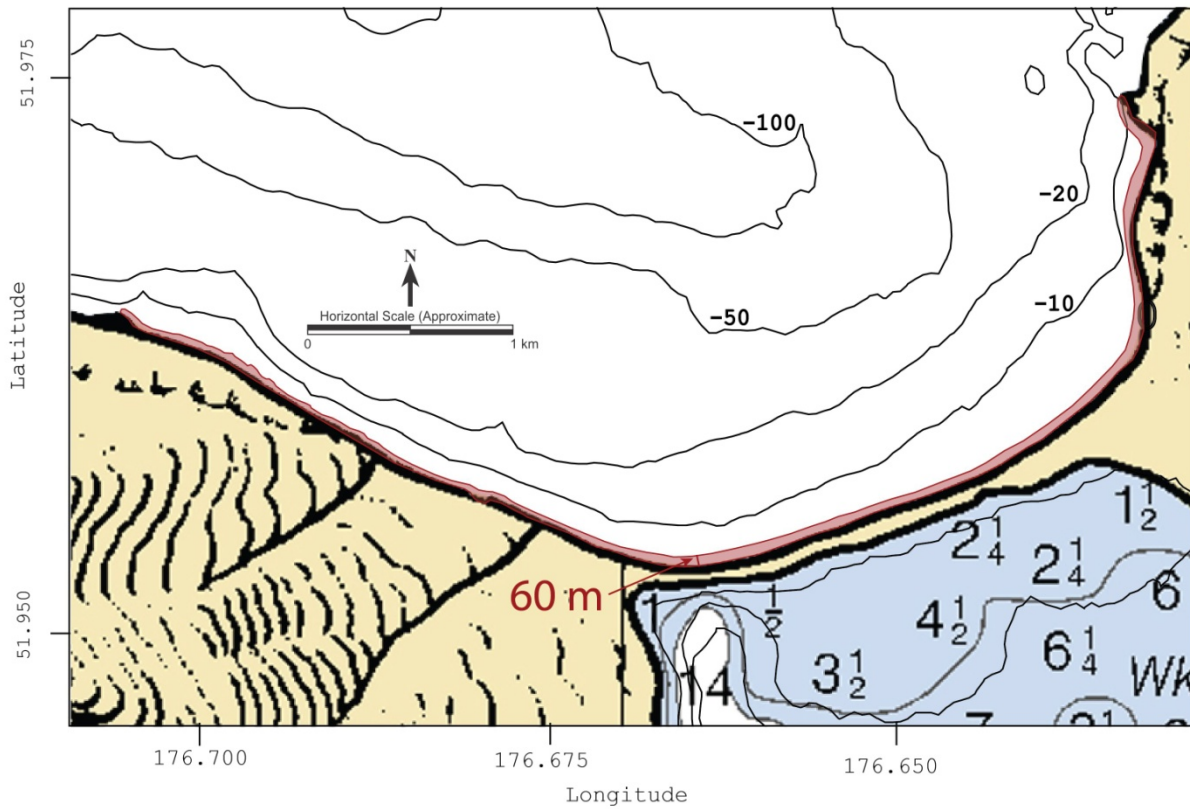


**Figure 4-3. Critical Zone Mapping (red) for the 2000 lb Bomb**  
(Within the critical zone, a 0.11% probability exists of a 2000 lb bomb moving further onshore over a 20-year period. The area in red is within the zone of active seasonal beach profile change and would be included in a beach profile monitoring program of the barrier spit beach for future monitoring and remediation planning.)

### **Section 5.0: RECOMMENDATIONS FOR FUTURE WORK**

To improve the analysis results of the bottom wind hypothesis, it is necessary to reduce uncertainties on UXO location, bottom type, bathymetric roughness, and directional wave and current variability. Reducing these uncertainties leads to recommendations already proposed in a previous UXO study at Andrew Bay by Jones and Israel (2002), namely:

- Bathymetric measurements. The Carignan et al. (2009) bathymetry is adequate over the farfield of Andrew Bay, but additional bathymetric surveys are needed to better resolve micro-bathymetry over the critical zone of the inner 2 km of Andrew Bay. When converted to digital formats, this critical zone bathymetry should provide at least 10 m horizontal resolution of bottom roughness features.
- Directional wave measurements in Andrew Bay. Bottom-mounted, self-recording ADCPs could provide these measurements. A single ADCP with co-located pressure sensor mounted at closure depth (28 m) could provide the first three moments of the shoaling wave direction spectra. A shore parallel line array of four such sensors at 50 m spacing could resolve the complete direction spectra.
- Current measurements in Andrew Bay. These measurements could be provided by the bottom-mounted ADCP measurements described above, augmented by a deep water monitoring site at the outer edge of the critical zone, 2 km offshore of the barrier spit. This deep water mooring would require an ADCP mounted to a clump weight with acoustic release, as it would be located at about 100 m depth, below operational depth of most divers.
- Sediment samples collected throughout Andrew Bay to characterize the bottom.
- UXO underwater survey using towed array magnetometers.

Improvements to the analysis results of the beach churn hypothesis require improved information on the resident UXO population numbers, types, and spatial distribution, beach aggregate size distribution, seasonal beach profile change, and directional wave and current variability. These improvements can be achieved by implementing the following recommendations, some of which are included above:

- Higher resolution bathymetric measurements, shoreward of closure depth (inside the 28 m isobath), as described above under additional bottom wind measurements.
- Shoaling wave measurements with bottom-mounted ADCPs, as described above under additional bottom wind measurements.
- Beach profile surveys in both summer and winter.
- Samples of beach aggregate and follow-on size and roundness analysis.
- Electro-magnetic or magnetic gradiometer surveys to detect and classify UXO blended in the beach deposits of the barrier spit. These types of land surveys have demonstrated extremely high probabilities of detection (Pd) and classification (Pc) of UXO and fragments under ESTCP-sponsored programs. The equipment would require large diameter wheeled or tracked vehicles for adequate mobility and maneuverability over the beach rock and cobble fields on the beach of the barrier spit at Andrew Bay.

## Section 6.0: REFERENCES

- Bagnold, R.A. 1956. "The flow of cohesionless grains in fluids," *Philos. Trans. R. Soc. London Ser. A*, 249(964), 235-297.
- Bagnold, R.A. 1963. "Mechanics of marine sedimentation," in *The Sea, Ideas and Observations on Progress in the Study of the Seas*, Vol. 3, The Earth Beneath the Sea, History, edited by M.N. Hill, Wiley, New York, 507-528.
- Berkoff, J.C.W. 1972. "Computation of combined refraction-diffraction," *Proc. 13th Coastal Eng. Conf.*, 471-490.
- Carignan, K.S., L.A. Taylor, B.W. Eakins, R.R. Warnken, P.R. Medley, E. Lim. 2009. "Digital Elevation Model of Adak, Alaska: Procedures, Data Sources and Analysis," Technical Memorandum NESDIS NGDC-31, National Geophysical Data Center, Marine Geology and Geophysics Division, Boulder, Colorado.
- Dalrymple, R.A., J.T. Kirby, and P.A. Hwang. 1984. "Wave diffraction due to areas of energy dissipation," *J. Waterway Port, Coast, and Ocean Engin.*, Vol. 110, 67-79.
- Dalrymple, R.A., D.W. Mann, and N. Kobayashi. 1983. "Tidal flows in Indian River Inlet." Research Rept. No. CE-83-39, Dept. of Civil Engineering, University of Delaware.
- Foster Wheeler Environmental Corporation. 2000. "Selected Areas of Concern in Operable Unit B, Former Naval Air Facility, Adak, Alaska," Delivery Order No. 0083, Foster Wheeler Environmental Corporation, Anchorage, Alaska.
- Garrod, D. 2008. *UXO Mobility Model Users' Manual*, NAVFAC ESC Technical Report, Revision 8.4, ESTCP 200417, 79 pp.
- Jenkins, S.A. and J. Wasyl. 1990. "Resuspension of Estuarial Fine Sediments by Tethered Wings," *J. Coastal Res.*, Vol. 6, No. 4, pp. 961-980.
- Jenkins, S.A. and D.L. Inman. 2002. "Model for Mine Scour and Burial: An Illustrated Abstract with Technical Appendix," University of California, San Diego, Scripps Institution of Oceanography, SIO Reference Series 02-2, 42 pp.
- Jenkins, S.A. and J. Wasyl. 2005. "Model for Prediction and Updates for UXO Transport during MMFT 1 & 2, Ocean Shores, WA," submitted to Sound and Sea Technologies, 170 pp.
- Jenkins, S.A. and D.L. Inman. 1985. "On a submerged sphere in a viscous fluid excited by small-amplitude periodic motions," *J. Fluid Mechanics*, Vol. 157, 199-224.
- Jenkins, S.A. and D.L. Inman. 2006. "Thermodynamic Solutions for Equilibrium Beach Profiles," *J. Geophysical Res.*, 111, C02003.
- Jenkins, S.A., D.L. Inman, M.D. Richardson, T.F. Wever, and J. Wasyl. 2007. "Scour and Burial Mechanics of Objects in the Nearshore," *IEEE J. Ocean Eng.*, Vol. 32, No. 1, pp. 78-90.
- Jenkins, S.A., G. D'Spain, and J. Wasyl. 2012. "Vortex Lattice UXO Mobility Model for Reef-Type Range Environment," ESTCP Tech. Rpt. No. MR-201003, 101 pp.

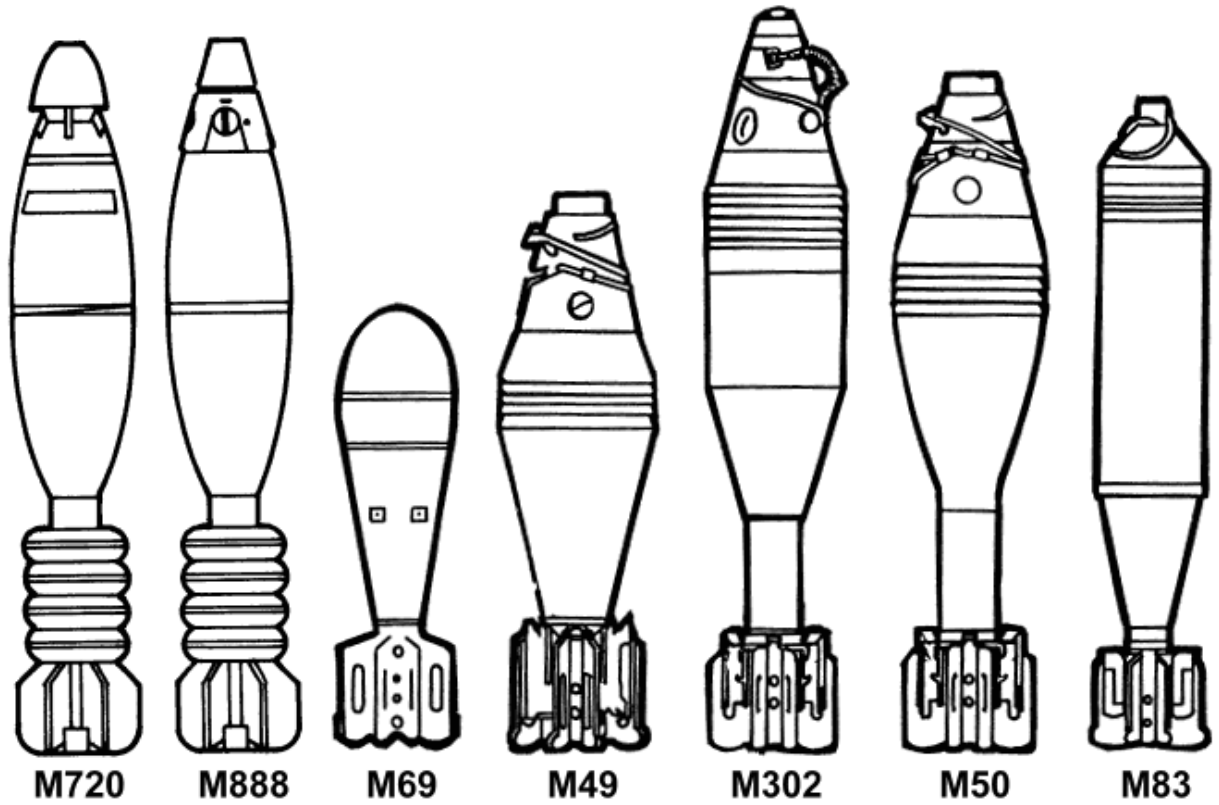
- Jones, C. and K. Israel. 2002. "Assessment of Potential Areas of UXO Transport Andrew Bay Adak Island, Alaska," Woods Hole Group, prepared for Environmental Chemical Corporation, 54 pp.
- Kirby, J.T. 1986. "Higher-order approximations in the parabolic equation method for water-waves," *J. Geophys. Res.*, Vol. 91, No. C1, 933-952.
- Kirby, J.T. and R.A Dalrymple. 1994. *Combined Refraction/Diffraction Model REF/DIF 1 Documentation and User's Manual*, CACR Report No. 94-22. Univ. of Delaware, Newark, DE.
- Naval Facilities Engineering Service Center (NFESC). 2008. *Applications Guidance Document: Predicting the Mobility and Burial of Underwater Unexploded Ordnance (UXO) Using the UXO Mobility Model*, Naval Facilities Engineering Service Center, Ocean Engineering Division, OP51. Port Hueneme, CA, ESTCP Project 200417, Contract N62473-06-D-3005, 82 pp.
- Madsen, O.S. and P.N. Wikramanayake. 1991. "Simple Models for Turbulent Wave-current Bottom Boundary Layer Flow," U.S. Army Corps of Engineers Contract Report DRP-91-1, USACE-WES, Vicksburg, MI.
- Radder, A.C. 1979. "On the parabolic equation method for water-wave propagation," *Jour. Fluid Mech.*, Vol. 95, pt. 1, 159-176.
- Wilson, J.V. and S.A. Jenkins. 2005. "UXO Measurement Method Field Tests (MMFT1&2) and Mobility Model Modification, final report," Sound & Sea Technology Report 05-07.
- Wilson, J.V., A. DeVisser, and B. Sugiyama. 2008. "(ESTCP) 200417 Predicting the Mobility and Burial of Underwater Unexploded Ordnance (UXO) Using the UXO Mobility Model, field test report (FRF Duck, NC)," NAVFAC ESC Technical Report.
- Wilson, J.V., A. DeVisser, and B. Sugiyama. 2008e. "TO-2008-09-16-T061, Example Applications Analysis Using the UXO Mobility Model: Lake Erie Impact Range Analysis," NAVFAC ESC Technical Report, 53 pp.

**APPENDIX A**  
**UXO Types in Andrew Bay**

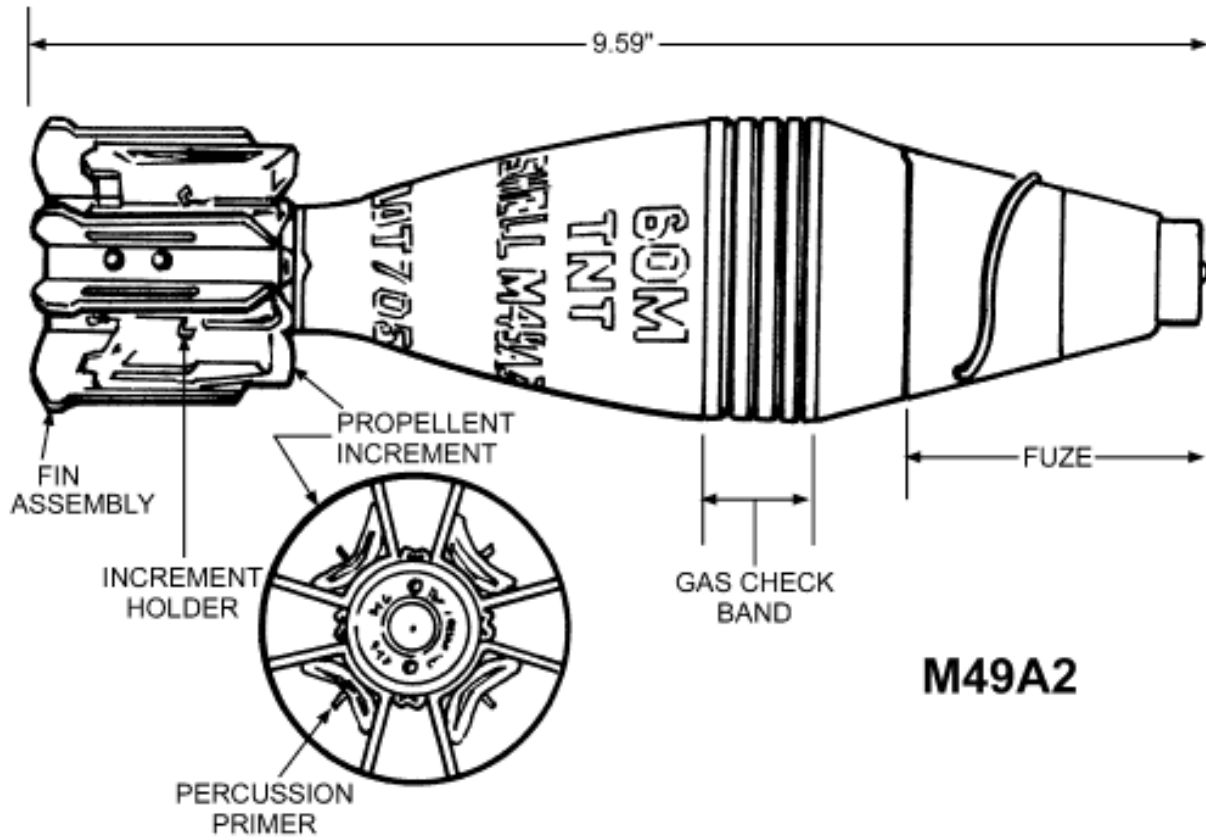
<b>Ordnance Type</b>	<b>Diameter</b>	<b>Length</b>	<b>Weight</b>
30 Cal Carbine, Complete Round (CR)	.36 inch	1.68 inch	.4 oz
30-06 Small Arms, CR, Springfield	.473 inch	3.34 inch	.9 oz
45 Cal Small Arms, CR, M1911	.48 inch	1.275 inch	.8 oz
38 Cal Special, Small Arms, Ball, CR	.38 inch	1.53 inch	.5 oz
50 Cal Small Arms, CR, M-2 Ball	.75 inch	5.45 inch	4 oz
50 Cal Small Arms, Projectile	.50 inch	2.31 inch	1.6 oz
50 Cal Small Arms, Cartridge Case	.75 inch	4 inch	1.9 oz
12 Gauge Shot shell	.797 inch	2.75 inch	1.5 oz
20MM Projectile, Ball, CR	1.17 inch	5.45 inch	<b>Average-10 oz</b>
20MM Projectile, assorted	.787 inch	3.4 inch	Average-4 oz
20MM Projectile Cartridge Case, assorted	1.17	Average-4.2 inch	Average 6 oz
37MM Projectile, M63, HE, CR	1.55 inch	14.9 inch	3.8 lbs
37MM Projectile, M63	1.45 inch	6 inch	1.36 lbs
37MM Projectile Cartridge Case, M63	1.55 inch	8.75 inch	.75 lbs
40MM Projectile, Bofore, HE, CR	1.87 inch	17.64 inch	4.64 lbs
40MM Projectile, Bofore, HE	1.56 inch	5.17 inch	1.5 lbs
40MM Projectile, AP, M81, CR	2.375 inch	17.6inch	4.58 lbs
40MM Projectile, AP, M81	1.57 inch	6 inch	2.73 lbs
40MM Projectile, HEI, M811, CR	2.375 inch	21.4 inch	5.5 lbs
40MM Projectile, HEI M811	1.57 inch	7.5 inch	2.5 lbs
40MM Projectile Cartridge Case	2.375 inch	12.25 inch	1.2 lbs
2.36 Rocket, HEAT, M6A1, CR (pointed nose)	2.245 inch	21.6 inch	3.4 lbs
2.36 Rocket, HEAT, M6A1 Warhead	2.23 inch	8.6 inch	2.4 lbs
2.36 Rocket, HEAT, M6A3, CR (round blunt nose)	2.245 inch	19 inch	3.4 lbs
2.36 Rocket, HE, M6A3 Warhead	2.245 inch	8.6 inch	2.4 lbs
2.36 Rocket Motor/with fins	1.24 inch	9.32 inch	1 lb
Grenade, Hand, Frag, MK-II	2.25 inch	4.5 inch	21 oz
Grenade, Hand, WP Smoke, M-15	2.375 inch	4.5 inch	31 oz
Grenade, Hand Thermite, M14	2.5 inch	5.7 inch	32 oz
Fuze, Grenade, M204	1 to 1/4 in	4 inch	2.6 oz
Grenade, Rifle, Anti-tank, M-9	2.25 inch	11.24 inch	1.23 lbs
Grenade, Rifle, WP Smoke, M-19	2 inch	11.31 inch	1.57 lbs
Grenade, Rifle, HEAT, M-31	2.61 inch	16.96 inch	1.56 lbs
3.5 inch Rocket, HEAT, M-28A2, CR	3.5 inch	23.55 inch	9 lbs
3.5 inch Rocket, HEAT, M-28A2, Warhead	3.5 inch	10.5 inch	4.5 lbs
3.5 inch Rocket, WP, M-30, CR	3.5 inch	23.55 inch	9 lbs
3.5 inch Rocket, M-30 Warhead, WP	3.5 inch	10.5 inch	4.5 lbs
3.5 inch Rocket, Motor with fuze	2 inch	14.89	4.46 lbs
3.5 inch Rocket, Motor only	2 inch	10.4 inch	4.3 lbs
57MM Recoilless Rifle, HE, M306, CR	2.24 inch	17.54 inch	5.46 lbs
57MM, Warhead, HE, M306	2.24 inch	6.47 inch	2.78 lbs
57MM Recoilless Rifle, HEAT, M307, CR	2.24 inch	18.78 inch	5.43 lbs
57MM, Warhead, HEAT, M307/with fuze	2.24 inch	8.343 inch	2.75 lbs
57MM Recoilless Rifle, WP, M308, CR	2.24 inch	17.64 inch	5.43 lbs
57MM, Warhead, WP, M308	2.24 inch	6.43 inch	2.75 lbs
57MM, Cartridge Case	2.24 inch	12 inch	2.68 lbs
60MM Mortar, HE, M49, CR	2.36 inch	9.5 inch	2.94 lbs
60MM Mortar, WP, Smoke, M302	2.36 inch	8.62 inch	4 lbs
60MM Illumination, M83	2.36 inch	14.28 inch	4.2 lbs
81MM Mortar, HE, M43, CR	3.16 inch	13.25 inch	7.05 lbs
81MM Mortar, HE, M82, CR	3.16 inch	20 inch	8.96 lbs

81MM Mortar, HE, high capacity/Heavy, M56	3.16 inch	23.5 inch	15.1 lbs
81MM Mortar, WP Smoke, CR, M370	3.16 inch	20.8 inch	9.34 lbs
81MM Mortar, WP Smoke, high capacity, M57	3.16 inch	22.91 inch	11.38 lbs
81MM Mortar, Illumination, M301, CR	3.16 inch	24.7 inch	10.1 lbs
90MM Projectile, HE-T, M 71, CR	4.5 inch	37.45 inch	41.5 lbs
90MM Projectile, HE-T, M 71	3.62 inch	16 Inch	25 lbs
90MM Projectile, APC-T, M 82, CR	4.5 inch	38.24 inch	43.25
90MM Projectile, APC-T, M 82	3.62 inch	16 inch	25 lbs
3 inch Projectile, Common, MK3	2.98 inch	10.04 inch	13 lbs
3 inch Projectile, Mk 31, AA/without fuze	2.98 inch	8.5 inch	12.9 lbs
4.5 inch Barrage Rocket, MK3, CR	4.5 inch	30 inch	28.7 lbs
4.5 inch Barrage Rocket, MK3, Warhead	4.5 inch	13 inch	19.9 lbs
4.5 inch Barrage Rocket, MK3, Motor	2.25 inch	15.5 inch	8.8 lbs
5 inch Cartridge Case, Mk-5	6.2 inch base	26.75 inch	12.31 lbs
6 inch/47 Projectile, Mk 35 with cap & windshield	5.99 inch	27 inch	130 lbs
6 inch/47 Projectile, Mk 35 no cap or windshield	5.99 inch	17.19 inch	114 lbs
Projectile Fuze, M52	1.93 inch	2.95 inch	.35 lbs
Projectile Fuze, 40MM, PD, MK-27	1.2 inch	2.45 inch	.22 lbs
Projectile Fuze, M48/M51 series	Aver 2.5 inch	5.9 inch	2.2 lbs
Projectile Fuze, M503/57MM RR	2 inch	2.6 inch	.34 lbs
Bomb, Incendiary/thermite, 4lb, M126	1.58 inch	19.5 inch	4 lbs
4 lb Incendiary/thermite Bomblet, M50	1.7 inch	21.35 inch	4 lbs
Incendiary Bomb, M74A1	2.875 inch	19.5 inch	8.5 lbs
Incendiary Bomb, AN-M76, 500 lb	14 inch	45.3 inch	475 lbs
500 lb AP/HE, AN-M58	11.8 inch	46.8 inch	494 lbs
1000 lb Bomb, M65, CR	19 inch	67 inch	1016 lbs
1000 lb Bomb, M65 (no fins)	19 inch	Approx. 50 inch	Approx 990 lbs
Bomb Fuze, M103, (Nose)	2.5 inch	7.1 inch	Approx 2 lbs
Bomb Fuze, AN-M112 (Tail)	1.75 inch	11 inch	Approx 2 lbs
Bomb Fuze, M100 Series (Tail)	Vane 5 inch/ Body 1.75 in Average	9 - 16 inch	1 - 4 lbs
Bomb Fuze, M123, (Tail)	Vane 5 inch/ Body 1.75 in	9.4 inch	Approx 3 lbs
Aircraft Parachute Flare, Mk5	4.75 inch	27 inch	18 lbs
References: TM 9 series/TM 43 series/OP 1664/Internet			

**APPENDIX B**  
**Photographs and Engineering Drawings of Each Ordnance Type Found in the Canonical Listing in**  
**Table 2-2**



Typical 60 mm mortars used at ADAK range



M49A2 60 mm mortar



**60 mm mortar**



**81 mm mortar**

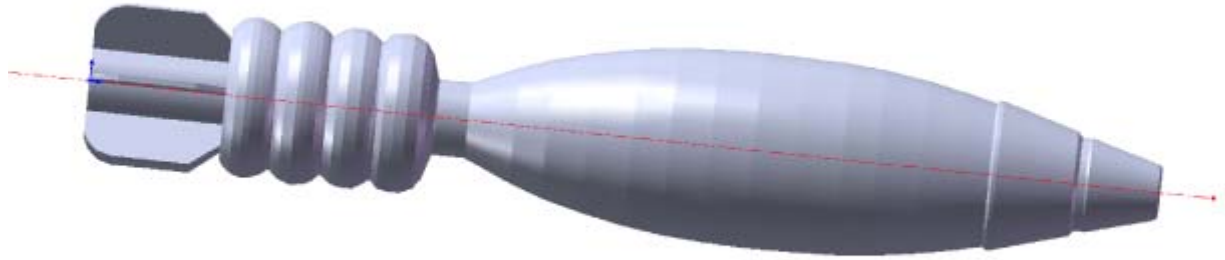


Expended 60MM M721

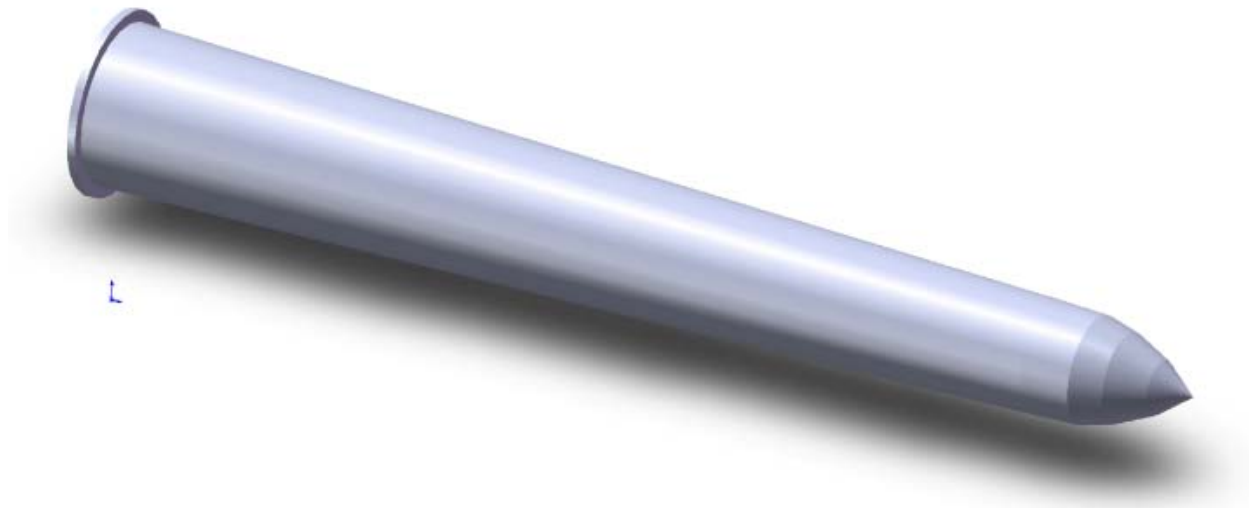


57x307R 47x376R 40x304R 57x441R

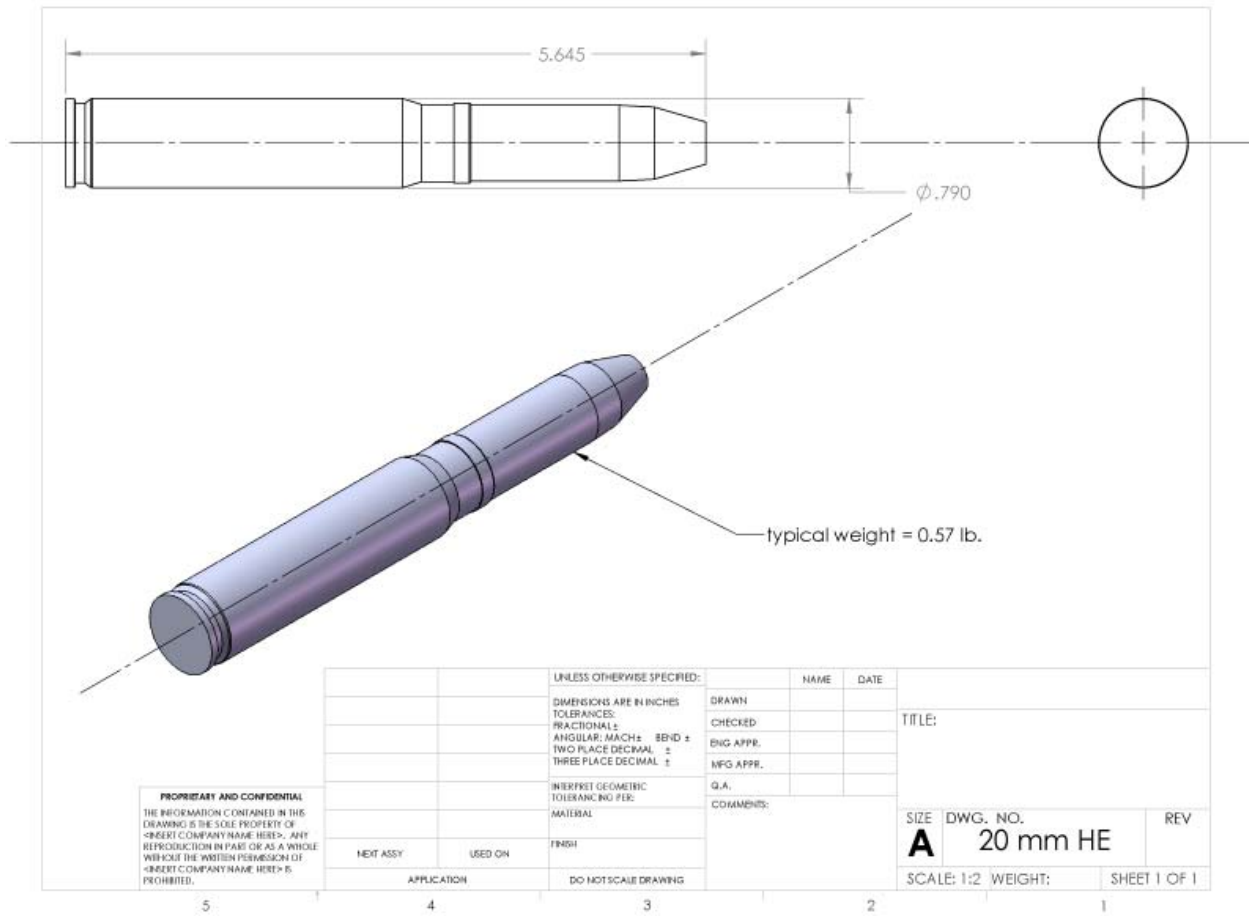
Typical tank gun ammo, 40 mm – 57 mm



**Modeled M888 60 mm mortar**



**Modeled 40 mm tank ammo**



**Modeled 20 mm HE round**

**APPENDIX C**  
**Combined Peer Review Comments and Author Responses**

**(Peer Review Comments in Black Font, Author Responses in Red Font)**

**Comments on Jenkins, D'Spain and AW and Wasyl by Justin Peach.**

1. Cover and title page, electronic deliverable needs to be to Navy deliverable SOP.
2. Introduction, 5<sup>th</sup> line down. Delete the sentence that begins "The United States navy has deposited Ordnance in the bay for approximately ... " That is not accurate. Delete "... from these deposits ... " from the next sentence.  
**Response: This sentence has been deleted.**
3. Do a global search for "Andre" as in Andre Cove, Andre Bay, Andre Lake, etc. I believe it should be Andrew everywhere.  
**Response: Done**
4. Do a global search for "Bearing" as in Bearing Sea. I believe it should be Bering Sea.  
**Response: Done**
5. Do a global search for far-field, farfield, near-field, and nearfield. Pick a format and be consistent.  
**Response: Done**
6. Page 43, 4<sup>th</sup> line. Do you mean rocking or rocky?  
**Response: rocky**

**Comments on Jenkins, D'Spain and AW and Wasyl by Mike Richardson.**

This report is a good start to determining the dominate mechanisms to account for the presence of UXO on a high energy exposed rocky beaches such as found near Adak, Alaska. It is obvious that the available data are inadequate for an accurate prediction of the distribution of UXO at this site. The following data are required 1) long-term wave and current data 2) seasonal beach slopes, 3) grain size distribution over the entire area, 4) numbers and initial distribution of UXO, 5) bottom roughness related to rolling resistance of UXO over the seafloor.

**Response: We agree. These points have been detailed at the end of the Executive Summary and Conclusions and have included recommendations for additional studies.**

There is no way at present to validate these mobility model predictions.

**Response: We fully agree that it is hard to "certify" the accuracy of a model prediction when there really isn't enough data to run the model to its designed potential. The model predictions have been validated at other sites, under less extreme conditions than Adak Alaska. The UXO Mobility Model (UXO-MM) was initially field validated using 20mm UXO surrogates at Pt Mugu, CA (Wilson 2004) and 5"/38 naval round surrogates at Pacific Beach and Ocean Shores, WA (Wilson and Jenkins, 2005). Subsequently, the UXO-MM was field validated at the U.S. Army Corps Of Engineers Engineering, Research & Development Center, Field Research Facility (FRF), Duck, North Carolina. Data were collected at various points over a 22-28 month period, 2005-2008. A follow-up ESTCP UXO field validation test demonstration was conducted off the coast of the Pacific Missile Range Facility (PMRF) on the southwestern coast of Kauai, Hawaii in 2007. Both ESTCP funded validation tests were fully successful in that all the required**

data were obtained and the behavior of the test items matched the predictions from the UXO-MM within measurement error.

In the Executive Summary: Certify may be the wrong word. The UXO Mobility Model was successfully demonstrated. The Mobility Model has not been certified by ESTCP.

Response: Corrected, “demonstrated” was substituted for “certified”.

The use of a 4-year wave record looped 5 times to obtain a 20-year continuous record is a questionable approach as wave heights might have exceeded those during the 4-year period.

Response: We fully agree. Data gaps are a serious problem when modeling time-stepped, time-evolving processes such as UXO migration; introducing significant uncertainty related to what occurred during the time period that the model is forced to stop and re-start across a data gap. Four years is the longest unbroken wave record available from any wave buoy in the region. The largest wave height in our 4-year unbroken wave data block was 11 m. Analysis of NOAA buoy data fragments going back to 1985 show that the largest wave over that 27 year span was 12 m. Probability densities and cumulative probabilities for wave heights in Figure 2.6a show about a 1% difference between the 4-year unbroken wave record and the full 27 years of data fragments in the occurrence of waves greater than 6 m height; and less than a 0.5% difference in occurrence of the largest waves. We have added additional figures and text in Section 2.4 explaining these points.

Given the grain size distribution in Figure 2.3, I doubt that grabs or cores are the best tools for collecting sediment samples at this site.

Response: We have changed the wording of our last recommendation in both the Executive Summary and in Section 5 to read simply, “Samples of beach aggregate and follow-on size and roundness analysis”...leaving it up to the geotechnical experts to decide how those samples should be collected.

A scale would be useful on Figures 1.2 and 1.3.

Response: We have added that feature to both figures.

Page 12: There are statistics associated with sorting; for example Folk and Ward, 1957.  
Figure 2.3: How many samples were used to generate the size distribution histogram? How variable is the sediment distribution, especially with water depth? Is there a gradient in size distribution with depth in the seafloor; perhaps smaller sizes on the surface and larger sizes below? Is a single size distribution adequate to characterize sediment (if you can call it sediment) distribution for the Mobility Model?

Response: The size distribution was derived from what was reported as a “composite sample” (blended from an unspecified number of sub-samples) taken from the beach deposits of the barrier spit at Andrew Bay from Carignan et al., 2009, which referenced a US Army Corps of Engineers dredge permit application to dredge an inlet to Andrew Cove by broaching the barrier

spit. A size distribution table with inferred sample mass has been added to Section 2.2 to lend appreciation for the difficulty of measuring such a size distribution when some of the larger sized beach rock are over 700 kg each! If data are available, we can apply different size distributions to various provinces of the model grid; but the size distribution data in Section 2.2 is the only data available, and is specific to only the beach rock, cobble and gravels found on the beach deposits of the barrier spit of Andrew Bay. No sediment size distribution data is available on the bottom types in the offshore regions of Andrew Bay where NOAA charts indicate the presence of shells, sands, and gravels. Acquisition of such data is among our list of recommendations in both the Executive Summary and in Section 5. In the absence of sediment data in the offshore domain, the initialization of the UXO-MM is based on the choice of bottom composition that separately maximizes risk and seeks the most pessimistic plausible outcome by either of the two hypotheses of the. When evaluating risk associated with the *Beach Churn Hypothesis*, we assume that the size distribution of beach aggregate in Figure 2.3 and Table 2.1 persists between the beach of the barrier spit and the 30 m depth contour, which is the estimated seaward limit of the beach rock, cobble and gravel deposits of the barrier spit based on EOD communications of visual surveys during EOD sweeps reported in Jones and Israel, 2002, (cf Section 2.0; and Figure 2.2 indicates the offshore reach of those visual surveys). Offshore of the 30 m depth contour, we assume under the *Beach Churn Hypothesis* that a coarse-sand and gravel bottom type exists based on a proxy grain size distribution (Figure 2.3a) adopted from a high energy coast at Ocean Shores, WA, where the first UXO mobility experiments were conducted in 2005, (Wilson and Jenkins, 2005). Median grain size of this proxy grain size distribution according to percent by weight is 384 microns. This assumption (*movable bottom* formulation) maximizes co-mingling of offshore UXO with the beach deposits of the barrier spit by sorting mechanisms. In evaluating risk associated with the *Bottom Wind Hypothesis*, we make the same inshore bottom composition assumption; but assume a bare bedrock bottom seaward of the 30 m depth contour. This assumption (the *rigid bottom* formulation) maximizes shoreward transport of UXO due to the hydrodynamic forces of shoaling waves and currents acting directly on exposed UXO. These details are explained in a new **Section 2.2.1 Modeling Choices Related to Bottom Composition** and in some additional text in the **Section 4.0 Risk Assessment**. We have also added notes to each flow simulation figure indicating which bottom formulation is shown.

Pages 15-18: Why was NOAA buoy 46073 chosen to drive the Mobility Model? It is the closest buoy to Adak but NOAA buoy #46035 has a continuous record on the waves since 1985.

Response: The period of record for buoy#46035 was 13 Sept 1985 - present. There are more than 100 data gaps in that period of record accounting for 10% of the total record length; 7 of those data gaps are longer than 1 month, and 3 of these data gaps are a half-year or more in length. Again, we emphasize that data gaps are a serious problem when modeling time-stepped, time-evolving processes such as UXO migration, introducing significant uncertainty related to what occurred during the time period that the model is forced to stop and re-start across a data gap. Consequently Buoy #46073 was selected to drive the UXO Mobility model, as it provided an unbroken record of deep water wave height, period and direction at hourly sampling intervals over a period of 4 years from 2005-2009. We added several new figures and a new section to give more detail on this issue. The new section is **2.4.1 Modeling Choices Related to Wave Climate**. In that section we give histograms of wave height and periods to assess the statistical fidelity of the wave forcing derived from looping the 2005-2009 period of record from Buoy

#46073 (red) versus the data fragments from the 1985-2011 period of record for NOAA Buoy #46035 (green). What we found was that the longer, fragmented record from Buoy #46035 gives wave heights that on average are about 5% higher than the 4-year unbroken record from Buoy #46073; and waves that are 1% higher or less for extreme events. The cumulative probability curves for wave period in Figure 2.6b show virtually no significant difference in the wave period data between the two records. Since there is no apparent modeling work-around for the missing data from Buoy #46035, because the statistical differences between the two records is small, and because it is located closer to the study site, the choice was made to use the looped 4-year unbroken record from Buoy #46073 to drive the UXO Mobility Model.

Page 43: Bottom roughness (friction) may be a very important mechanism that retards UXO migration. I agree that bottom roughness needs to be measured but wonder why the authors did not estimate that roughness from the grain size distribution as a first step to determine its importance.

Response: This question is addressed in our new **Section 2.2.1 Modeling Choices Related to Bottom Composition**. Inside the 30 m depth contour we assume from EOD observation that the bottom composition is characterized by the size distribution of the beach deposits of the barrier spit, where roughness is one half the median size fraction, or 0(12 cm). Seaward of the 30 m depth contour, roughness relates to choices of bottom composition in the offshore domain in the absence of bottom composition and roughness data in that domain. Under the *moveable bottom* formulation where sedimentary bottom deposits are assumed to be distributed everywhere, roughness is based on scour bedform parameters 0(5 cm) appropriate to the proxy grain size distribution adopted from a high energy coast at Ocean Shores, WA. Under the *rigid bottom* formulation, where the bottom is assumed to be bare bedrock offshore of the beach deposits of the barrier spit, bottom roughness consists of faceted plane surfaces defined by the resolution of the digital bathymetry data base, 0(30 m) in the horizontal for each facet.

Other comments:

- 1) Does the density of the UXO compared to similar-sized cobbles and boulders have any effects on UXO migration and or burial? If so, the densities should be given in sections 2.2 and 2.5.

Response: The answer is yes, as detailed in numerical sensitivity analyses in Wilson and Jenkins (2005). The nominal density of the large and mid-sized rounds used in the modeling (81 mm Mortors and 2000 lb bombs) is  $3 \text{ g/cm}^3$  as compared to  $2.65 \text{ g/cm}^3$  if the beach rock and cobble is granitic; or  $2.8 \text{ g/cm}^3$  to  $3 \text{ g/cm}^3$  if it is basaltic. These large and mid-sized rounds are the simulation specimens that predominate in the sorting of Beach Churn Hypothesis. Smaller rounds tend to have higher densities. Density was added to Table 4.1 where the risk assessment of the Beach Churn hypothesis is evaluated.

- 2) The grain size in Figure 2.3 appears to be determined from beach samples. Have you assumed that same distribution for other sites with the critical zone?

Response: This issue now is explicitly addressed in our new **Section 2.2.1 Modeling Choices Related to Bottom Composition**.

- 3) Does the vortex lattice model indicate any burial of UXO? You only report migration.

**Response:** Yes, burial was calculated in simulations under the *moveable bottom* formulation, where sedimentary bottom deposits are assumed to be distributed everywhere. Varying degrees of burial are shown in simulations of Figures 3.14, 3.17, 3.21; and 3.27 (lower panel).

- 4) A sensitivity analysis of the effects of seafloor roughness on roll resistance (friction) would be useful. By roughness I mean roughness on the same scale or slightly larger than the UXO.

**Response:** We agree but to achieve closure with this comment requires the recommended additional studies which are outside the scope of the present study.

- 5) Seasonal measurement of beach profiles should be made to validate the thermodynamic approach to prediction beach profiles (Jenkins and Inman, 2006) for rocky beaches (Figure 13.2).

**Response:** We agree. Hopefully the recommended additional site studies can be conducted to collect the necessary data.

#### **Comments on Jenkins, D’Spain and AW and Wasyl by Bryan Harre.**

Pg. 8, 1.0 Introduction – The following statement isn’t quite correct “The United States Navy has deposited ordnance in the bay for approximately the last 60 years through various mechanisms (barge dumps, firing ranges, airplanes, etc.)”. There has been a DoD prohibition on sea dumping of munitions since 1970. While there may have been some type of “rogue/prohibited” dumping by individual sailors, the munitions dumped in the bay should be overwhelmingly from earlier than 1970. Not sure about the use of ranges and when they were in use in that area, but the facility closed in 1990’s and I thought the ranges were WWII era.

**Response:** This sentence has been deleted.

Pg. 9, Figure 1.2 – Suggest adding a label/arrow for the location of Andrew Bay.

**Response:** Done

Pg. 15, 2.4 Wave Climate – Suggest adding a statement that the wave data in the 4 year period underwent quality control checks/procedures from the NDBC.

**Response:** A new section **2.4.1 Modeling Choices Related to Wave Climate** has been added in which the statistics of the 4-year record and its quality compared to other wave data in the region has been discussed in detail.

Pg. 19, 2.5 UXO types – A modification to the inputs of the UXO types present should be considered.

1. The modeled shapes of the mortar rounds includes the propelling charges. It would be very unlikely that these charges would remain intact on the rounds in such a dynamic environment if they were dumped. The dumped munitions would have had either a cellophane or cloth bag to hold the propellant depending upon the exact type of round

- and were designed for easy removal to adjust range (TM9-1901, Artillery Ammunition, 1944 and TM9-1300-203, Artillery Ammunition, 1967). If the round was fired, the propellant would have been expended and the shape would be different than the currently modeled shapes.
2. Depending upon the exact type of mortar round and date of issuance, they often had the fin assembly made out of an aluminum alloy. When connected to the steel body and immersed in seawater, this would result in galvanic corrosion. The fin assembly would then be the “sacrificial anode”. This would impact the shape and weight of the mortar round and thus the mobility.
  3. Modeled shapes for the 40mm round includes the casing. If the release scenario is from a fired projectile, the casing would not be present.

**Response:** We have addressed this point at the end of Section 2.5. The choice to model intact rounds was not only based on the practical requirement to have standardized and known shapes in the model gridding exercise, but also to assure the model analysis was maximizing risk in the risk assessment and seeking the most pessimistic plausible outcome by the two operative hypotheses. The inclusion of guidance fins, propellant charges and charge casings in the modeled UXO shapes (in spite of the fact these features are typically obliterated over time in this high energy environment) increases the wetted area and hydrodynamic drag on these shapes, while reducing the net density and rendering the UXO more mobile to any given fluid forcing.

Pg. 39 Simulation, - Please check to make sure the following statement is correct “The uniform distribution was limited from the 1000 m depth contour into the shore, and confined between the headlands of the Bay.” Figure 1.2 has the 1000m depth contour well outside the bay, so this reader assumes the statement should be 1000m from shore.

**Response:** Good catch...we meant 1000 ft ...a hold-over from an earlier draft before we converted globally to metric throughout the document. It is now changed to 300 m.

Pg 39 Simulation and figure 3.13 – The figure gives the impression that the area modeled is a finer sediment. Suggest modifying this figure and other figures to account for the cobbles that exist at the site.

**Response:** We believe the figure is correct and based on the rigid bottom formulation for the UXO\_MM under which the cobbles stop beyond the 30m depth contour to be consistent with NOAA charts and to obtain the most pessimistic plausible outcome in the Bottom Wind Hypothesis. This issue now is explained in detail in our new **Section 2.2.1 Modeling Choices Related to Bottom Composition**. The bottom type is now identified in the Figure 3.13 caption.

Pg 43. Some limitations of this mobility study would be the fact that biofouling can occur on the item, potentially altering its shape and its mobility. Also, since the area has kelp, this

would impact the simulation as well, potentially changing the simulation results. Please discuss how this may affect the results

Response: At high latitudes, the kelp only grows shoreward of the 30m depth due to depth attenuation of ambient light; (a consequence of turbidity from spring melt pulses and high waves with short daylight periods in winter). This limited depth regime of kelp at Andre Bay is consistent with notations in NOAA charts; (cf. Section 2.0s and 2.2.1). In these nearshore locations, kelp stands are uprooted during the high-energy winter months by shoaling, long-period waves, 6m and higher. Winter months are also when most of the UXO mobility occurs. The kelp grows back rapidly during the long arctic summer days, but the waves are generally very small at this time, (cf Figure 2.7), when little UXO mobility would occur. Because of this seasonality, we are not convinced that kelp is a direct factor on predominant UXO transport processes. The biofouling is neglected under the premise that we are conducting the model analysis under a set of simplifying assumptions that maximizes risk in the risk assessment and seeks the most pessimistic plausible outcome by the two hypotheses. Biofouling would impede mobility by creating angularity on otherwise smooth rounded shapes and by cementing the UXO rounds to hard bottom substrate. We have added comments on these issues to the front end of Section 3.5.

Pg 43. Suggest adding more discussion on the impact of the results from the following statement “Rocky crags and crevices acting to wedge the UXO in place on a hard bottom were not explicitly treated by the model physics herein”. Since this isn’t accounted for, are the current simulation results more conservative (potentially overestimating the mobility upslope and downslope)? Since the 20mm and 40mm are smaller than the average cobble size, would the results be more conservative for these items since they may “find more holes to fall in” than the larger items? Would their mobility be more “rate limited” by the movement of the larger cobbles around them since they aren’t exposed to the shear forces?

Response: This topic is another example of how we are conducting the model analysis under a set of simplifying assumptions that maximizes risk in the risk assessment and seeks the most pessimistic plausible outcome by the two hypotheses. We have added that phrase to the end of the above quote and in the second paragraph of the Executive Summary to emphasize the conservative (most-pessimistic) nature of modeled outcomes.

Pg 65. In thinking about long term management of these sites, it would be useful to estimate the overall long term trend at the site. Something like x percent moved upslope onto the beach, y percent moved to the closure depth, and z percent are still in the dynamic zone with potential mobility either way.

Response: Those percentages can be obtained from the end points of the cumulative probability curves (blue) in each of the transport histogram plots in Section 3.5 for a uniformly distributed population shoreward the 300 m (1000 ft) depth contour. What isn’t known is whether the real population is uniformly distributed or in patches offshore. That’s why an offshore UXO survey is necessary.

Pg. 77 Note that manuals mentioned above in the comments give slightly different dimensions “9.54 inches versus 9.59 inches. TM43-0001-28 gives 9.61 inches.

Pg. 79 Note Al alloy fin assembly

Pg. 80 picture is of an 81 mm mortar round, not 60mm

**Response: Corrected**

Overall – Excellent, well written report

### **Comments on Jenkins, D’Spain and AW and Wasyl by Barbara Sugiyama.**

We have data that shows that there is a probability that UXO will continue to show up on the beach due to two separated mechanisms. How valuable or what specifically, will additional data collection due to our knowledge base? Will doing some of the recommendations such as wave and current measurements provide any benefit? The other recommendations will be costly. What is the trade off benefit for additional investment? Is there a ball park cost for each additional data element?

**Response:** It seems to us the answer to these cost-trade-off questions depends on the programmatic objectives. Assuming the offshore UXO population is not concentrated in patches very close to shore (and EOD surveys suggest they are not); then we believe we’ve this report provides a worst-case assessment to estimate high-end costs of monitoring and remediation. We have added several sentences of prioritization of the recommended studies based on the most-cost effective way to proceed in filling the critical knowledge gaps. In our judgment, offshore surveys of bottom composition based on collecting sediment samples would provide the greatest cost-benefit to evaluating the *Bottom Wind Hypothesis* because it would resolve the question concerning the movable bottom vs rigid bottom formulation of the UXO-MM in the offshore domain. Samples of beach aggregate with follow-on size and roundness analysis, combined with Electro-magnetic or magnetic gradiometer surveys to detect and classify UXO blended in the beach deposits of the barrier spit, would provide the greatest cost-benefit to evaluating the *Beach Churn Hypothesis*, because such studies would resolve the long-term persistence of this UXO exposure mechanism.

A table summarizing the results in the executive summary may make it easier to read.

**Response:** Three such tables have been added to the Executive Summary